Identification of Novel Benzimidazole Derivatives as NPY Y5 Receptor Antagonists

田村, 友亮

https://doi.org/10.15017/1398444

出版情報：九州大学, 2013, 博士（理学）, 論文博士
バージョン：

Identification of Novel Benzimidazole Derivatives as NPY Y5 Receptor Antagonists

May 2013

Yuusuke Tamura

Contents

Abbreviations

ADME : absorption, distribution, metabolism, and excretion

AUC : area under the (blood concentration-time) curve

BA : bioavailability

BID : bis in die

BMI : body mass index

B/P ratio : brain concentration / plasma concentration ratio

CL_{tot} : total body clearance

C_{max} : maximum concentration

CSF : cerebrospinal fluid

CYP450 : cytochrome P450

DIO : diet-induced obese

HTS : high throughput screening

IC_{50} : half maximal inhibitory concentration

icv : intracerebroventricular

iv : intravenous

NPY : neuropeptide Y

PK : pharmacokinetic

po : per oral

SAR : structure-activity relationship

Chapter 1.

Introduction

Obesity is associated with several comorbidities, including hypertension, type 2 diabetes, and dyslipidemia, and these lifestyle-related diseases are independent risk factors for cardiovascular diseases. When these risk factors accumulate, the risk of cardiovascular diseases severely increases. The effects of this syndrome over time are now being referred to as 'metabolic domino effect'.[1]

Body mass index (BMI) criteria are currently the primary focus in obesity treatment recommendations. Health information regarding the relationship between BMI and above metabolic diseases is obtained through the use of the following two surveys. The National Health and Nutrition Examination Surveys (NHANES) in the United States and the Study to Help Improve Early evaluation and management of risk factors Leading to Diabetes (SHIELD), which are well-recognized and independently conducted surveys, showed similar results (*e. g*. prevalences of diabetes mellitus (types 1 and 2) and hypertension by BMI level).[2] Both surveys showed that the prevalence of these metabolic diseases increases in a linear fashion as BMI levels increases.

In addition, the economic cost of obesity-associated diseases is approaching five to ten percent of medical expenses in the United States.[3]

Many of these diseases can be prevented or ameliorated by a reduction in body weight. However, diet and exercise strategies alone, although successful in the short term, are difficult to maintain in the long term for the majority of patients. Given these limitations in achieving weight control, medications and alternative treatment options have been sought. Although the efficacy and safety of long-term drug therapy are very important in the obesity management, many anti-obesity drugs have been withdrawn because of their adverse effects. Some examples of side effects are valvulopathy associated with fenfluramine, the abuse potential and psychiatric side effects associated with rimonabant, and, most recently reported cardiac adverse events associated with sibutramine.[4] Therefore, there is significant medical need, which drives the search for new, safe, and effective anti-obesity drugs.

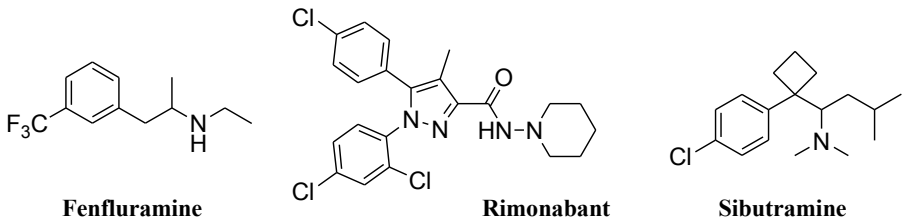

Fenfluramine **Rimonabant** **Sibutramine**

Figure 1_1. Structures of fenfluramine, rimonabant and sibutramine.

Neuropeptide Y (NPY) is a 36-amino acid peptide[5] which is widely distributed in the central[6-8] and peripheral nervous systems.[9-11] The biological effects of NPY are mediated through its interaction with G-protein coupled receptors (Y1, Y2, Y4 and Y5).[12] Among them, the Y5 receptor is thought to play a key role in the central regulation of food intake and energy balance.[13-16] Therefore, antagonism of the Y5 receptor represents an attractive target for potential therapeutic application against obesity. Recently, two Y5 antagonists, MK-0577[17] from Merck and Velneperit[18] from Shionogi, have advanced to clinical trials (Figure 1_2). However, these Y5 antagonists showed only modest, but statistically meaningful, effects on weight loss.

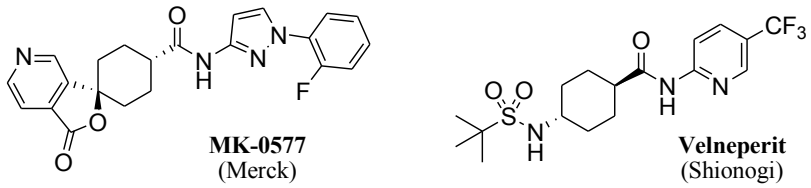

MK-0577 (Merck) **Velneperit** (Shionogi)

Figure 1_2. Structures of MK-0577 and Velneperit.

These results prompted the author to explore for more efficacious compounds. The author set an initial goal of in vitro profile suitable for progression to in vivo studies (Y5 IC_{50} < 10 nM, CYP450 inhibition > 10 μM, solubility > 10 μM, metabolic stability: human / rat > 80% / > 80%).

Chapter 2.

Identification of novel benzimidazole derivatives as highly potent NPY Y5 receptor antagonists with attractive in vitro Absorption, Distribution, Metabolism, and Excretion (ADME) profiles

To explore for novel Y5 antagonists, the author conducted a high throughput screening (HTS) campaign of compound library and selected structurally diverse compounds.[19] Among them, benzimidazole **2_1** was one of the attractive hit compounds.

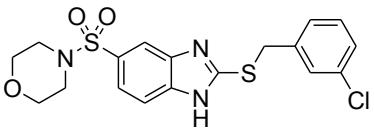

HTS hit 2_1

Y5 IC_{50} (nM) : 19.8

CYP450 inhibition (μM)
1A2 / 2C19 / 2C9 / 2D6 / 3A4 : >10 / 0.4 / 1.5 / >10 / 1.9

Solubility (μM) : 8.9

Metabolic stability
in human / rat liver microsomes (%) : 6.7 / 0.2

Figure 2_1. In vitro profiles of HTS hit **2_1**.

Velneperit that possesses a pharmacophore including SO_2 moiety, acidic N-H and terminal lipophilic groups, has a specific Y5 receptor binding affinity. Compound **2_1** also possesses a similar pharmacophore and it was expected to be a promising Y5 antagonist.

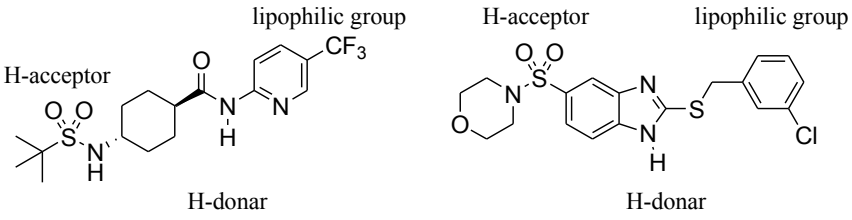

Velneperit **HTS hit 2_1**

Figure 2_2. Comparison of the structural features of Velneperit and HTS hit **2_1**.

However, while **2_1** exhibited Y5 antagonistic activity, the IC50 value is modest and its profile regarding CYP450 inhibition and metabolic stability needed to be improved. The author hypothesized

that these issues could arise from conformational flexibility and low oxidation tolerance of the -S-CH_2- linker of **2_1**. On the basis of this hypothesis, the author focused on the introduction of metabolically stable and rigid linkers in place of the -S-CH_2- moiety of **2_1**.

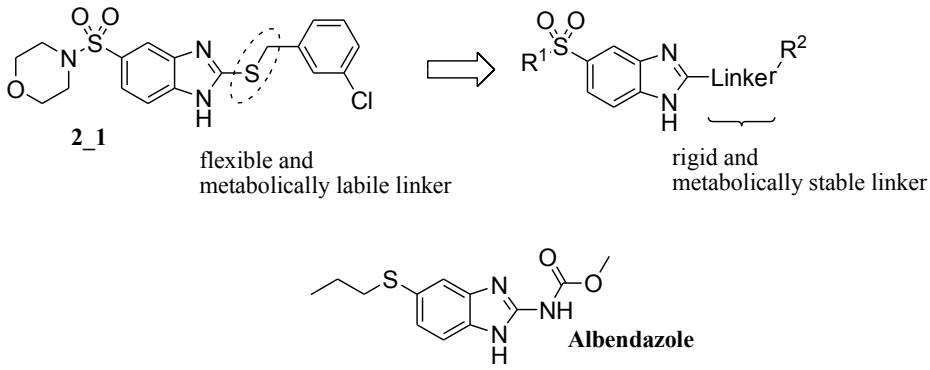

Figure 2_3. Design concept for new Y5 antagonists and structure of a possible starting material.

As the first approach to resolving the issues of HTS hit **2_1**, the author conducted the conversion of the -S-CH_2- moiety into an aryl linker that is connected to an additional phenyl ring as the lipophilic group (R^2). Considering availability and ease of derivatization, Albendazole (Figure 2_3) was utilized as the starting material, in which the sulfide group at the C-5 position could be easily converted into the sulfonyl moiety during synthesis and would be equivalent to the sulfonyl moiety of **2_1**. As shown in Table 2_1, positional scanning with the phenyl ring was investigated and showed a preference for the *meta*-position. While the *ortho*-phenyl **2_2b** lost Y5 receptor binding affinity, the *meta*-phenyl **2_2c** had very high binding affinity, which was 10,000-fold more potent than unsubstituted **2_2a**. The *para*-phenyl **2_2d** showed single digit nanomolar binding affinity, which was less potent than **2_2c**. On the basis of these observations, additional *meta*-substituted derivatives were explored and the author found

that the most favorable substituent was phenyl group (**2_2c**), followed by trifluoromethoxy (**2_2f**) and trifluoromethyl groups (**2_2e**).

Table 2_1. IC_{50} values, CYP450 inhibition profiles and solubilities of **2_2a-f**.

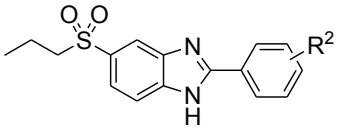

2_2

compds	R^2	Y5 IC_{50} (nM)[a]	CYP450 inhibition (μM) 1A2 / 2C19 / 2C9 / 2D6 / 3A4	Solubility (μM)[b]
2_2a	H	4657	2.9 / >10 / 9.5 / >10 / >10	>50
2_2b	*ortho*-Ph	4065	>10 / >10 / 4.5 / >10 / >10	23.6
2_2c	*meta*-Ph	0.43	2.7 / >10 / 9.5 / >10 / 6.0	0.50
2_2d	*para*-Ph	6.3	>10 / 5.9 / 2.4 / >10 / 2.9	0.50
2_2e	*meta*-CF_3	44.5	0.4 / >10 / 7.4 / >10 / >10	2.5
2_2f	*meta*-OCF_3	1.9	1.9 / 10 / 5.6 / >10 / 10	3.6

[a] Concentration of the compound that inhibited 50% of the total specific binding of ^{125}I-PYY as a ligand to mouse NPY Y5 receptors; obtained from the mean value of two or more independent assays.
[b] Solubility was measured as kinetic solubility using 1% DMSO solution at pH 6.8.

These results prompted the author to verify the pharmacophore of the highly potent derivative **2_2c** by investigating the corresponding indole analogues **2_3a** and **2_3b** for their Y5 receptor binding affinity (Figure 2_4). Interestingly, compound **2_3a** was approximately 60-fold more potent than **2_3b**, although both indole analogues showed decreased binding affinity relative to **2_2c**. The moderate potency of **2_3a** and the loss of potency with **2_3b** suggested that the form **I** of **2_2c** would be the preferred binding mode of the two possible tautomers, whose N-H is attached at the *para*-position to the sulfonyl group.

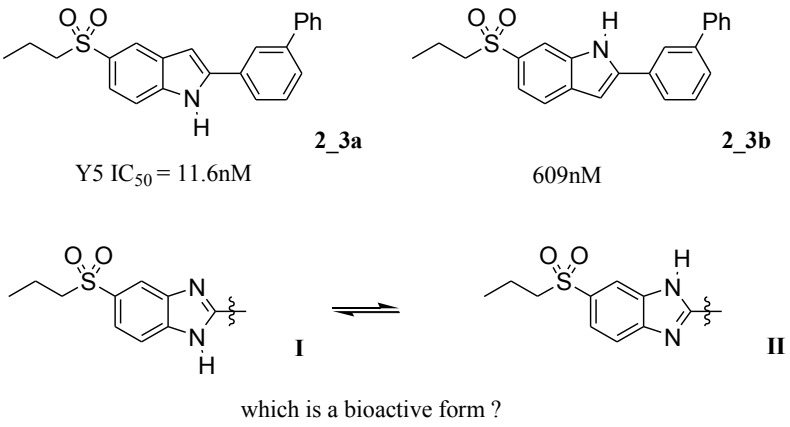

Figure 2_4. Elucidation of the preferred binding mode.

As for in vitro metabolic stabilities**,** derivative **2_2c** exhibited improved metabolic stabilities in liver microsomes (human 68.6%, rat 57.1%) relative to HTS hit **2_1** (human 6.7%, rat 0.2%).[20] In addition, replacement of the *n*-propanesulfonyl group with ethanesulfonyl group (**2_2g**, Table 2_2) resulted in further improved metabolic stabilities in liver microsomes (human 85.2%, rat 79.1%) along with retention of high affinity for the Y5 receptor. In this way, derivative **2_2g** was found to be a highly potent Y5 antagonist with improved metabolic stabilities; however, there was a room for improvement in the CYP450 inhibition profiles and the solubility.

Table 2_2. IC_{50} values, CYP450 inhibition profiles and solubilities of **2_2c** and **2_2g**.

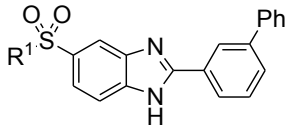

compds	R^1	Y5 IC_{50} (nM)[a]	CYP450 inhibition (μM) 1A2 / 2C19 / 2C9 / 2D6 / 3A4	Solubility (μM)[b]
2_2c	*n*-Pr	0.43	2.7 / >10 / 9.5 / >10 / 6.0	0.50
2_2g	Et	0.46	0.4 / >10 / 9.9 / >10 / 9.0	0.90

[a, b] See Table 2-1.

Some CYP450 subfamilies preferentially bind planar and lipophilic molecules.[21] In addition, solubility of a molecule in water is dependent on its crystallinity, which correlates with molecular planarity, and ability to interact with water. Therefore, the author next turned his attention to the introduction of different substituents on the central phenyl ring of **2_2g**. The dihedral angle between two phenyl rings is related to molecular planarity and affect the physicochemical profile.[22] In fact, the *ortho*-phenyl **2_2b** has larger dihedral angle than the *meta*-phenyl **2_2c** and the *para*-phenyl **2_2d** and it exhibited high solubility relative to **2_2c** and **2_2d** (Table 2_1).

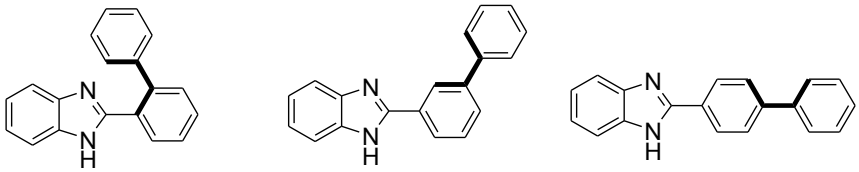

Φ = 67.2 Φ = 52.7 Φ = 52.2

Figure 2_5. Dihedral angles calculated by Molecular Operating Environment (MOE) 2011.10.

As shown in Table 2_3, relatively bulky substituents, such as the chloro and methyl groups, at the 2'- or 4'-position (**2_4d**, **4e**, **4g** and **4h**) were not tolerated, probably due to prevention of the interaction between benzimidazole N-H and the Y5 receptor. In contrast, compounds bearing a substituent at the 6'-position (**2_4c**, **4f** and **4i**) exhibited excellent binding affinity. However, they did not show acceptable improvement in the CYP450 inhibition profiles and the solubility. Effect of the introduced substituents on molecular planarity may have been offsets by its enhanced lipophilicity, and high lipophilicity due to the biphenyl moiety seemed to be the reason for the CYP450 inhibition and the low solubility.

Table 2_3. IC_{50} values, CYP450 inhibition profiles and solubilities of **2_2g** and **2_4a-i**

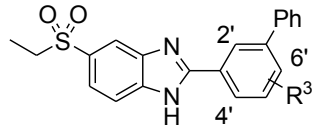

2_4

compds	R^3	Y5 IC_{50} (nM)[a]	CYP450 inhibition (μM) 1A2 / 2C19 / 2C9 / 2D6 / 3A4	Solubility (μM)[b]
2_2g	H	0.46	0.4 / >10 / 9.9 / >10 / 9.0	0.90
2_4a	2'-F	2.7	1.1 / >10 / 7.2 / >10 / 6.6	0.60
2_4b	4'-F	0.54	2.2 / >10 / >10 / >10 / >10	0.60
2_4c	6'-F	0.16	3.4 / >10 / 9.5 / >10 / 5.6	0.20
2_4d	2'-Cl	40.5	3.0 / 9.3 / 4.0 / >10 / 3.8	1.5
2_4e	4'-Cl	31.1	0.4 / 4.9 / 7.1 / >10 / 5.0	0.40
2_4f	6'-Cl	0.16	8.5 / >10 / 5.4 / >10 / 2.6	N.D.
2_4g	2'-Me	21.8	7.8 / >10 / 4.4 / >10 / 5.2	3.2
2_4h	4'-Me	383	0.4 / 4.2 / 6.8 / >10 / 5.9	0.50
2_4i	6'-Me	0.20	3.2 / >10 / 8.3 / >10 / 5.7	N.D.

[a, b] See Table 2-1.

To reduce the lipophilicity of **2_2g** (CLopP = 4.94),[23] the author sought to incorporate a polar linker in place of the phenyl linker. One strategy was use of pyridine analogues. As shown in Table 2_4, the first example was **2_5a** (CLopP = 3.95), which unfortunately resulted in significant decreases in the Y5 receptor binding affinity.

Table 2_4. IC_{50} values, CYP450 inhibition profiles and solubilities of **2_2g** and **2_5a**.

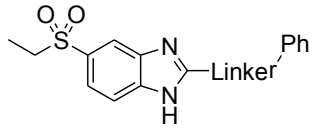

compds	-Linker-	Y5 IC_{50} (nM)[a]	CYP450 inhibition (μM) 1A2 / 2C19 / 2C9 / 2D6 / 3A4	Solubility (μM)[b]
2_2g	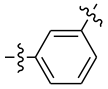	0.46	0.4 / >10 / 9.9 / >10 / 9.0	0.90
2_5a	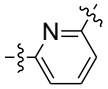	38.9	0.4 / >10 / >10 / >10 / 7.7	4.0

[a, b] See Table 2-1.

This negative effect of the nitrogen atom in the pyridine linker of **2_5a** on the binding affinity could be rationalized as follow. Assuming that conformer **IV** in Figure 2_6 is best fit into the key site of Y5 receptor and the pyridine nitrogen indirectly affects the binding affinity by changing the conformational preference, the decreased potency of **2_5a** would be reasonable. In the case of **2_5a**, the proposed bioactive form **IV** should be destabilized by unfavorable lone pair repulsion between the benzimidazole nitrogen and the pyridine nitrogen, while the bio-inactive form **III** or **V** would be favored owing to the intramolecular hydrogen bond formation between the benzimidazole N-H and the pyridine nitrogen.

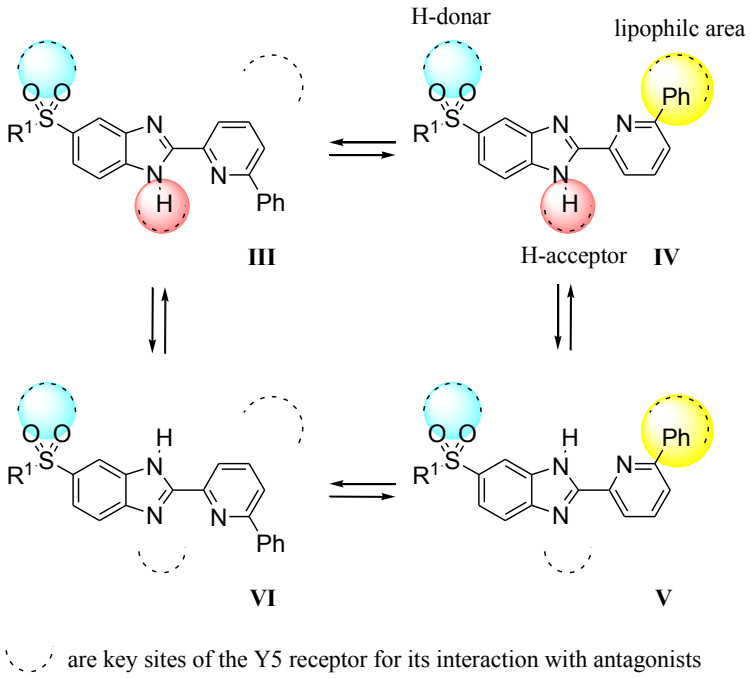

Figure 2_6. Proposed active conformation.

In fact, the Φ = 0° rotamer corresponding to **III** or **V** is 10 kcal/mol more favorable than the Φ = 180° rotamer corresponding to **IV** or **VI** (Figure 2_7).

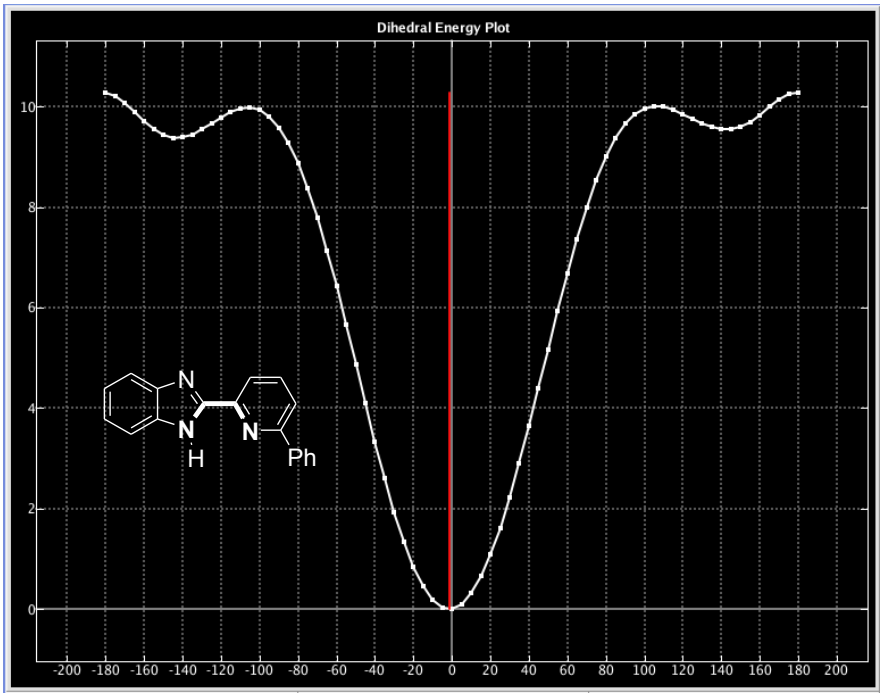

Figure 2_7. Dihedral energy plot calculated by MOE 2011.10.

To test the author's hypothesis, other pyridine analogues **2_5b-d**, which could not form the undesirable intramolecular hydrogen bond and were expected to exhibit the high binding affinity, were explored. Compounds **2_5b-d** maintained similar Y5 receptor affinity for **2_2g** as expected. In addition, the pyridine nitrogen of **2_5c** or **2_5d** contributed to solubility presumably because of reduced lipophilicity (**2_5c** CLogP = 3.53, **2_5d** CLogP = 3.74). These investigations yielded additional information about the preferred binding mode. However, pyridine analogues did not show acceptable improvement in the CYP450 inhibition profiles.

Table 2_5. IC_{50} values, CYP450 inhibition profiles and solubilities of **2_2g** and **2_5a-d**.

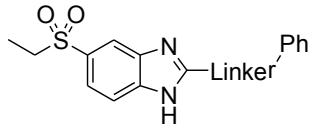

compds	-Linker-	Y5 IC_{50} (nM)[a]	CYP450 inhibition (μM) 1A2 / 2C19 / 2C9 / 2D6 / 3A4	Solubility (μM)[b]
2_2g	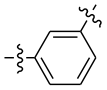	0.46	0.4 / >10 / 9.9 / >10 / 9.0	0.90
2_5a	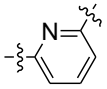	38.9	0.4 / >10 / >10 / >10 / 7.7	4.0
2_5b	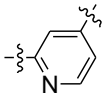	0.55	1.6 / >10 / 10 / >10 / 7.0	1.6
2_5c	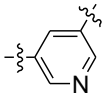	1.8	6.3 / >10 / 9.8 / >10 / 7.8	12.1
2_5d	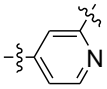	0.31	3.4 / >10 / >10 / >10 / 8.7	20.3

[a, b] See Table 2-1.

In an attempt to resolve this issue, the author next figured out use of less lipophilic pyridone rings in place of phenyl linker. Considering the results of Tables 2_3 and 2_5, the author adopted substitution pattern **2_8** as a linker.

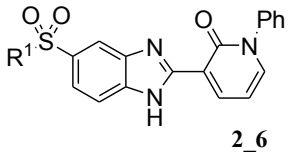

2_6

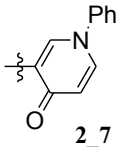

2_7

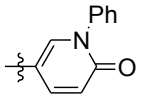

2_8

Figure 2_8.Substitution pattern of pyridone analogues.

As expected, pyridone analogue **2_8a** exhibited acceptably high binding affinity with dramatic improvement of the CYP450 inhibition profiles and the solubility, consistent with its less lipophilicity (CLogP = 2.92). This result prompted the author to investigate the *n*-propanesulfonyl derivative **2_8b**. Replacement of ethyl group with *n*-propyl group led to the enhanced binding affinity and retention of improved CYP450 inhibition profiles and high solubility. In addition, the pyridone analogues showed high metabolic stabilities in liver microsomes: human / rat (**2_8a**, 99.2% / >99.9%; **2_8b**, 88.5% / 78.6%).

Table 2_6. IC_{50} values, CYP450 inhibition profiles and solubilities of **2_8a-b**

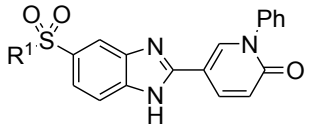

2_8

compds	R^1	Y5 IC_{50} (nM)[a]	CYP450 inhibition (μM) 1A2 / 2C19 / 2C9 / 2D6 / 3A4	Solubility (μM)[b]
2_8a	Et	7.7	All > 10	>50
2_8b	*n*-Pr	1.9	All > 10	43.3

[a, b] See Table 2-1.

In summary, the optimization of HTS hit **2_1** led to identification of the highly potent derivative **2_2c**. Modification of **2_2c** gave pyridone analogues **2_8a-b** which had nanomolar Y5 receptor binding affinities with improved CYP450 inhibition profiles, enhanced solubilities and metabolic stabilities.

Chapter 3.

Identification of a novel and orally available benzimidazole derivative as an NPY Y5 receptor antagonist

In chapter 2 the author described the optimization of HTS hit **2_1** and the discovery of a novel NPY Y5 receptor antagonist **2_8b** that exhibits high binding affinity and attractive in vitro profiles with respect to CYP450 inhibition, solubility and metabolic stabilities. Despite these attractive in vitro properties, the pyridone analogue exhibited only little absorption after oral administration.[24] Although the reason was unclear, the author tried to find a second-generation derivative with improved oral absorption together with in vitro profiles comparable to **2_8b**. The new strategy was to replace the aromatic linker of **2_2c** with several saturated rings to reduce structural planarity and change the ADME profiles (Figure 3_1).[22]

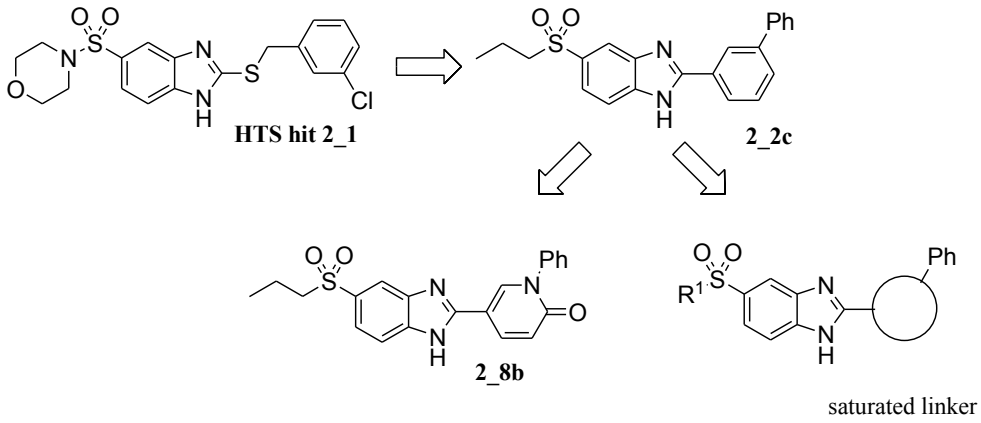

Figure 3_1. Design concept.

The first strategy was to replace the phenyl linker of **2_2c** with a pyrrolidine or piperidine ring (Table 3_1). As expected, both saturated derivatives showed moderate to appreciable improvement in the CYP450 inhibition profiles and the solubility. Piperidine **3_2a** exhibited sub-nanomolar binding affinity, which was equipotent to **2_2c**. Pyrrolidine **3_1a** was 3-fold less potent than **3_2a**. These results suggest that the right-hand part, which is similar in shape to the biphenyl moiety of **2_2c**, is

important for the binding affinity. While **3_2a** afforded the best potency, its metabolic stabilities in human and rat liver microsomes were unacceptable.

Table 3_1. IC_{50} values, CYP450 inhibition profiles, solubilities and metabolic stabilities of compounds **2_2c**, **3_1a**, and **3_2a**.

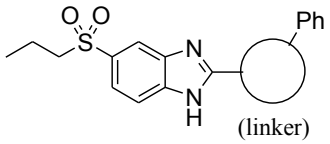

compds	linker	Y5 IC_{50} (nM)[a]	CYP450 inhibition (μM) 1A2 / 2C19 / 2C9 / 2D6 / 3A4	Solubility (μM)[b]	Metabolic stability (%)[c] human / rat
2_2c	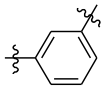	0.43	2.7 / >10 / 9.5 / >10 / 6.0	0.50	68.6 / 57.1
3_1a	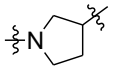	1.01	All >10	15.4	74.9 / 19.2
3_2a	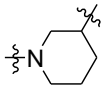	0.29	>10 / >10 / 9.4 / >10 / 6.9	19.1	45.2 / 2.2

[a] Concentration of the compound that inhibited 50% of total specific binding of ^{125}I-PYY as a ligand to mouse NPY Y5 receptors; obtained from the mean value of two or more independent assays.
[b] Solubility was measured as kinetic solubility using 1% DMSO solution at pH 6.8.
[c] Metabolic stability in human or rat liver microsomes was measured as the percentage of the compound remaining after 30 min incubation.

The metabolic instablility of **3_2a** may arise from the aliphatic carbon around the benzylic position. This hypothesis prompted the author to incorporate heteroatoms into the piperidine moiety. Thus, piperazine **3_3a-4a** and morpholine **3_5a** were examined. Among them, derivatives **3_3a** and **3_5a** showed improvement in metabolic stabilities. While piperazine **3_3a** exhibited a 20-fold decrease in the binding affinity, morpholine **3_5a** was equipotent to piperidine **3_2a**.

Table 3_2. IC_{50} values, CYP450 inhibition profiles, solubilities and metabolic stabilities of compounds **3_2a-5a**.

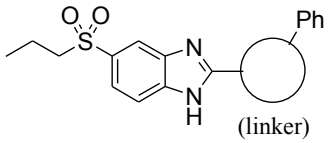

compds	linker	Y5 IC_{50} (nM)[a]	CYP450 inhibition (μM) 1A2 / 2C19 / 2C9 / 2D6 / 3A4	Solubility (μM)[b]	Metabolic stability (%)[c] human / rat
3_2a	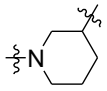	0.29	>10 / >10 / 9.4 / >10 / 6.9	19.1	45.2 / 2.2
3_3a	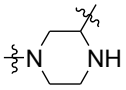	6.82	All >10	>50	64.4 / 44.0
3_4a	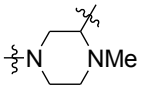	4.99	All >10	>50	21.9 / 21.1
3_5a	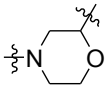	0.60	All >10	>50	77.9 / 45.9

[a, b, c] See Table 3-1.

On the other hand, utilization of tetrahydropyran ring in place of morpholine ring resulted in a decrease of the Y5 receptor binding affinity (Table 3_3). These results suggest that the sp^3 hybridized carbon atom, which is directly bonded with the C-2 position of benzimidazole core, have a negative influence on the binding affinity.

Table 3_3. IC_{50} values, CYP450 inhibition profiles, solubilities and metabolic stabilities of compounds **3_5a** and **3_6a**.

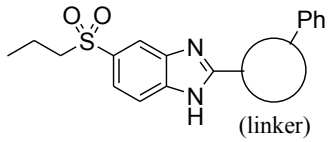

compds	linker	Y5 IC_{50} (nM)[a]	CYP450 inhibition (μM) 1A2 / 2C19 / 2C9 / 2D6 / 3A4	Solubility (μM)[b]	Metabolic stability (%)[c] human / rat
3_5a	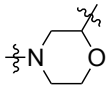	0.60	All >10	>50	77.9 / 45.9
3_6a[d]	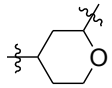	17.2	All >10	>50	65.0 / 74.0

[a, b, c] See Table 3-1.
[d] *Cis*/*trans* mixture.

To further explore the potential of morpholine **3_5a**, we investigated the effect of its subunits on binding affinity and in vitro profiles. Initial investigations were focused on the left-hand part of **3_5a**, namely alkyl substitutions on the sulfonyl group (R^1SO_2). The replacement of *n*-$PrSO_2$ with $EtSO_2$ led to equipotent compound **3_5b** with further improved metabolic stabilities. The binding affinity decreased as the bulkiness of the α-position of the alkylsulfonyl group became larger (**3_5b-d**). In contrast, the bulkiness of the β-position of the alkylsulfonyl group showed a positive effect on the binding affinity (**3_5e** and **3_5g**). While **3_5g** showed high Y5 binding affinity with appreciable CYP450 profiles and high solubility, the $CF_3CH_2SO_2$ moiety was easily hydrolyzed under basic condition due to its high susceptibility to elimination reaction (Figure 3_2).[25] An attempt to improve the physicochemical stability of **3_5g** by replacing the α-protons with methyl group worsened the CYP450 inhibition profiles and the solubility (**3_5h**), in accord with the above observation.

Table 3_4. IC_{50} values, CYP450 inhibition profiles, solubilities and metabolic stabilities of compounds **3_5a-h**.

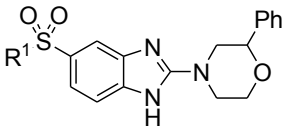

compds	R^1	Y5 IC_{50} (nM)[a]	CYP450 inhibition (μM) 1A2 / 2C19 / 2C9 / 2D6 / 3A4	Solubility (μM)[b]	Metabolic stability (%)[c] human / rat
3_5a	*n*-Pr	0.60	All >10	>50	77.9 / 45.9
3_5b	Et	0.43	All >10	>50	89.0 / 76.1
3_5c	*i*-Pr	1.33	All >10	>50	87.0 / 49.5
3_5d	*t*-Bu	4.27	All >10	10.7	78.5 / 56.4
3_5e	*i*-Bu	0.28	>10 / >10 / >10 / >10 / 9.3	43.2	55.1 / 2.4
3_5f	CF_3	0.73	>10 / 1.7 / 4.5 / 5.5 / 2.3	3.7	81.7 / 67.9
3_5g	CH_2CF_3	0.21	All >10	>50	85.0 / 63.5
3_5h	$C(CH_3)_2CF_3$	1.43	>10 / >10 / >10 />10 / 8.2	11.6	60.2 / 37.8

[a, b, c] See Table 3-1.

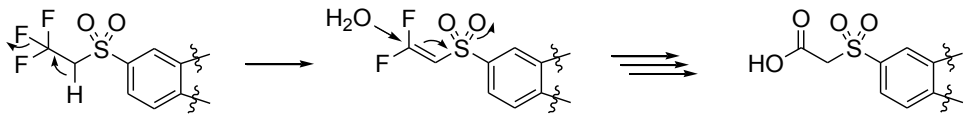

Figure 3_2. Mechanism for decomposition of **3_5g**

Retaining the ethanesulfonyl group the author next turned his attention to investigation of the influence of various substituents on the right-hand phenyl ring of **3_5b** (Table 3_5). While all the examined

substituents on the outer phenyl ring did not give adverse effect on Y5 binding affinities, **3_5j** showed CYP450 inhibition potential and **3_5k-l** were metabolically unstable in rat liver microsomes.

Table 3_5. IC_{50} values, CYP450 inhibition profiles, solubilities and metabolic stabilities of compounds **3_5b** and **3_5i-l**.

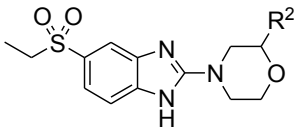

compds	R^2	Y5 IC_{50} (nM)[a]	CYP450 inhibition (μM) 1A2 / 2C19 / 2C9 / 2D6 / 3A4	Solubility (μM)[b]	Metabolic stability (%)[c] human / rat
3_5b	Ph	0.43	All >10	>50	89.0 / 76.1
3_5i	4-F-Ph	1.05	All > 10	>50	92.4 / 87.1
3_5j	4-Cl-Ph	0.85	9.2 / 9.1 / >10 / >10 / >10	38.1	94.6 / 87.2
3_5k	4-Me-Ph	0.80	All > 10	21.6	87.8 / 34.0
3_5l	4-OMe-Ph	3.03	All >10	>50	81.0 / 48.0

[a, b, c] See Table 3-1.

On the basis of these results, morpholine **3_5b** was selected for further investigation. An in vivo cassette study in rats for **3_5b** (0.5 mg/kg iv, 1.0 mg/kg po) was conducted to examine the oral absorption[26] and showed acceptable plasma exposure with moderate blood clearance (C_{max} = 64.2 ng/ml, CL_{tot} = 9.9 ml/min/kg), indicating some effect of the saturated linker on the PK profiles.

To evaluate in vivo efficacy, compound **3_5b** (12.5 mg/kg) was orally administered 1 h before the mice were treated with Y5 selective agonist[27] (0.1 nmol icv) and cumulative food intake was measured for the following 4 h. As shown in Figure 3_3, compound **3_5b** blocked the increase in food intake in this feeding model.

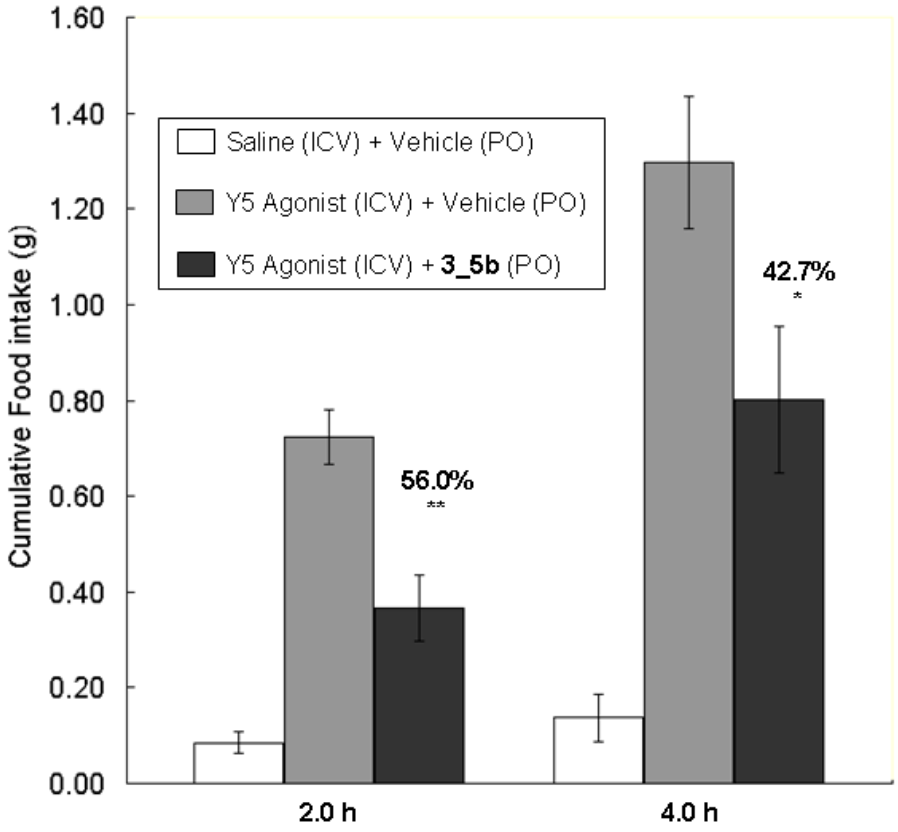

Figure 3_3. Effect of **3_5b** (12.5 mg/kg) on Y5 agonist-stimulated food intake in diet-induced obese mice (n = 4-6). Vehicle is 0.5% hydroxypropylmethyl cellulose solution. **p < 0.01 versus Y5 agonist and vehicle treated group.

In summary, replacement of the phenyl linker of the lead compound **2_2c** with the corresponding saturated linkers resulted in several potent derivatives. Among them, morpholine **3_5b** showed in vivo efficacy in the agonist-induced food intake model. However, its chronic oral administration (25 mg/kg bid) to diet-induced obese (DIO) mice did not cause reduction of body weight gain.

Chapter 4.

Identification of a novel benzimidazole derivative as a highly potent NPY Y5 receptor antagonist with an anti-obesity profile

In chapter 2 and 3 the author carried out optimization of HTS hit **2_1**, with a main focus on modification at the C-2 position of the benzimidazole core. Elimination of the flexible and metabolically liable -S-CH_2- part and utilization of pyridone and morpholine rings led to identification of novel NPY Y5 receptor antagonists **2_8b** and **3_5b**, respectively.

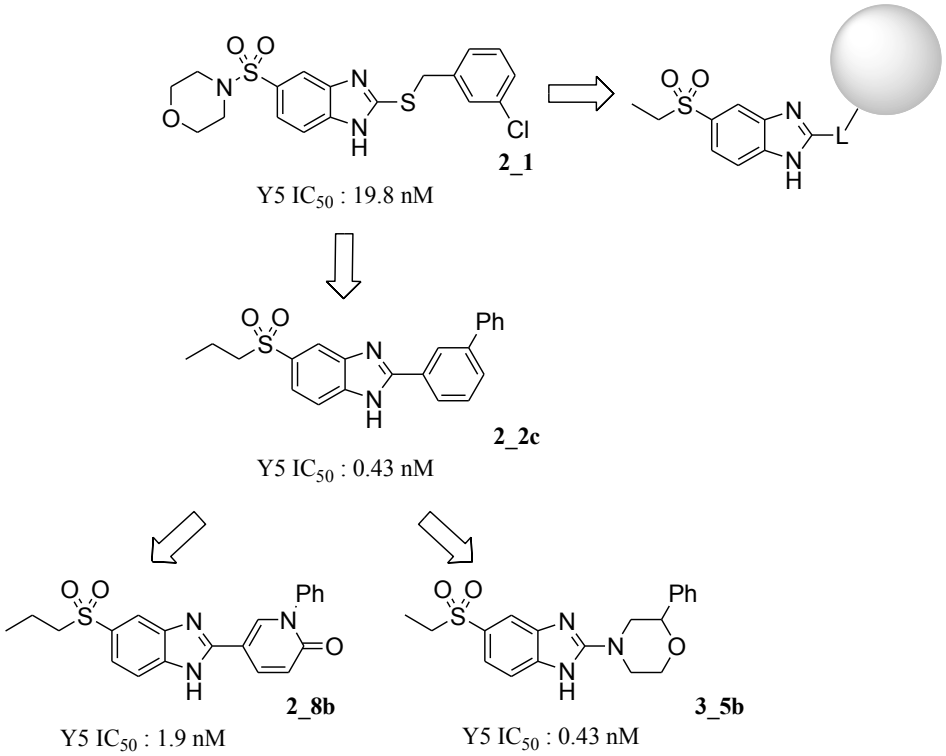

Figure 4_1. Design concept.

Although pyridone **2_8b** exhibited high affinity at the NPY Y5 receptor with attractive in vitro ADME profiles, it suffered from poor bioavailability. While morpholine **3_5b** was orally active for suppression of food intake induced by a NPY Y5 selective agonist, its chronic oral administration (25 mg/kg bid) to diet-induced obese (DIO) mice did not cause reduction of body weight gain. With regard to brain penetration, morpholine **3_5b** showed marginal brain exposure presumably due to the presence

of a guanidine-like substructure, which would have a negative effect on in vivo efficacy.[28] Lipophilicity is known to be an important parameter governing brain penetration and a guanidine-like substructure show the lowest CLogP value (Figure 4_2).

Figure 4_2. CLogP values estimated with ChemDraw Ultra, version 9.0.

Therefore, the author sought to eliminate this liability by replacing the nitrogen-linker with a sulfur-, oxygen- or carbon-linker. On the basis of findings in chapter 2 and 3, the initial structure-activity relationship (SAR) study was conducted by replacement of the sulfonamide moiety of HTS hit **2_1** with an ethanesulfonyl group. As shown in Table 4_1, derivative **4_1a** exhibited improved solubility and metabolic stability in human liver microsomes, however, its metabolic stability in rat liver microsomes was still low. This supports the author's previous inference that $–S-CH_2-$ unit is responsible for poor metabolic stability. Introduction of an $-O-CH_2-$ linker in place of the $-S-CH_2-$ moiety of **4_1a** led to improvement of metabolic stabilities in both human and rat liver microsomes to some extent but resulted in reduction of the Y5 receptor binding affinity.

Table 4_1. IC_{50} values, CYP450 inhibition profiles, solubilities and metabolic stabilities of compounds **2_1** and **4_1a-b**.

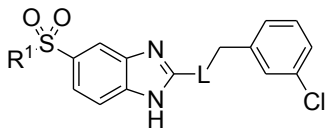

2_1 : L = S
4_1a : L = S
4_1b : L = O

compds	R^1	Y5 IC_{50} (nM)[a]	CYP450 inhibition (μM) 1A2 / 2C19 / 2C9 / 2D6 / 3A4	Solubility (μM)[b]	Metabolic stability (%)[c] human / rat
2_1	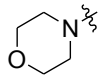	19.8	>10 / 0.4 / 1.5 / >10 / 1.9	8.9	6.7 / 0.19
4_1a		12.1	8.9 / 9.4 / >10 / >10 / 8.8	27.5	63.7 / 0.13
4_1b		80.4	8.9 / >10 / >10 / >10 / >10	49.9	88.5 / 37.9

[a] Concentration of the compound that inhibited 50% of total specific binding of ^{125}I-PYY as a ligand to mouse NPY Y5 receptors; obtained from the mean value of two or more independent assays.
[b] Solubility was measured as kinetic solubility using 1% DMSO solution at pH 6.8.
[c] Metabolic stability in human or rat liver microsomes was measured as the percentage of the compound remaining after 30 min incubation.

Compound **2_2c** exhibited high binding affinity (Chapter 2, Table 2_1). Therefore, the author expected that the compound bearing a 2-phenylethoxy moiety, the conformation of which overlaps the morpholine moiety of **2_2c**, would also show good binding affinity.

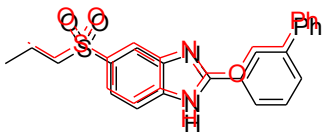

Figure 4_3. Overlay of morpholine derivative **2_2c** and 2-phenylethoxy derivative.

Although 2-phenylethoxy derivative **4_1c** had improved binding affinity relative to **4_1b**, its Y5 IC_{50} value was moderate. The author considered that the moderate binding affinity of **4_1c** could arise from the high conformational freedom of the -O-CH_2-CH_2- linker. Due to favorable gauche interaction [$\sigma_{C\text{-}H}$–$\sigma^*_{C\text{-}F}$ interaction] by C-F bond,[29] it was expected that the conformation of the linker would be fixed if C-F bonds are introduced at the benzylic position. The introduction of C-F bonds on the benzylic position was also expected to improve the metabolic liability. Indeed, derivative **4_1d** showed enhanced binding affinity with improved metabolic stabilities.

Table 4_2. IC_{50} values, CYP450 inhibition profiles, solubilities and metabolic stabilities of compounds **4_1c-d**.

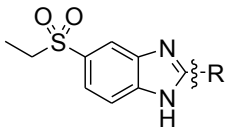

compds	R	Y5 IC_{50} (nM)[a]	CYP450 inhibition (μM) 1A2 / 2C19 / 2C9 / 2D6 / 3A4	Solubility (μM)[b]	Metabolic stability (%)[c] human / rat
4_1c	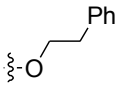	25.0	All >10	>50.0	88.1 / 37.6
4_1d	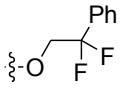	4.39	All >10	>50.0	97.9 / 83.8

[a, b, c] See Table 4-1.

This result prompted the author to conduct the next SAR study with phenoxy derivatives that seem to be a moderately flexible and has a related structure to **2_2c**. Thus the author investigated several *meta*- and *para*-substituted derivatives. *meta*- and *para*-CF_3 derivatives had modest binding affinities. The

most favorable substitution was *para*-phenyl, followed by *meta*-OCF_3. Interestingly, while *para*-phenyl was 3-fold more potent than the *meta*- phenyl, *para*-OCF_3 was less potent than *meta*- OCF_3.

Table 4_3. IC_{50} values, CYP450 inhibition profiles, solubilities and metabolic stabilities of compounds **4_2a-f**.

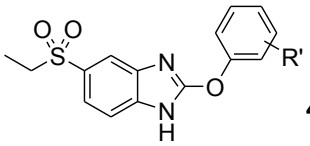

4_2

compds	R'	Y5 IC_{50} (nM)[a]	CYP450 inhibition (μM) 1A2 / 2C19 / 2C9 / 2D6 / 3A4	Solubility (μM)[b]	Metabolic stability (%)[c] human / rat
4_2a	*meta*-CF_3	41.2	>10 / >10 / >10 / 0.4 / >10	>50	>99.9 / 88.4
4_2b	*para*-CF_3	98.1	All >10	>50	95.2 / 86.9
4_2c	*meta*-OCF_3	7.11	All > 10	>50	97.1 / 86.2
4_2d	*para*-OCF_3	22.4	All > 10	>50	92.8 / 91.6
4_2e	*meta*-Ph	9.55	8.3 / >10 / 8.4 / >10 />10	4.2	29.1 / 77.3
4_2f	*para*-Ph	2.82	>10 / >10 / 6.9 / >10 / 7.7	2.5	>99.9 / >99.9

[a, b, c] See Table 4-1.

To further explore a more potent biphenyl derivative **4_2f**, the oxygen linker was replaced with a -CH_2-, -CO- or -CF_2- linker (Table 4_4). While -CH_2- and -CF_2- derivatives resulted in significant decreases in the Y5 receptor binding affinity, the carbonyl derivative **4_4a** retained high binding affinity with improved CYP450 inhibition profiles but suffered from decreased solubility, probably due to its rigid structural nature.

Table 4_4. IC_{50} values, CYP450 inhibition profiles, solubilities and metabolic stabilities of compounds **4_2f** and **4_3a-5a**.

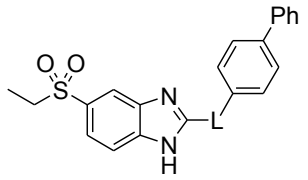

compds	L	Y5 IC_{50} (nM)[a]	CYP450 inhibition (μM) 1A2 / 2C19 / 2C9 / 2D6 / 3A4	Solubility (μM)[b]	Metabolic stability (%)[c] human / rat
4_2f		2.82	>10 / >10 / 6.9 / >10 / 7.7	2.5	>99.9 / >99.9
4_3a		112	>10 / 10 / >10 / 3.5 / 10	3.0	87.6 / 74.3
4_4a		2.61	All >10	0.3	>99.9 / >99.9
4_5a		48.6	10 / 8.4 / 2.7 / 4.1 / 10	0.3	0.10 / 78.3

[a, b, c] See Table 4-1.

Derivative **4_2f** was a highly potent Y5 antagonist with appreciable metabolic stabilities, but several drawbacks were identified; it had potent CYP450 inhibition and low solubility which might be a consequence of its high lipophilicity or rigid nature. To address this problem, the author planed to synthesize a series of **4_2f** derivatives, in which one phenyl group of the biphenyl moiety was replaced with pyridiyl group to reduce its lipophilicity (Figure 4_4). However, among five possible derivatives, regioisomer **4_6a** may be unpromising due to undesirable conformational preference via intramolecular hydrogen bonding between benzimidazole N-H and pyridine nitrogen (Figure 4_5). Regioisomers **4_6d**

and **4_6e** possess a naked pyridine and should cause high CYP450 inhibition. Therefore, the author selected regioisomers **4_6b** and **4_6c** for a SAR study.

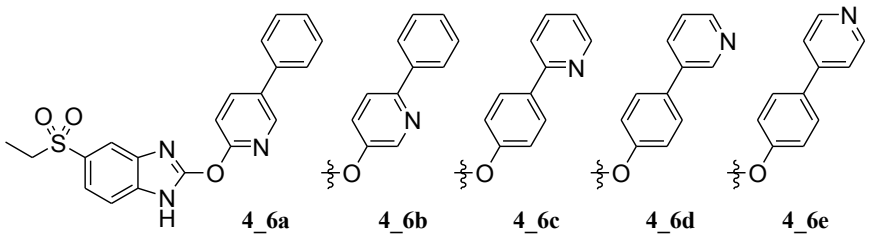

Figure 4_4. Regioisomers of pyridine analogues.

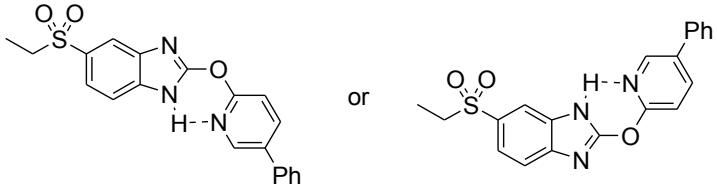

Figure 4_5. Preferred but undesirable conformations of **4_6a**.

As shown in Table 4_5, derivatives **4_6b** and **4_6c** retained Y5 receptor binding affinity with improved CYP450 inhibition profiles and solubility. Next, we replaced the inner phenyl ring of **4_2f** with a cyclohexyl substructure to reduce structural planarity and to change ADME profiles.[22] Cyclohexyl derivative **4_7a** maintained high binding affinity and metabolic stabilities, but did not show acceptable improvement in the CYP450 inhibition profiles and solubility.

Table 4_5. IC_{50} values, CYP450 inhibition profiles, solubilities and metabolic stabilities of compounds **4_2f**, **4_6b**, **4_6c**, and **4_7a**.

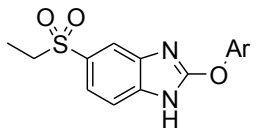

compds	Ar	Y5 IC_{50} (nM)[a]	CYP450 inhibition (μM) 1A2 / 2C19 / 2C9 / 2D6 / 3A4	Solubility (μM)[b]	Metabolic stability (%)[c] human / rat
4_2f	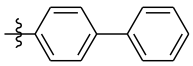	2.82	>10 / >10 / 6.9 / >10 / 7.7	2.5	>99.9 / >99.9
4_6b	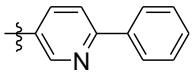	2.92	All >10	39.7	98.6 / >99.9
4_6c	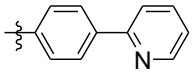	4.07	All >10	>50	99.1 / 99.3
4_7a	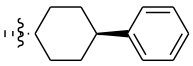	3.75	>10 / >10 / 7.3 / >10 / 2.7	6.1	>99.9 / 93.8

[a, b, c] See Table 4-1.

Through efforts, some derivatives presented an in vitro profile suitable for progression to in vivo studies (Y5 IC_{50} < 10 nM, CYP450 inhibition > 10 μM, solubility > 10 μM, metabolic stability: human / rat > 80% / > 80%). In vivo cassette studies in rat for **4_1d**, **4_2c**, **4_6b** and **4_6c** were conducted and their pharmacokinetic (PK) parameters are shown in Table 4_6.[26] While derivative **4_2c** exhibited high brain/plasma (B/P) ratio, the plasma level was low probably due to high clearance. Derivatives **4_1d**, **4_6b** and **4_6c** had acceptable plasma levels with low clearance. Additionally, derivatives **4_1d** and **4_6b** had moderate to good B/P ratios.

Table 4_6. Rat PK profile of **4_1d**, **4_2c**, **4_6b** and **4_6c** (0.5 mg/kg iv, 1.0 mg/kg po)

compds	CL_{tot} (ml/min/kg)	AUC (ng hr/ml)	C_{max} (ng/ml)	BA (%)[a]	B/P ratio[b]
4_1d	5.29	2160	166	68.3	0.58
4_2c	30.7	74.8	17.9	13.5	0.98
4_6b	2.13	3630	320	46.5	0.14
4_6c	2.04	2880	287	33.9	0.04

[a] Bioavailability. [b] Brain / plasma ratio

Derivatives **4_1d** and **4_6b** were thus selected for evaluation of in vivo efficacy and tested in a Y5 selective agonist-induced food intake model.[27] While derivative **4_6b** (12.5 mg/kg po) blocked the increase in food intake in this feeding model (Figure 4_6), derivative **4_1d** (12.5 mg/kg po) was not efficacious in spite of its desirable PK profile. To determine what led to the difference between **4_1d** and **4_6b**, the cerebrospinal fluid (CSF) concentrations of these compounds were measured. At 30 min after administration of **4_1d** (0.5 mg/kg iv) and **4_6b** (0.5 mg/kg iv), the CSF concentrations were 1.7 ng/ml and 2.9 ng/ml, respectively. This suggested that the CSF concentration has a stronger correlation with in vivo efficacy than the B/P ratio.

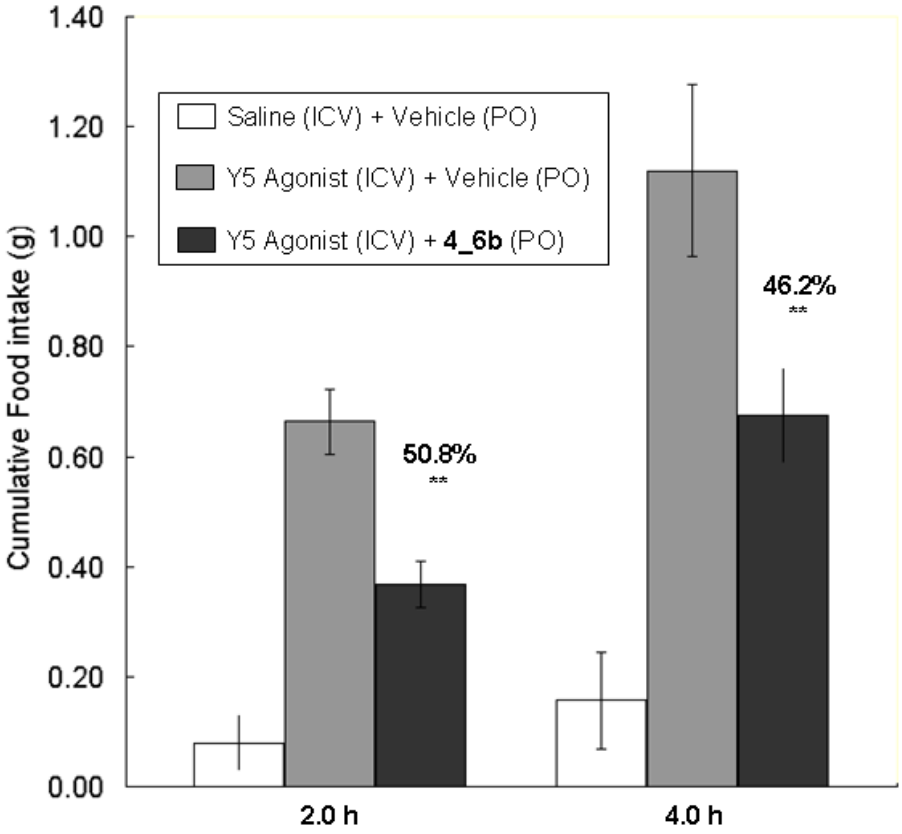

Figure 4_6. Effect of **4_6b** (12.5 mg/kg) on Y5 agonist-stimulated food intake in diet-induced obese mice (n = 4-7). Vehicle is 0.5% hydroxypropylmethyl cellulose solution. **p < 0.01 versus Y5 agonist and vehicle treated group.

In addition to the in vivo efficacy stated above, oral administration of **4_6b** to DIO mice for 21 days caused a dose-dependent reduction that was significantly different from the control group without any abnormal behavior (Figure 4_7).

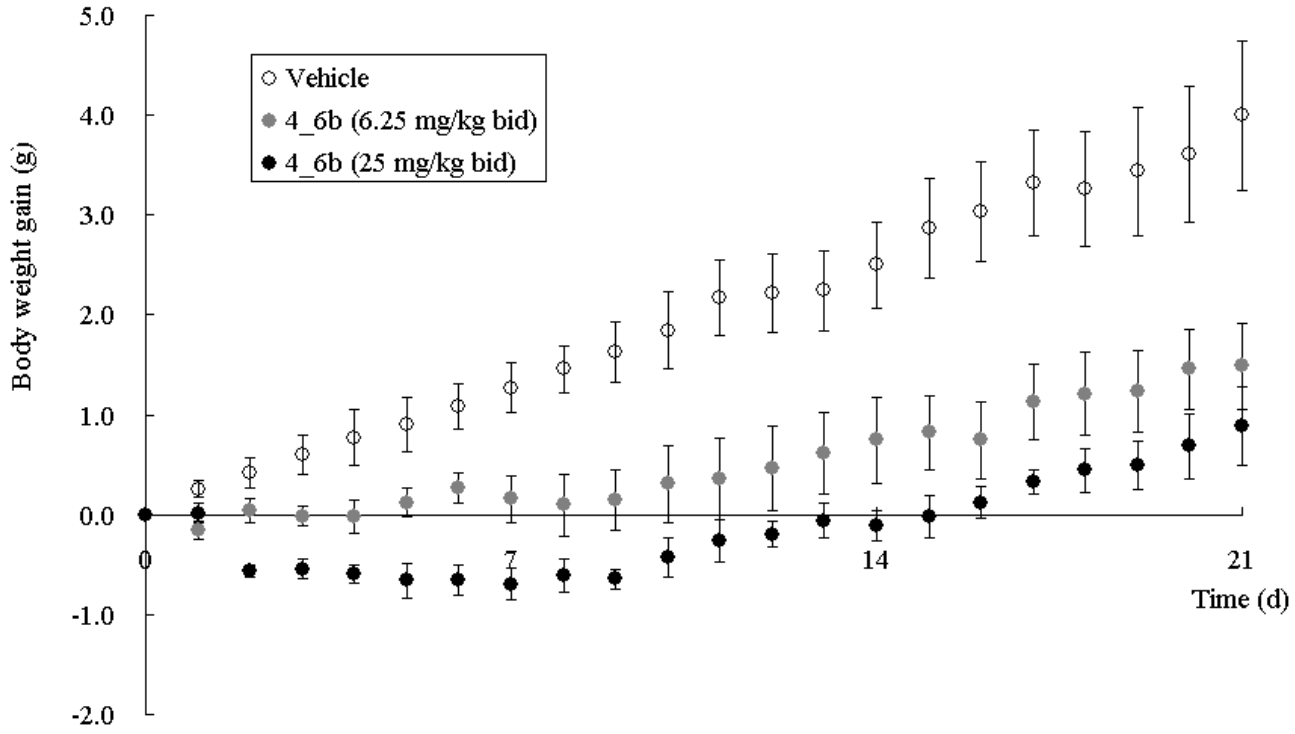

Figure 4_7. Effect of chronic oral administration of **4_6b** on body weight gain in diet-induced obese mice (n = 7).

In summary, a series of novel and potent NPY Y5 receptor antagonists were identified by modification of HTS hit **2_1**. Among them, derivative **4_6b** exhibited an acceptable PK profile and inhibited food intake induced by the NPY Y5 selective agonist, which resulted in reduction of body weight gain in DIO mice.

Chapter 5.

Summary

In this research, the author first selected **2_1** as a HTS hit compound for developing novel NPY Y5 receptor antagonists, extensively conducted SAR study retaining three point pharmacophores (SO_2, acidic N-H, and lipophilic group) of **2_1**, and could identify novel benzimidazole derivatives as highly potent NPY Y5 receptor antagonists with improved in vitro ADME profiles. Among the benzimidazole derivatives, derivative **4_6b** exhibited an acceptable PK profile and inhibited food intake induced by the NPY Y5 selective agonist, which resulted in reduction of body weight gain in DIO mice.

Moreover, through the study described in chapter 2, the author proposed a best fit conformation model for NPY Y5 receptor by considering the presence or absence of hydrogen bonding and the coordination ability of the introduced pyridine linker, which gives a reasonable explanation for the unique relationship between the structure of pyridine linker and the NPY Y5 receptor binding affinity (Chapter 2, Figure 2_6) and should serve as a useful concept for further development of NPY Y5 receptor antagonists.

It was also found that *N*-phenylpyridone and 2-phenylmorpholine could be substituted for a biphenyl moiety with improved CYP450 inhibition profiles, enhanced solubilities, and high metabolic stabilities. Since biphenyl moieties are found in some useful bioactive compounds, this knowledge should be a useful tool for drug discovery research.

Chapter 6.

Synthetic routes to benzimidazole derivatives and experimentals

Synthetic routes to derivatives **2_2a-f** are shown in Scheme 6_1. Intermediate **6_1** was synthesized from commercially available Albendazole, which has a benzimidazole core. Albendazole was first treated with *m*-CPBA to oxidize the *n*-propylthio group and then subjected to hydrolysis of the methyl carbamate group. The resulting amino compound was subjected to the Sandmeyer reaction condition to give 2-bromobenzimidazole **6_1**. Suzuki cross-coupling between bromide **6_1** and boronic acids **6_2** provided derivatives **2_2a-f.**

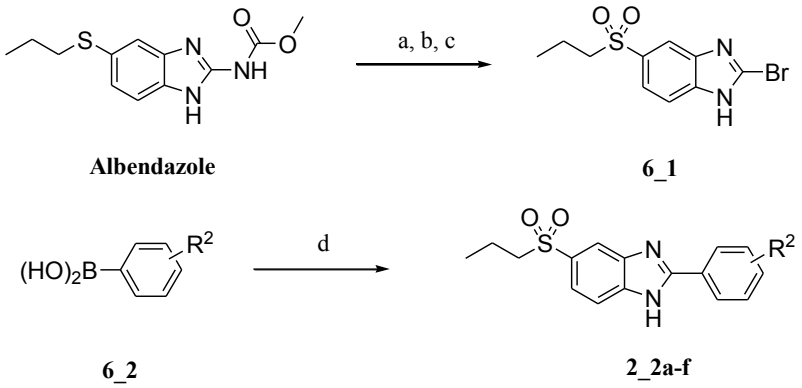

Scheme 6_1. Synthetic routes of analogues **2_2a-f**. Reagents and conditions: (a) *m*-CPBA, CH_2Cl_2, 0 °C to rt; (b) 2 M NaOH aq., 85 °C; (c) conc. HCl, $NaNO_2$, CuBr, 60 °C; (d) **6_1**, $Pd(PPh_3)_4$, Cs_2CO_3, 1,4-dioxane, H_2O, 180 °C (microwave).

Derivatives **2_2g**, **2_4a-i** and **2_5a-d** were synthesized by amidation of carboxylic acids with phenylenediamines and subsequent cyclocondensation to construct the benzimidazole core. Scheme 6_2 shows the preparation of the phenylenediamines. To prepare **6_5**, nucleophilic aromatic substitution of chloride **6_3** with $EtSO_2Na$[30] was carried out,[31] followed by hydrogenation of the nitro group in the presence of Pd/C. Compound **6_6** was reduced using $Na_2S_2O_4$ and the resulting **6_7** was

used for next step without purification. The other phenylenediamines **6_8** and **6_9** were commercially available.

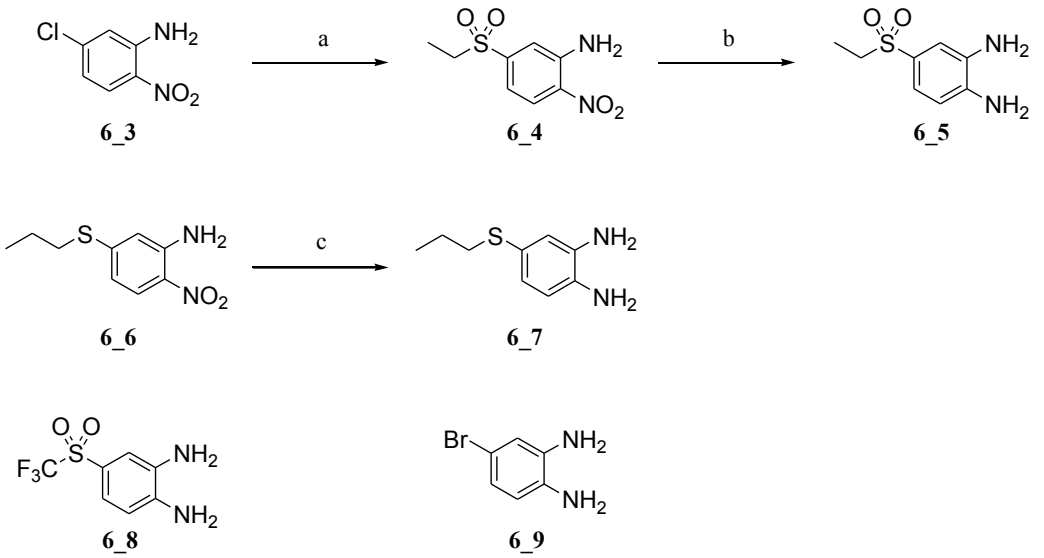

Scheme 6_2. Preparation of phenylenediamines. Reagents and conditions: (a) $EtSO_2Na$, DMSO, 100 °C; (b) Pd/C, H_2, MeOH, rt; (c) $Na_2S_2O_4$, EtOH, H_2O, 60 °C.

The synthesis of derivatives **2_2g** and **2_4a-i** is shown in Scheme 6_3. Carboxylic acids **6_10** were made to react with phenylenediamine **6_5** in the presence of *O*-(7-azabenzotriazole-1-yl)-*N*,*N*,*N*',*N*'-tetramethyluronium hexafluorophospate (HATU) and Et_3N to produce a mixture of regioisomeric amides. The amides were subsequently cyclized in acetic acid to prepare **6_11a-b**. MOM-protection of the resulting benzimidazole N-H followed by phenylation of the halide using Suzuki cross-coupling[32] and removal of the MOM-protection provided **2_4a-b**. The other derivatives were synthesized in a more efficient manner. Carboxylic acids **6_10** was converted in three steps to **2_4c-i** by the sequence: i)

phenylation, ii) amidation and iii) cyclization. Pyridine analogues **2_5a-d** were prepared in a similar manner to the biphenyl derivatives.

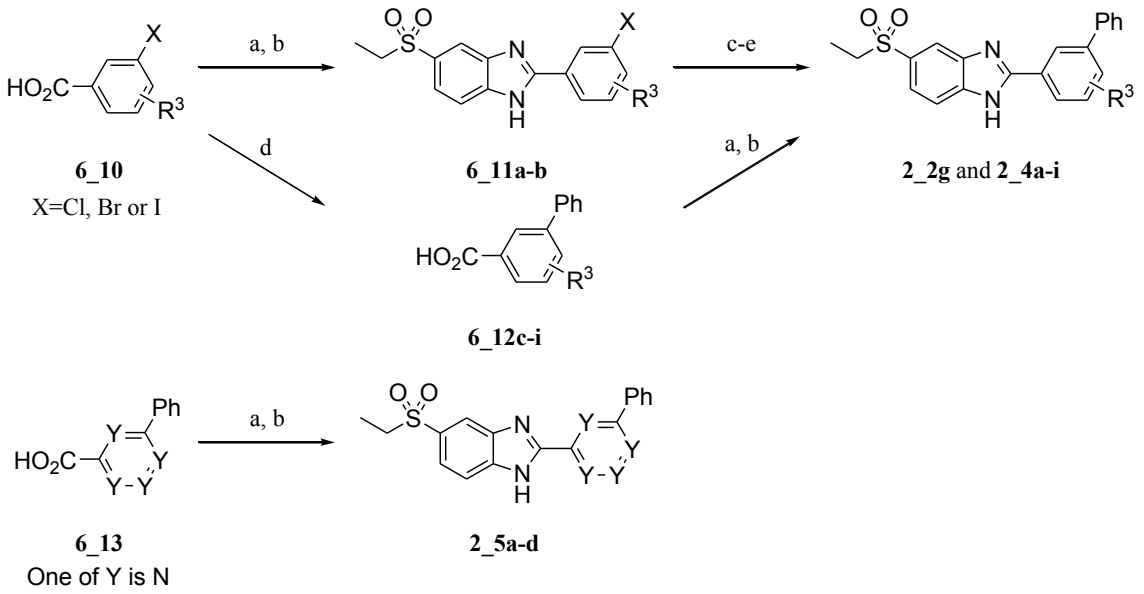

Scheme 6_3. Synthetic routes to analogues **2_2g**, **2_4a-i** and **2_5a-d**. Reagents and conditions: (a) **6_5**, HATU, Et_3N, DMF, 0 °C to rt; (b) AcOH, reflux. (c) MOM-Cl, 60% NaH, DMF, rt; (d) $Pd(dtbpf)Cl_2$, $PhB(OH)_2$, K_2CO_3, DMF or EtOH, H_2O, rt to 60 °C; (e) 2 M HCl in MeOH, 60 °C.

Syntheses of pyridone analogues **2_8a-b** commenced from carboxylic acid **6_14**. Its carboxylic group was protected as methyl ester to provide **6_15**. N-Phenylation of **6_15** by Chan-Lam-Evans coupling reaction[33] was followed by hydrolysis under basic condition to give **6_17**. Carboxylic acid **6_17** was made to react with phenylenediamines in the presence of HATU and Et_3N to produce a mixture of regioisomeric amides, which was subsequently cyclized in acetic acid to construct benzimidazole core. The synthesis of **2_8b** starting from phenylenediamine **6_7** needed another step, the oxidation of *n*-propylthio group at the C-5 position with *m*-CPBA.

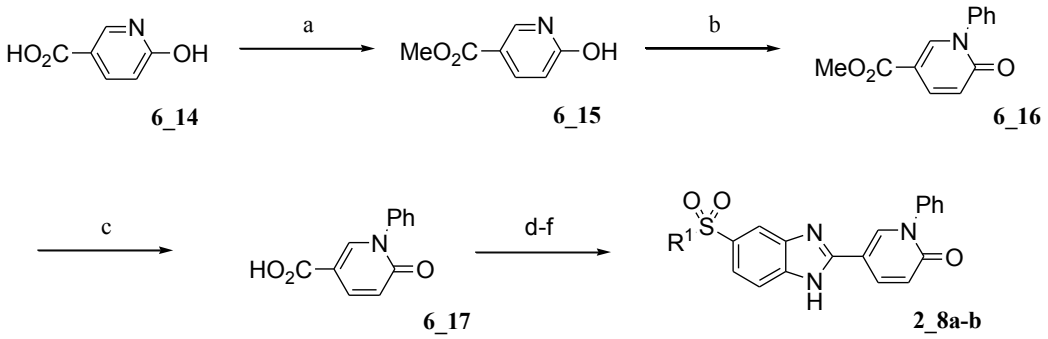

Scheme 6_4. Representative synthetic routes to pyridone analogues **2_8a-b**. Reagents and conditions: (a) 2 M HCl in MeOH, rt to 50 °C; (b) $PhB(OH)_2$, $Cu(OAc)_2$, TEMPO, pyridine, CH_2Cl_2, rt; (c) 2 M NaOH aq., MeOH, rt; (d) **6_5** or **6_7**, HATU, Et_3N, DMF, 0 °C to rt; (e) AcOH, reflux; (f) *m*-CPBA, CH_2Cl_2, rt.

Synthetic routes for derivatives **3_1a-5a** are shown in Scheme 6_5. 2-Bromobenzimidazole **6_1** was coupled with various secondary amines **6_18** to afford derivatives **3_1a-2a** and **3_4a-5a**. For the synthesis of **3_3a**, the benzyloxycarbonyl (Cbz) group was removed by hydrogenation.

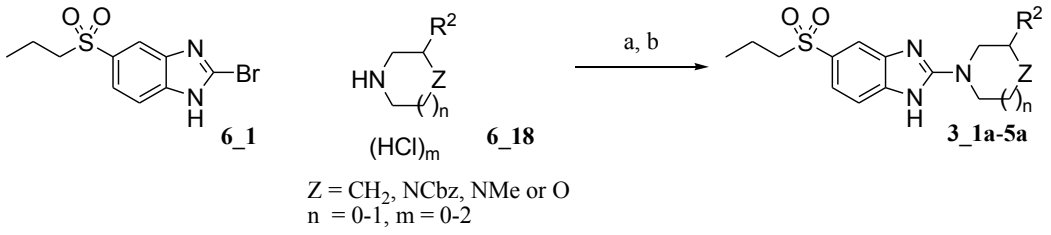

Scheme 6_5. Synthetic routes for compounds **3_1a-5a**. Reagents and conditions: (a) K_2CO_3, CH_3CN, 120 °C (microwave); (b) Z = NCbz : Pd/C, H_2, MeOH, rt.

As shown in Scheme 6_6, the synthesis of **3_6a** commenced from the alcohol **6_19**. The hydroxyl group was mesylated and subsequently substituted with cyanide to prepare **6_20**. The resulting cyano group was hydrolyzed under basic condition to afford **6_21**. Carboxylic acid **6_21** was treated with phenylenediamine **6_7** in the presence of HATU and Et_3N to produce a mixture of regioisomeric amides. The amides were subsequently cyclized in acetic acid to construct the benzimidazole core, followed by oxidation of the *n*-propylthio group with *m*-CPBA to provide **3_6a**.

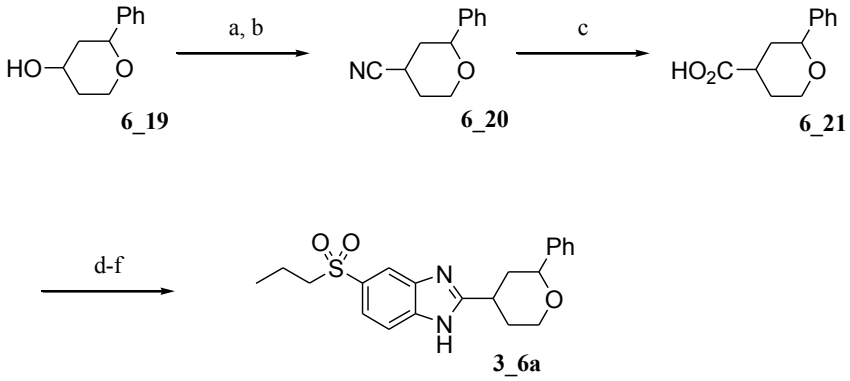

Scheme 6_6. Synthetic route to compound **3_6a**. Reagents and conditions: (a) MsCl, Et_3N, THF, 0 °C; (b) NaCN, Bu_4NCN, DMF, 100 °C; (c) 28% NaOMe in MeOH, 100 °C then H_2O; (d) **6_7**, HATU, Et_3N, DMF, 0 °C to rt; (e) AcOH, reflux; (f) *m*-CPBA, CH_2Cl_2, 0 °C to rt.

To systematically evaluate the SAR of the right hand part and the left hand part of morpholine derivative, a series of morpholine compounds were prepared. Phenylenediamines **6_5** and **6_8** were treated with 1,1'-carbonyldiimidazole (CDI), followed by chlorination in $POCl_3$ to give 2-chlorobenzimidazole **6_22** and **6_23**, respectively, which were subsequently coupled with **6_18** (Z = O) to afford derivatives **3_5b**, **3_5i-l** and **3_5f**. To explore the other R^1 groups, 2-chlorobenzimidazole **6_24** was coupled with **6_18** (Z = O) to give **6_25**. Then various alkylthio (R^1S) groups were

introduced at the C-5 position of **6_25** using a coupling reaction[34] and oxidized to the corresponding alkylsulfonyl (R^1SO_2) groups.

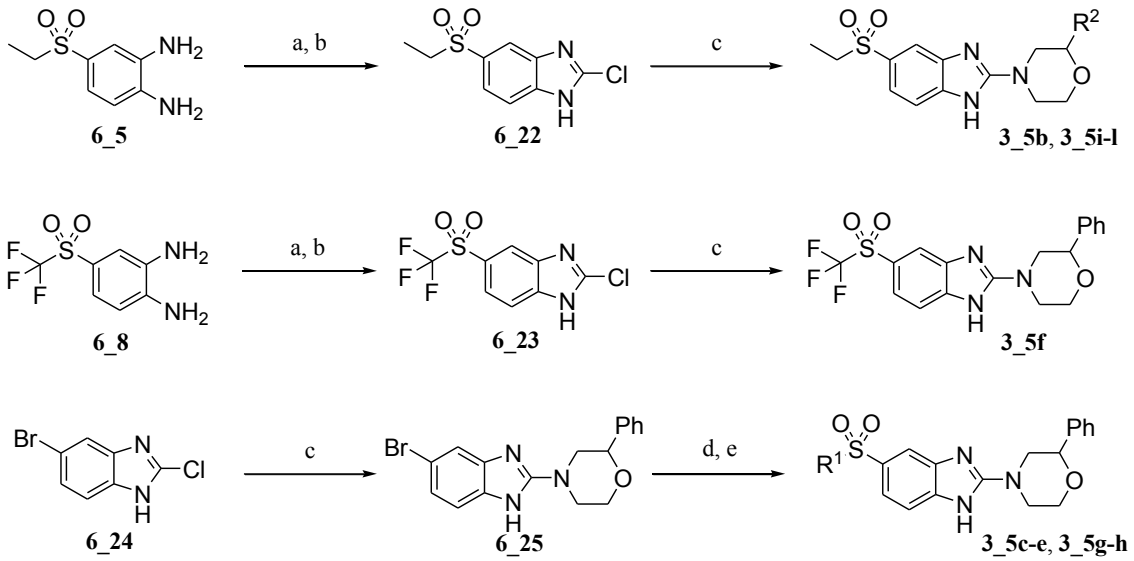

Scheme 6_7. Synthetic routes to compounds **3_5b-l**. Reagents and conditions: (a) CDI, THF, rt; (b) $POCl_3$, 100 °C; (c) **6_18**, *i*-Pr_2NEt, *i*-PrOH, 180 °C (microwave); (d) R^1SH, Hunig's base, $Pd_2(dba)_3$, xantphos, 1,4-dioxane, 130 °C (microwave); (e) *m*-CPBA, CH_2Cl_2, 0 °C to rt.

The syntheses of derivatives **4_1a-d**, **4_2a-f**, **4_6b-c** and **4_7a** bearing a sulfur- or oxygen-linker at the C-2 position are shown in Scheme 6_8. Phenylenediamine **6_5** was treated with 1,1'-thiocarbonyldiimidazole (TCDI), followed by alkylation to give sulfur-linker derivative **4_1a**. On the other hand, 2-chlorobenzimidazole **6_22** was protected with 2-(trimethylsiloxy)ethoxymethyl (SEM) chloride, followed by the coupling with alcohols and removal of the SEM-protection to give oxygen-linker derivatives.

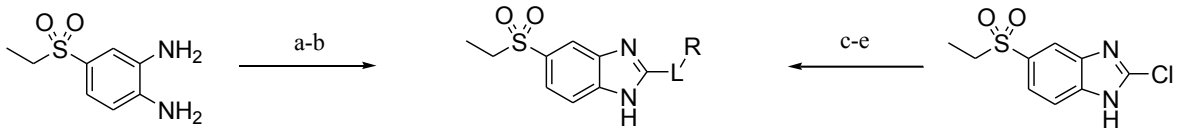

6_5 **4_1a-d**, **4_2a-f**, **4_6b-c**, **4_7a** **6_22**

Scheme 6_8. Syntheses of derivatives **4_1a-d**, **4_2a-f**, **4_6b-c** and **4_7a**. Reagents and conditions: (a) TCDI, DMF, rt; (b) 28% NH_3 aq., 1-(bromomethyl)-3-chlorobenzene, CH_3CN, rt; (c) SEM-Cl, 60% NaH, DMF, rt; (d) R-LH, Cs_2CO_3 or 60% NaH, DMF, 0 to 50 °C; (e) TBAF, THF, 70 °C; or TFA, CH_2Cl_2, rt, then MeOH.

The synthetic routes of derivative **4_3a-5a** are shown in Scheme 6_9. Carboxylic acid **6_26** was made to react with **6_5** in the presence of HATU and Et_3N to produce a mixture of regioisomeric amides. The resulting amides were subsequently cyclized in acetic acid to obtain **4_3a**. The benzyl position of **4_3a** was oxidized with SeO_2[35] to afford **4_4a**, which was deoxofluorinated using bis(2-methoxyethyl) aminosulfur trifluoride (deoxofluor) to give **4_5a**.

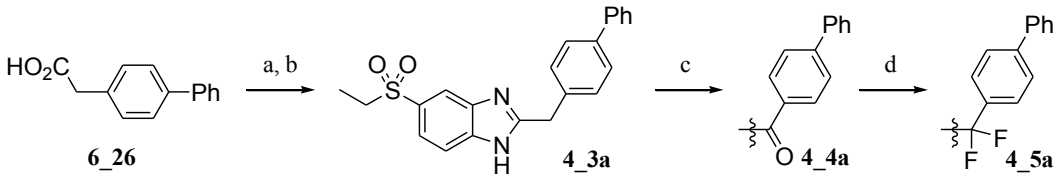

6_26 **4_3a** O **4_4a** **4_5a**

Scheme 6_9. Syntheses of benzimidazole derivatives **4_3a**, **4a** and **5a**.Reagents and conditions: (a) **6_5**, HATU, Et_3N, DMF, 0 °C to rt; (b) AcOH, reflux; (c) SeO_2, 1,4-dioxane, 80 °C; (d) deoxofluor, THF, 60 °C.

Experimentals

General

All reactions were carried out in an oven-dried glassware with magnetic stirring. ^{1}H NMR spectra were measured on a BRUKER ULTRASHIELD 400 PLUS. Tetramethylsilane (TMS) served as the internal standard (0 ppm) for ^{1}H NMR. High resolution mass spectra were mesured on Thermo SCIENTIFIC LTQ Orbitrap. Infrared spectra were measured on a BRUKER vertex 70.

Synthesis of compound **6_1**

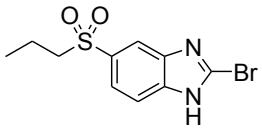

A solution of *m*-CPBA (68%, 2.10 g, 8.29 mmol) in CH_2Cl_2 (15.0 mL) was added to a suspension of Albendazole (1.00 g, 3.77 mmol, Figure 2_3) in CH_2Cl_2 (5.0 mL) and the mixture was stirred at room temperature. After 2 hours, 1.0 M K_2CO_3 aq. (20.0 mL) was added. The resulting precipitates were collected by filtration and washed with water (2 x 2.0 mL) and CH_2Cl_2 (2 x 5.0 mL). The resulting solid was suspended in 2.0 M NaOH aq. (13.2 mL, 26.4 mmol) and stirred at 90 °C. After 3 hours, the reaction mixture was cooled to room temperature, neutralized by conc. HCl and extracted with $CHCl_3$/MeOH=5/1 (5 x 10.0 mL). The organic phase was dried with $MgSO_4$. After removal of the drying agent by filtration, the filtrate was concentrated under reduced pressure. The residue (543 mg) was suspended in water (8.0 mL). After addition of conc. HCl (0.945 mL) and CuBr (976 mg, 6.80 mmol), the mixture was stirred at 60 °C. After 1 hour, reaction mixture was cooled to room temperature, neutralized by NaOH aq. and extracted with $CHCl_3$/MeOH=9/1 (3 x 100 mL). The organic phase was dried with $MgSO_4$. After removal of the drying agent by filtration, the filtrate was

concentrated under reduced pressure. The resulting precipitates were suspended in EtOAc and collected by filtration to give compound **6_1** (289 mg, 25.8%).

Cream solid; ^{1}H NMR (DMSO-d_6): δ = 0.90 (3H, t, J = 7.4 Hz), 1.54 (2H, tq, J = 7.4, 7.4 Hz), 7.62-8.16 (3H, m), 13.87 (1H, br s), two protons are buried in solvent peak; HRESI-MS, calcd for $C_{10}H_{11}BrN_2O_2S$+H m/z 302.9797, found m/z 302.9798 $(M+H)^+$.

Typical procedure for synthesis of compounds **2_2a-f**

Boronic acid **6_2** (0.396 mmol), tetrakis(triphenylpohosphine)palladium (19.1mg, 0.016mmol) and Cs_2CO_3 (161mg, 0.495mmol) were added to a solution of compound **6_1** (100 mg, 0.330 mmol) in 1,4-dioxane (4.0 mL) and water (0.5 mL). The mixture was stirred at 180 ℃ under microwave irradiation. The reaction mixture was concentrated under reduced pressure and the residue was purified by column chromatography on silica gel ($CHCl_3$/MeOH) to give the target compound.

Compound **2_2a**

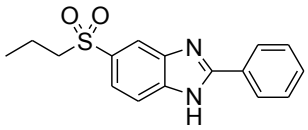

Cream solid, 28.3% yield; ^{1}H NMR (DMSO-d_6): δ = 0.91 (3H, t, J = 7.4 Hz), 1.51-1.64 (2H, m), 7.57-8.23 (8H, m), 13.47 (1H, br s), two protons are buried in solvent peak; HRESI-MS, calcd for $C_{16}H_{16}N_2O_2S$+H m/z 301.1005, found m/z 301.1006 $(M+H)^+$.

Compound **2_2b**

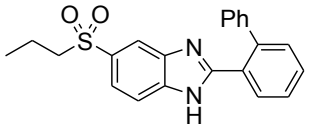

White solid, 15.5% yield; ^{1}H NMR (DMSO-d_6): δ = 0.90 (3H, t, *J* = 7.5 Hz), 1.55 (2H, tq, *J* = 7.5, 7.5 Hz), 3.24-3.30 (2H, m), 7.16-7.31 (5H, m), 7.54-8.08 (7H, m), 12.71 (1H, br s); HRESI-MS, calcd for $C_{22}H_{20}N_2O_2S$+H m/z 377.1318, found m/z 377.1326 $(M+H)^+$.

Compound **2_2c**

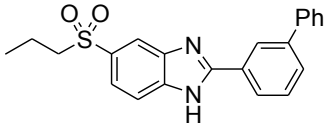

White solid, 55.6% yield; ^{1}H NMR (DMSO-d_6): δ = 0.91 (3H, t, *J* = 7.4 Hz), 1.52-1.64 (2H, m), 7.43-7.48 (1H, m), 7.53-7.58 (2H, m), 7.67-7.76 (2H, m), 7.78-8.27 (6H, m), 8.51 (1H, s), 13.56 (1H, br s), two protons are buried in solvent peak; HRESI-MS, calcd for $C_{22}H_{20}N_2O_2S$+H m/z 377.1318, found m/z 377.1310 $(M+H)^+$.

Compound **2_2d**

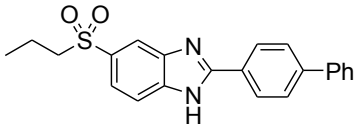

Cream solid, 30.6% yield; ^{1}H NMR (DMSO-d_6): δ = 0.92 (3H, t, *J* = 7.4 Hz), 1.58 (2H, tq, *J* = 7.4, 7.4 Hz), 7.40-7.46 (1H, m), 7.49-7.55 (2H, m), 7.72 (1H, dd, *J* = 8.6, 1.5 Hz), 7.77-8.17 (6H, m), 8.31 (2H, d, *J* = 8.6 Hz), 13.50 (1H, br s), two protons are buried in solvent peak; HRESI-MS, calcd for $C_{22}H_{20}N_2O_2S$+H m/z 377.1318, found m/z 377.1310 $(M+H)^+$.

Compound **2_2e**

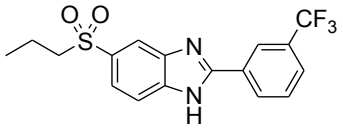

Cream solid, 83.1% yield; ^{1}H NMR (DMSO-d_6): δ = 0.92 (3H, t, J = 7.4 Hz), 1.59 (2H, tq, J = 7.4, 7.4 Hz), 7.76 (1H, dd, J = 8.6, 1.5 Hz), 7.81-8.21 (4H, m), 8.53 (1H, d, J = 8.1 Hz), 8.56 (1H, s), 13.70 (1H, br s), two protons are buried in solvent peak; HRESI-MS, calcd for $C_{17}H_{15}F_3N_2O_2S$+H m/z 369.0879, found m/z 369.0882 $(M+H)^+$.

Compound **2_2f**

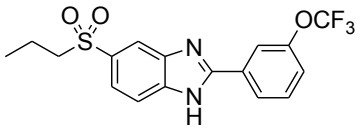

Cream solid, 36.3% yield; ^{1}H NMR (DMSO-d_6): δ = 0.92 (3H, t, J = 7.4 Hz), 1.58 (2H, tq, J = 7.4, 7.4 Hz), 7.58 (1H, d, J = 8.6 Hz), 7.72-8.22 (5H, m), 8.26 (1H, d, J = 7.6 Hz), 13.64 (1H, br s), two protons are buried in solvent peak; HRESI-MS, calcd for $C_{17}H_{15}F_3N_2O_3S$+H m/z 385.0828, found m/z 385.0832 $(M+H)^+$.

Synthesis of compound **6_4**

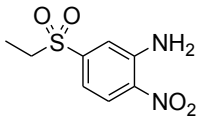

5-Chloro-2-nitroaniline (138 g, 0.800 mol) and $EtSO_2Na$ (279 g, 2.40 mol) were dissolved in DMSO (800 mL) and stirred at 100 °C. After 11 hours, the reaction mixture was cooled to room temperature and poured into a stirred solution of 5.0% NaCl aq. (6.00 L). The resulting precipitates were collected by filtration and washed with water (4.00 L) to give compound **6_4** (177 g, 96.2%).

Yellow solid; ^{1}H NMR (DMSO-d_6): δ = 1.13 (3H, t, J = 7.4 Hz), 3.32 (2H, q, J = 7.4 Hz), 7.00 (1H, dd, J = 8.8, 2.0 Hz), 7.60 (1H, d, J = 2.0 Hz), 7.73 (2H, s), 8.18 (1H, d, J = 8.8 Hz); HRESI-MS, calcd for $C_8H_{10}N_2O_4S$-H m/z 229.0278, found m/z 229.0286 $(M-H)^-$.

Synthesis of compound **6_5**

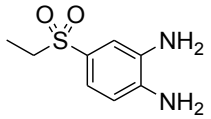

Compound **6_4** (170 g, 738 mmol) was dissolved in MeOH (1.7 L). After addition of Pd/C (17.0 g), the solution was stirred under H_2 atmosphere for 2 hours. After removal of the catalyst, the filtrate was concentrated under reduced pressure. The residue was suspended in (i-Pr)$_2$O (1.5 L) and the resulting precipitates were collected by filtration and washed with (i-Pr)$_2$O (500 mL) to give compound **6_5** (90.4 g, 61.1%)

Brown solid; ^{1}H NMR (DMSO-d_6): δ = 1.05 (3H, t, J = 7.4 Hz), 3.01 (2H, q, J = 7.4 Hz), 4.90 (2H, br s), 5.39 (2H, br s), 6.59 (1H, d, J = 8.1 Hz), 6.86 (1H, dd, J = 8.1, 2.5 Hz), 6.93 (1H, d, J = 2.5 Hz); HRESI-MS, calcd for $C_8H_{12}N_2O_2S$+H m/z 201.0692, found m/z 201.0691 $(M+H)^+$.

Typical procedure for synthesis of compounds **6_11a-b**

Et_3N (0.472 mL) and the corresponding *m*-bromobenzoic acid **6_10** (2.27 mmol) were added to a solution of compound **6_5** (500 mg, 2.50 mmol) in DMF (5.0 mL). After addition of HATU (1.04 g, 2.72 mmol) at 0 °C, the mixture was stirred at room temperature. The reaction mixture was diluted with EtOAc (20 mL) and washed with 2.0 M K_2CO_3 aq. (5.0 mL) and water (3 x 5.0 mL). The organic phase was dried with $MgSO_4$. After removal of the drying agent by filtration, the filtrate was concentrated under reduced pressure. The residue was dissolved in acetic acid (5.0 mL) and refluxed. After

concentration of the reaction mixture under reduced pressure, the residue was neutralized with 2.0 M K_2CO_3 aq. and extracted with $CHCl_3$. After concentration of the organic phase under reduced pressure, the residue was purified by column chromatography on silica gel ($CHCl_3$/MeOH) to give compound **6_11**.

Compound **6_11a**

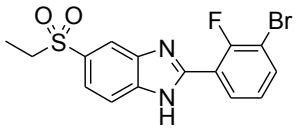

White solid, 76.2% yield; ^{1}H NMR (DMSO-d_6): δ = 1.12 (3H, t, *J* = 7.3 Hz), 7.40 (1H, dd, *J* = 7.8, 7.8 Hz), 7.75 (1H, dd, *J* = 8.4, 1.6 Hz), 7.88 (1H, d, *J* = 8.4 Hz), 7.92-7.96 (1H, m), 8.15-8.18 (1H, m), 8.22-8.26 (1H, m), 13.26 (1H, br s), two protons are buried in solvent peak; HRESI-MS, calcd for $C_{15}H_{12}BrFN_2O_2S$+H m/z 382.9860, found m/z 382.9855 $(M+H)^+$.

Compound **6_11b**

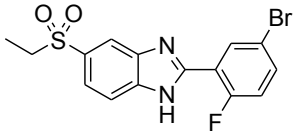

White amorphous, 93.3% yield; ^{1}H NMR (DMSO-d_6): δ = 1.12 (3H, t, *J* = 7.4 Hz), 7.51 (1H, dd, *J* = 10.8, 8.8 Hz), 7.75 (1H, dd, *J* = 8.5, 1.8 Hz), 7.79-7.85 (1H, m), 7.88 (1H, d, *J* = 8.5 Hz), 8.15-8.19 (1H, m), 8.39 (1H, dd, *J* = 6.5, 2.5 Hz), 13.21 (1H, br s), two protons are buried in solvent peak; HRESI-MS, calcd for $C_{15}H_{12}BrFN_2O_2S$+H m/z 382.9860, found m/z 382.9854 $(M+H)^+$.

Typical procedure for synthesis of compounds **2_4a-b**

60% NaH (15.7 mg, 0.391 mmol) was added at 0 °C to a solution of compound **6_11** (0.261 mmol) in DMF (1.0 mL). After addition of MOM-Cl (30 µl, 0.391 mmol) at 0 °C, the mixture was stirred at 0 °C. The reaction mixture was diluted with EtOAc (10 mL) and washed with water (3 x 2.0 mL). The organic phase was dried with $MgSO_4$. After removal of the drying agent by filtration, the filtrate was concentrated under reduced pressure. The residue was dissolved in DMF (1.0 mL) and water (0.1 mL). After addition of phenylboronic acid (38.2 mg, 0.313 mmol), K_2CO_3 (108 mg, 0.783 mmol) and $Pd(dtbpf)Cl_2$ (25.5 mg, 0.039 mmol), the mixture was stirred at room temperature over night. The reaction mixture was diluted with EtOAc (10 mL) and washed with water (3 x 2.0 mL). The organic phase was dried with $MgSO_4$. After removal of the drying agent by filtration, the filtrate was concentrated under reduced pressure. The residue was dissolved in 2.0 M HCl in MeOH (2.0 mL) and stirred at 50 °C. The reaction mixture was neutralized with 2.0 M K_2CO_3 aq. and extracted with $CHCl_3$. After concentration of the organic phase under reduced pressure, the residue was purified by column chromatography on silica gel ($CHCl_3$/MeOH) to give the target compound.

Compound **2_4a**

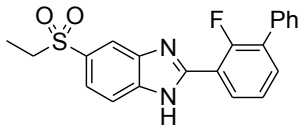

Cream solid, 65.9% yield; ^{1}H NMR (DMSO-d_6): δ = 1.12 (3H, t, *J* = 7.4 Hz), 7.45-7.59 (4H, m), 7.63-7.77 (4H, m), 7.84-7.91 (1H, m), 8.16 (1H, br s), 8.25-8.29 (1H, m), 13.17 (1H, br s) , two protons are buried in solvent peak; HRESI-MS, calcd for $C_{21}H_{17}FN_2O_2S$+H m/z 381.1068, found m/z 381.1070 $(M+H)^+$.

Compound **2_4b**

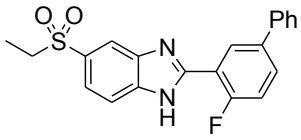

Cream solid, 51.4% yield; ^{1}H NMR (DMSO-d_6): δ = 1.12 (3H, t, *J* = 7.4 Hz), 7.41-7.46 (1H, m), 7.51-7.56 (2H, m), 7.59 (1H, dd, *J* = 10.9, 8.9 Hz), 7.73-7.80 (3H, m), 7.85-7.96 (2H, m), 8.18 (1H, br s), 8.49 (1H, dd, *J* = 7.1, 2.0 Hz), 13.21 (1H, br s), two protons are buried in solvent peak; HRESI-MS, calcd for $C_{21}H_{17}FN_2O_2S$+H m/z 381.1068, found m/z 381.1070 $(M+H)^+$.

Typical procedure for synthesis of compound **6_12c-i**

Compound **6_10** (2.33 mmol) was dissolved in 95% EtOH (5.0 mL). After addition of phenylboronic acid (340 mg, 2.79 mmol), K_2CO_3 (482mg, 3.49 mmol) and Pd(dtbpf)Cl_2 (25.5 mg, 0.039 mmol), the mixture was stirred at 60 °C. After 2 hours, the reaction mixture was concentrated under reduced pressure, and water (15 mL) was added to the residue. After removal of insoluble matter by filtration, the filtrate was neutralized with 2.0 M HCl aq. The resulting precipitates were collected by filtration and washed with water (3 x 5.0 mL) to give compound **6_12**.

Compound **6_12c**

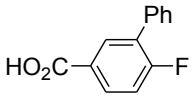

Light brown solid, 97.9% yield; ^{1}H NMR (DMSO-d_6): δ = 7.41-7.61 (6H, m), 7.96-8.07 (2H, m), 13.15 (1H, br s); HRESI-MS, calcd for $C_{13}H_9FO_2$-H m/z 215.0503, found m/z 215.0511 $(M-H)^-$.

Compound **6_12d**

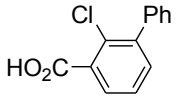

light brown solid, 66.3% yield; ^{1}H NMR (DMSO-d_6): δ = 7.38-7.52 (7H, m), 7.64-7.71 (1H, m), 13.48 (1H, br s); HRESI-MS, calcd for $C_{13}H_9ClO_2$-H m/z 231.0207, found m/z 231.0216 $(M-H)^-$.

Compound **6_12e**

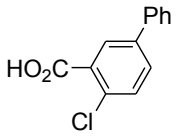

White solid, 46.8% yield; ^{1}H NMR (DMSO-d_6): δ = 7.39-7.45 (1H, m), 7.46-7.53 (2H, m), 7.63 (1H, d, J = 8.3 Hz), 7.68-7.73 (2H, m), 7.83 (1H, dd, J = 8.3, 2.5 Hz), 8.02 (1H, d, J = 2.5 Hz), 13.52 (1H, br s); HRESI-MS, calcd for $C_{13}H_9ClO_2$-H m/z 231.0207, found m/z 231.0217 $(M-H)^-$.

Compound **6_12f**

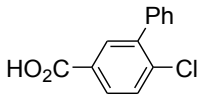

White solid, 48.9% yield; ^{1}H NMR (DMSO-d_6): δ = 7.42-7.53 (5H, m), 7.71 (1H, d, J = 8.3 Hz),7.88 (1H, d, J = 2.0 Hz), 7.93 (1H, dd, J = 8.3, 2.0 Hz), 13.28 (1H, br s). HRESI-MS, calcd for $C_{13}H_9ClO_2$-H m/z 231.0207, found m/z 231.0216 $(M-H)^-$.

Compound **6_12g**

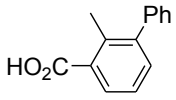

Light brown solid, 79.2% yield; ^{1}H NMR (DMSO-d_6): δ = 2.33 (3H, s), 7.28-7.49 (7H, m), 7.70-7.76 (1H, m), 12.93 (1H, br s); HRESI-MS, calcd for $C_{14}H_{12}O_2$-H m/z 211.0754, found m/z 211.0761 $(M-H)^-$.

Compound **6_12h**

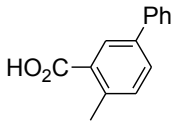

Cream solid, 66.6% yield; ^{1}H NMR (DMSO-d_6): δ = 2.54 (3H, s), 7.35-7.40 (2H, m), 7.45-7.50 (2H, m), 7.64-7.68 (2H, m), 7.72 (1H, dd, *J* = 7.9, 2.1 Hz), 8.04 (1H, d, *J* = 2.1 Hz), one proton is buried in solvent peak; HRESI-MS, calcd for $C_{14}H_{12}O_2$-H m/z 211.0754, found m/z 211.0758 $(M-H)^-$.

Compound **6_12i**

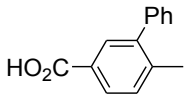

White solid, 75.2% yield; ^{1}H NMR (DMSO-d_6): δ = 2.29 (3H, s), 7.36-7.49 (6H, m), 7.74 (1H, d, *J* = 1.8 Hz), 7.84 (1H, dd, *J* = 7.9, 1.8 Hz), 12.89 (1H, br s); HRESI-MS, calcd for $C_{14}H_{12}O_2$-H m/z 211.0754, found m/z 211.0760 $(M-H)^-$.

Synthesis of compound **6_15**

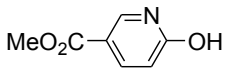

6-hydroxynicotinic acid (5.00 g, 35.9 mmol) was dissolved in 2.0 M HCl in MeOH (50 mL) and stirred at 50 °C. After concentration of the reaction mixture under reduced pressure, the residue was suspended in water (50 mL), neutralized with sat. $NaHCO_3$ aq. and extracted with $CHCl_3$. The organic

phase was dried with $MgSO_4$. After removal of the drying agent by filtration, the filtrate was concentrated under reduced pressure to give compound **6_15** (4.31g, 78.3%).

White solid; ^{1}H NMR (DMSO-d_6): δ = 3.77 (3H, s), 6.37 (1H, d, J = 9.6 Hz), 7.80 (1H, dd, J = 9.6, 2.5 Hz), 8.04 (1H, d, J = 2.5 Hz), 12.02 (1H, brs); HRESI-MS, calcd for $C_7H_7NO_3$+H m/z 154.0499, found m/z 154.0496 $(M+H)^+$.

Synthesis of compound **6_16**

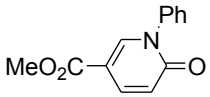

Compound **6_15** (3.94 g, 25.7 mmol) was suspended in CH_2Cl_2 (78 mL). After addition of pyridine (8.31 mL, 103 mmol), phenylboronic acid (6.27 g, 51.5 mmol), and TEMPO (4.42 g, 28.3 mmol), the mixture was stirred at room temperature under nitrogen atmosphere over night. The reaction mixture was diluted with $CHCl_3$ (100 mL) and washed with 2.0 M HCl aq. The organic phase was concentrated under reduced pressure. The residue was purified by column chromatography on silica gel ($CHCl_3$/MeOH) to give compound **6_16** (5.76 g, 97.7%).

Cream solid; ^{1}H NMR (DMSO-d_6): δ = 3.76 (3H, s), 6.56 (1H, d, J = 9.6 Hz), 7.45-7.57 (5H, m), 7.89 (1H, dd, J = 9.6, 2.5 Hz), 8.25 (1H, d, J = 2.5 Hz); HRESI-MS, calcd for $C_{13}H_{11}NO_3$+H m/z 230.0812, found m/z 230.0810 $(M+H)^+$.

Synthesis of compound **6_17**

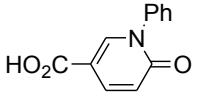

Compound **6_16** (3.00 g, 13.1 mmol) was dissolved in MeOH (15 mL). After addition of 2.0 M NaOH aq. (7.85 mL, 15.7 mmol), the mixture was stirred at room temperature. The reaction mixture was

neutralized with 2.0 M HCl aq. and concentrated under reduced pressure. The resulting precipitates were collected by filtration to give compound **6_17** (2.22 g, 78.8%).

White solid; ^{1}H NMR (DMSO-d_6): δ = 6.54 (1H, d, *J* = 9.5 Hz), 7.46-7.56 (5H, m), 7.87 (1H, dd, *J* = 9.5, 2.5 Hz), 8.17 (1H, d, *J* = 2.5 Hz), 12.92 (1H, br s); HRESI-MS, calcd for $C_{12}H_9NO_3$+H m/z 216.0655, found m/z 216.0654 $(M+H)^+$.

Typical procedure for synthesis of compounds **2_2g**, **2_4c-i**, **2_5a-d**, and **2_8a-b**

Compound **6_5** (120 mg, 0.599 mmol) was dissolved in DMF (1.0 mL). After addition of Et_3N (0.104 mL), the corresponding carboxylic acid (0.499 mmol) and HATU (228 mg, 0.599 mmol), the mixture was stirred at 40 °C. The reaction mixture was diluted with EtOAc (10 mL) and washed with water (3 x 2.0 mL). The organic phase was dried with $MgSO_4$. After removal of the drying agent by filtration, the filtrate was concentrated under reduced pressure. The residue was dissolved in acetic acid (5.0 mL) and refluxed. After concentration of the reaction mixture under reduced pressure, the residue was neutralized with 1.0 M K_2CO_3 aq. and extracted with $CHCl_3$. After concentration of the organic phase under reduced pressure, the residue was purified to give the target compound.

Compound **2_2g**

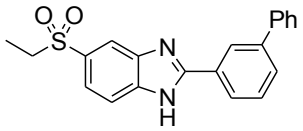

Light pink amorphous, 52.3% yield; ^{1}H-NMR (DMSO-d_6): δ = 1.12 (3H, t, J = 7.2 Hz), 7.45 (1H, t, J = 7.3 Hz), 7.52-7.59 (2H, m), 7.67-7.75 (2H, m), 7.78-7.90 (4H, m), 8.12 (1H, s), 8.23 (1H, d, J = 7.8 Hz),

8.52 (1H, s), 13.61 (1H, br s), two protons are buried in solvent peak; HRESI-MS, calcd for $C_{21}H_{18}N_2O_2S$+H m/z 363.1162, found m/z 363.1153 $(M+H)^+$.

Compound **2_4c**

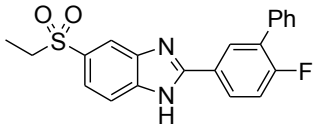

Cream amorphous, 28.7% yield; ^{1}H NMR (DMSO-d_6): δ = 1.12 (3H, t, *J* = 7.4 Hz), 7.46-7.52 (1H, m), 7.54-7.60 (3H, m), 7.66-7.74 (3H, m), 7.84 (1H, d, *J* = 8.1 Hz), 8.10 (1H, br s), 8.25-8.30 (1H, m), 8.38 (1H, dd, *J* = 7.6, 2.5 Hz), 13.52 (1H, br s) , two protons are buried in solvent peak; HRESI-MS, calcd for $C_{21}H_{17}FN_2O_2S$+H m/z 381.1068, found m/z 381.1068 $(M+H)^+$.

Compound **2_4d**

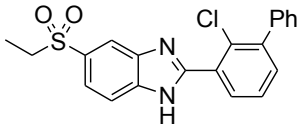

White amorphous, 57.0% yield; ^{1}H NMR (DMSO-d_6): δ = 1.12 (3H, t, *J* = 7.4 Hz), 7.43-7.55 (5H, m), 7.58-7.65 (2H, m), 7.74 (1H, dd, *J* = 8.4, 1.8 Hz), 7.83-7.89 (2H, m), 8.15 (1H, br s), 13.34 (1H, br s), two protons are buried in solvent peak; HRESI-MS, calcd for $C_{21}H_{17}ClN_2O_2S$+H m/z 397.0772, found m/z 397.0775 $(M+H)^+$.

Compound **2_4e**

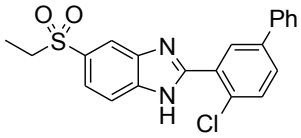

White solid, 68.4% yield; ^{1}H NMR (DMSO-d_6): δ = 1.12 (3H, t, *J* = 7.4 Hz), 7.41-7.47 (1H, m), 7.50-7.55 (2H, m), 7.74-7.81 (4H, m), 7.85-7.93 (2H, m), 8.14-8.22 (2H, m), 13.36 (1H, br s), two protons are buried in solvent peak; HRESI-MS, calcd for $C_{21}H_{17}ClN_2O_2S$+H m/z 397.0772, found m/z 397.0773 $(M+H)^+$.

Compound **2_4f**

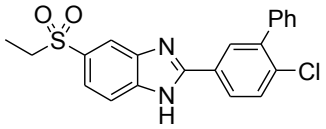

White amorphous, 78.8% yield; ^{1}H NMR (DMSO-d_6): δ = 1.11 (3H, t, *J* = 7.4 Hz), 7.47-7.57 (5H, m), 7.72 (1H, dd, *J* = 8.4, 1.8 Hz), 7.79-7.85 (2H, m), 8.10 (1H, s), 8.22-8.27 (2H, m), 13.56 (1H, br s), two protons are buried in solvent peak; HRESI-MS, calcd for $C_{21}H_{17}ClN_2O_2S$+H m/z 397.0772, found m/z 397.0771 $(M+H)^+$.

Compound **2_4g**

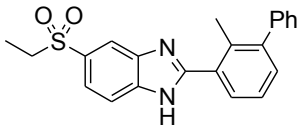

White amorphous, 27.5% yield; ^{1}H NMR (DMSO-d_6): δ = 1.12 (3H, t, *J* = 7.4 Hz), 2.38 (3H, s), 7.33-7.53 (7H, m), 7.69-7.88 (3H, m), 8.12 (1H, br s), 13.26 (1H, br s), two protons are buried in solvent peak; HRESI-MS, calcd for $C_{22}H_{20}N_2O_2S$+H m/z 377.1318, found m/z 377.1315 $(M+H)^+$.

Compound **2_4h**

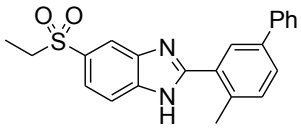

White amorphous, 58.8% yield; ^{1}H NMR (DMSO-d_6): δ = 1.13 (3H, t, *J* = 7.4 Hz), 2.69 (3H, s), 7.38-7.43 (1H, m), 7.48-7.55 (3H, m), 7.70-7.84 (5H, m), 8.00-8.25 (2H, m), 13.31 (1H, br s), two protons are buried in solvent peak; HRESI-MS, calcd for $C_{22}H_{20}N_2O_2S$+H m/z 377.1318, found m/z 377.1321 $(M+H)^+$.

Compound **2_4i**

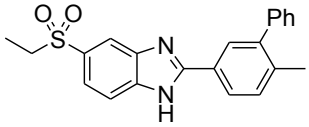

White amorphous, 73.1% yield; ^{1}H NMR (DMSO-d_6): δ = 1.11 (3H, t, *J* = 7.1 Hz), 2.33 (3H, s), 7.41-7.48 (3H, m), 7.49-7.56 (3H, m), 7.70 (1H, dd, *J* = 8.4, 1.8 Hz), 7.73-7.84 (1H, m), 8.00-8.11 (2H, m), 8.14 (1H, dd, *J* = 7.9, 1.8 Hz), 13.42 (1H, br s), two protons are buried in solvent peak; HRESI-MS, calcd for $C_{22}H_{20}N_2O_2S$+H m/z 377.1318, found m/z 377.1316 $(M+H)^+$.

Compound **2_5a**

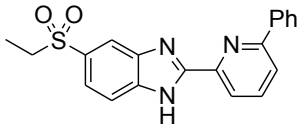

Light orange solid, 68.8% yield; ^{1}H-NMR ($CDCl_3$): δ = 1.31 (3H, t, *J* = 7.4 Hz), 3.15-3.23 (2H, m), 7.49-8.45 (11H, m), 10.71-10.84 (1H, br, overlap of NH peaks of two tautomeric forms); HRESI-MS, calcd for $C_{20}H_{17}N_3O_2S$+H m/z 364.1114, found m/z 364.1106 $(M+H)^+$.

Compound **2_5b**

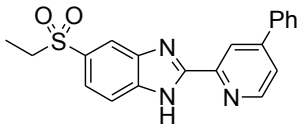

White solid, 93.4% yield; ^{1}H NMR (DMSO-d_6): δ = 1.13 (3H, t, *J* = 7.3 Hz), 7.52-7.65 (3H, m), 7.71-8.25 (6H, m), 8.64 (1H, d, *J* = 1.2 Hz), 8.85 (1H, d, *J* = 5.2 Hz), 13.74 (1H, br s), two protons are buried in solvent peak; HRESI-MS, calcd for $C_{20}H_{17}N_3O_2S$+H m/z 364.1114, found m/z 364.1108 $(M+H)^+$.

Compound **2_5c**

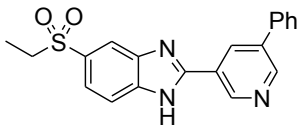

Cream amorphous, 72.1% yield; ^{1}H NMR (DMSO-d_6): δ = 1.13 (3H, t, *J* = 7.4 Hz), 7.48-7.53 (1H, m), 7.57-7.62 (2H, m), 7.76 (1H, dd, *J* = 8.4, 1.8 Hz), 7.86-7.93 (3H, m), 8.16 (1H, s), 8.82 (1H, dd, *J* = 2.0, 2.0 Hz), 9.07 (1H, d, *J* = 2.0 Hz), 9.38 (1H, d, *J* = 2.0 Hz), 13.73 (1H, br s), two protons are buried in solvent peak; HRESI-MS, calcd for $C_{20}H_{17}N_3O_2S$+H m/z 364.1114, found m/z 364.1107 $(M+H)^+$.

Compound **2_5d**

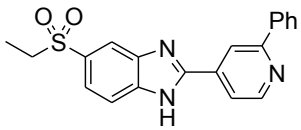

White solid, 42.8% yield; ^{1}H-NMR ($CDCl_3$): δ = 1.32 (3H, t, *J* = 7.4 Hz), 3.17-3.28 (2H, m), 7.44-8.50 (10H, m), 8.82-8.89 (1H, m), 10.74-11.32 (1H, br, overlap of NH peaks of two tautomeric forms); HRESI-MS, calcd for $C_{20}H_{17}N_3O_2S$+H m/z 364.1114, found m/z 364.1107 $(M+H)^+$.

Compound **2_8a**

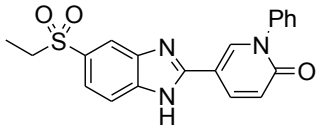

Cream solid, 41.3% yield; ^{1}H NMR (DMSO-d_6): δ = 1.10 (3H, t, *J* = 7.3 Hz), 6.71 (1H, d, *J* = 9.5 Hz), 7.50-7.63 (5H, m), 7.66 (1H, d, *J* = 8.4 Hz), 7.75 (1H, d, *J* = 8.4 Hz), 8.02 (1H, s), 8.30 (1H, d, *J* = 9.5 Hz), 8.57 (1H, s), 13.23 (1H, br s) , two protons are buried in solvent peak; HRESI-MS, calcd for $C_{20}H_{17}N_3O_3S$+H m/z 380.1063, found m/z 380.1060 $(M+H)^+$.

Compound **2_8b**

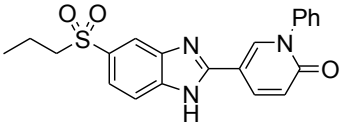

Cream solid, 19.1% yield; ^{1}H NMR (DMSO-d_6 and conc. DCl): δ = 0.91 (3H, t, *J* = 7.4 Hz), 1.52-1.63 (2H, m), 3.31-3.38 (2H, m), 6.79 (1H, d, *J* = 9.6 Hz), 7.52-7.63 (5H, m), 7.84 (1H, dd, *J* = 8.6, 1.5 Hz), 7.90 (1H, d, *J* = 8.6 Hz), 8.12 (1H, d, *J* = 1.5 Hz), 8.39 (1H, dd, *J* = 9.6, 2.5 Hz), 8.89 (1H, d, *J* = 2.5 Hz), one proton is buried in solvent peak; HRESI-MS, calcd for $C_{21}H_{19}N_3O_3S$+H m/z 394.1220, found m/z 394.1217 $(M+H)^+$.

Typical procedure for synthesis of compounds **3_1a**, **3_2a**, **3_3a**, **3_4a**, and **3_5a**,

Compound **6_1** (150 mg, 0.495 mmol) was dissolved in acetonitrile (4.0 mL). After addition of compound **6_18** (0.472 mmol) and K_2CO_3 (274 mg, 1.98 mmol), the mixture was stirred at 120 °C under micromave irradiation. After concentration of the reaction mixture under reduced pressure, the residue was purified by column chromatography on silica gel ($CHCl_3$/MeOH) to give the target compound.

Compound **3_1a**

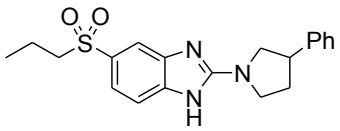

White solid, 38.3% yield; ^{1}H NMR (DMSO-d_6): δ = 0.89 (3H, t, *J* = 7.6 Hz), 1.47-1.60 (2H, m), 2.07-2.19 (1H, m), 2.36-2.46 (1H, m), 3.14-3.20 (2H, m), 3.45-3.65 (3H, m), 3.72-3.79 (1H, m), 3.95-4.03 (1H, m), 7.22-7.63 (8H, m), 11.58-11.82 (1H, br, overlap of NH peaks of two tautomeric forms); HRESI-MS, calcd for $C_{20}H_{23}N_3O_2S$+H m/z 370.1584, found m/z 370.1575 $(M+H)^+$.

Compound **3_2a**

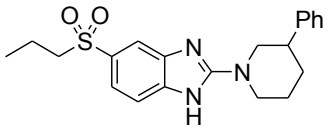

White solid, 90.9% yield; ^{1}H NMR (DMSO-d_6): δ = 0.89 (3H, t, *J* = 7.6 Hz), 1.53 (2H, tq, *J* = 7.6, 7.6 Hz), 1.63-1.88 (2H, m), 1.93-2.00 (1H, m), 2.76-2.86 (1H, m), 3.04-3.20 (4H, m), 4.16-4.28 (2H, m), 7.22-7.62 (8H, m), 11.68-11.92 (1H, br, overlap of NH peaks of two tautomeric forms); one proton is buried in solvent peak; HRESI-MS, calcd for $C_{21}H_{25}N_3O_2S$+H m/z 384.1740, found m/z 384.1729 $(M+H)^+$.

Compound **3_3a**

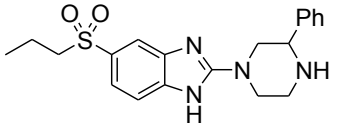

Cream amorphous, 45.1% yield; ^{1}H NMR (DMSO-d_6): δ = 0.85-0.91 (3H, m),1.46-1.58 (2H, m), 2.82-2.95 (2H, m), 3.04-3.21 (4H, m), 3.77-3.83 (1H, m), 4.03-4.13 (2H, m), 7.29-7.62 (8H, m), 11.78-11.90

(1H, br, overlap of NH peaks of two tautomeric forms), one proton is buried in solvent peak; HRESI-MS, calcd for $C_{20}H_{24}N_4O_2S$+H m/z 385.1693, found m/z 385.1692 $(M+H)^+$.

Compound **3_4a**

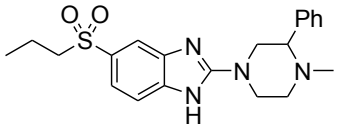

Cream amorphous, 48.5% yield; ^{1}H NMR (DMSO-d_6): δ = 0.85-0.91 (3H, m), 1.46-1.57 (2H, m), 1.99 (3H, s), 2.27-2.37 (1H, m), 2.96-3.12 (3H, m), 3.14-3.20 (2H, m), 3.93-4.01 (1H, m), 4.13-4.22 (1H, m), 7.31-7.63 (8H, m), 11.82-11.94 (1H, br, overlap of NH peaks of two tautomeric forms), one proton is buried in solvent peak; HRESI-MS, calcd for $C_{21}H_{26}N_4O_2S$+H m/z 399.1849, found m/z 399.1849 $(M+H)^+$.

Compound **3_5a**

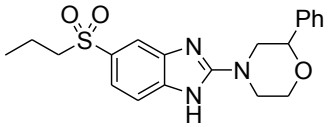

White solid, 54.5% yield; ^{1}H NMR (DMSO-d_6): δ = 0.83-0.92 (3H, m), 1.46-1.59 (2H, m), 2.99-3.10 (1H, m), 3.15-3.22 (2H, m), 3.22-3.28(1H, m), 3.76-3.84 (1H, m), 4.01-4.19 (3H, m), 4.61-4.67 (1H, m), 7.33-7.66 (8H, m), 11.90-12.01 (1H, br, overlap of NH peaks of two tautomeric forms); HRESI-MS, calcd for $C_{20}H_{23}N_3O_3S$+H m/z 386.1533, found m/z 386.1533 $(M+H)^+$.

Synthesis of compound **6_20**

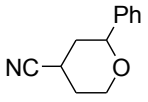

2-Phenyltetrahydro-2*H*-pyran-4-ol (260 mg, 1.46 mmol) was dissolved in THF (4.0 mL) and cooled to 0 °C. After addition of Et_3N (0.243 mL, 1.75 mmol) and MsCl (0.136 mL, 1.75 mmol), the mixture was stirred at 0 °C for 1 hour. The reaction mixture was quenched with water (2.0 mL) and extracted with EtOAc (20 mL). The organic phase was dried with $MgSO_4$. After removal of the drying agent by filtration, the filtrate was concentrated under reduced pressure. The residue was dissolved in DMF (3.5 mL). After addition of NaCN (107 mg, 2.19 mmol) and Bu_4NCN (618 mg, 2.19 mmol), the mixture was stirred at 100 °C. The reaction mixture was diluted with EtOAc (20 mL) and washed with water (4 x 10 mL). The organic phase was dried with $MgSO_4$. After removal of the drying agent by filtration, the filtrate was concentrated under reduced pressure. The residue was purified by column chromatography on silica gel (*n*-hexane/EtOAc) to give compound **6_20** (173 mg, 63.4%).
White solid; ^{1}H NMR ($CDCl_3$): δ = 1.84-1.92 (2H, m), 1.96-2.11 (2H, m), 3.20-3.25 (1H, m), 3.99 (1H, ddd, *J* = 12.3, 12.3, 2.4 Hz), 4.12-4.18 (1H, m), 4.71 (1H, dd, *J* = 11.2, 2.0 Hz), 7.28-7.38 (5H, m); HRESI-MS, calcd for $C_{12}H_{13}NO$+H m/z 188.1070, found m/z 188.1068 $(M+H)^+$.

Synthesis of compound **6_21**

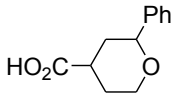

28% NaOMe in MeOH (2.00 g) was added to compound **6_20** (465 mg, 2.48 mmol) and the mixture was stirred at 100 °C. After 2 hours, 28% NaOMe in MeOH (1.0 mL) was added and the mixture was further stirred at 100 °C for 3 hours. The reaction mixture was quenched with water (1.5 mL) and cooled to 0 °C. The solution was neutralized with conc. HCl and extracted with $CHCl_3$. The organic phase was dried with $MgSO_4$. After removal of the drying agent by filtration, the filtrate was concentrated under reduced pressure to give compound **6_21** (515 mg, quant.).

Cream solid; ^{1}H-NMR (DMSO-d_6): δ = 1.43 (1H, dd, J = 24.5, 12.2 Hz), 1.58 (1H, ddd, J = 25.4, 12.6, 4.6 Hz), 1.78-1.85 (1H, m), 1.98-2.06 (1H, m), 2.62-2.72 (1H, m), 3.51-3.59 (1H, m), 4.03-4.11 (1H, m), 4.35 (1H, dd, J = 11.3, 2.3 Hz), 7.23-7.36 (5H, m), 12.28 (1H, br s); HRESI-MS, calcd for $C_{12}H_{14}O_3$-H m/z 205.0859, found m/z 205.0864 $(M-H)^-$.

Compound **3_6a**

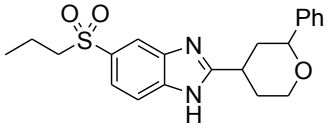

Cream solid, 32.4% yield; ^{1}H NMR (DMSO-d_6): δ = 0.88 (3H, t, *J* = 7.4 Hz), 1.53 (2H, tq, *J* = 7.4, 7.4 Hz),1.76-1.95 (2H, m), 2.03-2.11 (1H, m), 2.24-2.32 (1H, m), 3.70-3.79 (1H, m), 4.16-4.23 (1H, m), 4.55 (1H, d, *J* = 11.0 Hz), 7.26-7.98 (8H, m), 12.84 (1H, br s), three protons are buried in solvent peak; HRESI-MS, calcd for $C_{21}H_{24}N_2O_3S$+H m/z 385.1580, found m/z 385.1579 $(M+H)^+$.

Typical procedure for synthesis of compounds **6_22** and **6_23**

Compound **6_5** or **6_8** (50.4 mmol) was dissolved in DMF (100 mL). After addition of CDI (9.81 g, 60.5 mmol) at 0 °C, the solution was stirred at room temperature. After 2 hours, water (200 mL) was added to the reaction mixture. The resulting precipitates were collected by filtration and suspended in $POCl_3$ (62.1 mL). The suspension was stirred at 120 °C for 7 hours and cooled to room temperature. The reaction mixture was quenched with iced water, neutralized with NaOH aq. and extracted with $CHCl_3$. The organic phase was dried with $MgSO_4$. After removal of the drying agent by filtration, the filtrate was concentrated under reduced pressure. The residue was suspended in EtOAc and IPE. The resulting precipitates were collected by filtration to give 2-chlorobenzimidazole.

Compound **6_22**

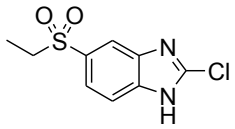

White powder, 28.3% yield; ^{1}H NMR (DMSO-d_6): δ = 1.09 (3H, t, *J* = 7.4 Hz), 3.31 (2H, q, *J* = 7.4 Hz), 7.71-7.78 (2H, m), 8.03 (1H, s), 13.91 (1H, br s); HRESI-MS, calcd for $C_9H_9ClN_2O_2S$+H m/z 245.0146, found m/z 245.0145 $(M+H)^+$.

Compound **6_23**

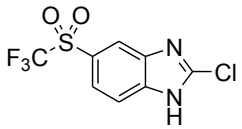

Cream solid, 68.7% yield; ^{1}H NMR (DMSO-d_6): δ = 7.88-7.91 (2H, m), 8.27 (1H, s), one proton is buried in solvent peak; HRESI-MS, calcd for $C_8H_4ClF_3N_2O_2S$+H m/z 284.9707, found m/z 284.9706 $(M+H)^+$.

Compound **3_5b**

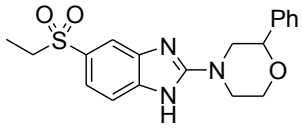

White solid, 56.6% yield; ^{1}H NMR ($CDCl_3$): δ = 1.24 (3H, t, J = 7.4 Hz), 3.08-3.18 (3H, m), 3.31-3.41 (1H, m), 3.84-3.94 (1H, m), 3.95-4.09 (1H, m), 4.13-4.26 (2H, m), 4.62 (1H, dd, J = 10.6, 2.0 Hz), 7.30-7.58 (7H, m), 7.79 (1H, br s), 9.98 (1H, br s); HRESI-MS, calcd for $C_{19}H_{21}N_3O_3S$+H m/z 372.1376, found m/z 372.1381 $(M+H)^+$.

Compound **3_5i**

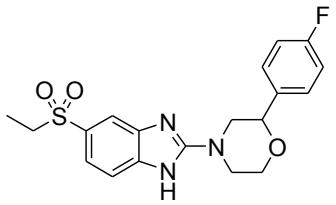

White solid, 36.6% yield; ^{1}H NMR ($CDCl_3$): δ = 1.26 (3H, t, *J* = 7.4 Hz), 3.08-3.17 (3H, m), 3.33-3.42 (1H, m), 3.86-3.94 (1H, m), 3.95-4.25 (3H, m), 4.62 (1H, dd, *J* = 10.4, 2.3 Hz), 7.04-7.12 (2H, m), 7.37-7.95 (5H, m), 9.75 (1H, br s); HRESI-MS, calcd for $C_{19}H_{20}FN_3O_3S$+H m/z 390.1282, found m/z 390.1283 $(M+H)^+$.

Compound **3_5j**

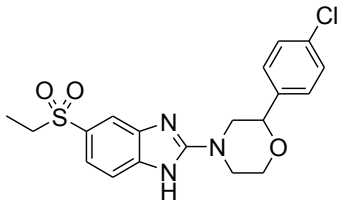

White solid, 49.0% yield; ^{1}H NMR ($CDCl_3$): δ = 1.26 (3H, t, *J* = 7.4 Hz), 3.05-3.18 (3H, m), 3.31-3.41 (1H, m), 3.84-3.93 (1H, m), 3.96-4.07 (1H, m), 4.14-4.26 (2H, m), 4.61 (1H, dd, *J* = 10.6, 2.5 Hz), 7.32-7.97 (7H, m), 9.87 (1H, br s); HRESI-MS, calcd for $C_{19}H_{20}ClN_3O_3S$+H m/z 406.0987, found m/z 406.0987 $(M+H)^+$.

Compound **3_5k**

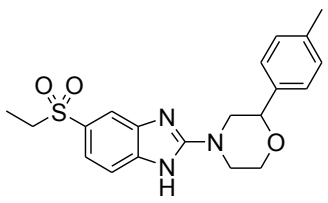

Light pink amorphous, 71.9% yield; ^{1}H NMR ($CDCl_3$): δ = 1.25 (3H, t, *J* = 7.6 Hz), 2.36 (3H, s), 3.09-3.20 (3H, m), .3.32-3.42 (1H, m), 3.85-3.94 (1H, m), 3.96-4.05 (1H, m), 4.09-4.16 (1H, m), 4.19 (1H, dd, *J* = 11.7, 3.0 Hz), 4.60 (1H, dd, *J* = 10.6, 2.5 Hz), 7.19 (2H, d, *J* = 8.1 Hz), 7.32 (2H, d, *J* = 8.1 Hz), 7.39-7.86 (3H, br m), 9.55 (1H, br s); HRESI-MS, calcd for $C_{20}H_{23}N_3O_3S$+H m/z 386.1533, found m/z 386.1538 $(M+H)^+$.

Compound **3_5l**

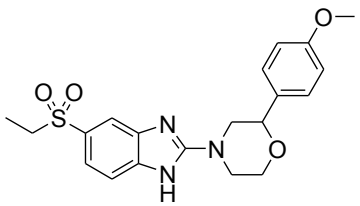

Light pink amorphous, 81.9% yield; ^{1}H NMR (DMSO-d_6): δ = 1.04-1.11 (3H, m), 2.99-3.10 (1H, m), 3.17-3.28 (3H, m), 3.73-3.82 (4H, m), 4.00-4.14 (3H, m), 4.56 (1H, dd, *J* = 10.4, 2.3 Hz), 6.96 (2H, d, *J* = 8.6 Hz), 7.37-7.71 (5H, m), 11.90-12.01 (1H, br, overlap of NH peaks of two tautomeric forms); HRESI-MS, calcd for $C_{20}H_{23}N_3O_4S$+H m/z 402.1482, found m/z 402.1486 $(M+H)^+$.

Compound **3_5f**

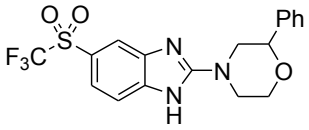

White solid, 96.3% yield; ^{1}H NMR ($CDCl_3$): δ = 3.19-3.27 (1H, m), 3.41-4.50 (1H, m), 3.89-4.16 (3H, m), 4.25 (1H, dd, *J* = 11.9, 3.3 Hz), 4.65 (1H, dd, *J* = 10.9, 2.8 Hz), 7.34-8.07 (8H, m), 8.72-8.78 (1H, br, overlap of NH peaks of two tautomeric forms); HRESI-MS, calcd for $C_{18}H_{16}F_3N_3O_3S$+H m/z 412.0937, found m/z 412.0937 $(M+H)^+$.

Synthesis of compound **6_25**

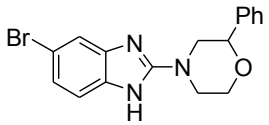

5-Bromo-2-chloro-1H-benzo[d]imidazole (300 mg, 1.30 mmol) and 2-phenylmorpholine hydrochloride (285 mg, 1.43 mmol) were suspended in *i*-PrOH (3.0 mL). After addition of $(i\text{-Pr})_2$NEt (0.566 mL, 3.24 mmol), the mixture was stirred at 180 °C under micromave irradiation. The reaction mixture was diluted with EtOAc (20 mL) and washed with water (3 x 2.0 mL). The organic phase was dried with $MgSO_4$. After removal of the drying agent by filtration, the filtrate was concentrated under reduced pressure. The residue was purified by reverse phase chromatography (0.1% HCO_2H in CH_3CN/0.1% HCO_2H aq.) to give compound **6_25** (361 mg, 77.8%)

Cream amorphous; ^{1}H NMR (DMSO-d_6): δ = 2.92-3.02 (1H, m), 3.13-3.23 (1H, m), 3.74-3.84 (1H, m), 3.99 (1H, d, J = 12.8 Hz), 4.06-4.15 (2H, m), 4.62 (1H, d, J = 10.3 Hz), 7.06 (1H, d, J = 8.3 Hz), 7.15 (1H, d, J = 8.3 Hz), 7.31-7.48 (6H, m), 11.66 (1H, br s); HRESI-MS, calcd for $C_{17}H_{16}BrN_3O$+H m/z 385.0550, found m/z 385.0547 $(M+H)^+$.

Typical procedure for synthesis of compounds **3_5c-e** and **3_5g-h**

Compound **6_25** (70 mg, 0.195 mmol) was dissolved in 1,4-dioxane (2.0 mL). After addition of $(i\text{-Pr})_2$NEt (68.0 μL, 0.391 mmol), $Pd_2(dba)_3$ (17.9 mg, 19.5 μmol), xantphos (22.6 mg, 39.0 μmol) and thiol (0.430 mmol), the mixture was stirred at 120 °C under micromave irradiation. The reaction mixture was diluted with EtOAc and washed with sat. $NaHCO_3$ aq. and brine. After concentration of the organic phase under reduced pressure, the residue was dissolved in CH_2Cl_2 (2.0 mL). After addition of *m*-CPBA (68%, 149 mg, 0.586 mmol), the mixture was stirred at room temperature. The reaction mixture was diluted with EtOAc and washed with sat. $NaHCO_3$ aq. and brine. The organic phase was

dried with $MgSO_4$. After removal of the drying agent by filtration, the filtrate was concentrated under reduced pressure. The residue was purified by column chromatography on silica gel ($CHCl_3$/MeOH) to give the target compound.

Compound **3_5c**

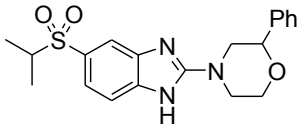

Cream solid, 52.0% yield; ^{1}H NMR ($CDCl_3$): δ = 1.26 (6H, d, J = 6.8 Hz), 3.13-3.23 (2H, m), 3.34-3.43 (1H, m), 3.86-3.95 (1H, m), 4.02 (1H, d, J = 12.8 Hz), 4.12-4.24 (2H, m), 4.64 (1H, dd, J = 10.7, 2.6 Hz), 7.32-7.46 (6H, m), 7.55 (1H, dd, J = 8.3, 1.7 Hz), 7.79 (1H, d, J = 1.7 Hz), the NH proton exchanged with water, stabilizer of $CDCl_3$, and gave a broad peak; HRESI-MS, calcd for $C_{20}H_{23}N_3O_3S$+H m/z 386.1533, found m/z 386.1532 $(M+H)^+$.

Compound **3_5d**

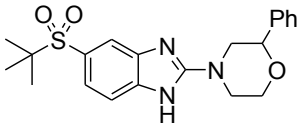

White solid, 41.1% yield; ^{1}H NMR ($CDCl_3$): δ = 1.31 (9H, s), 3.10-3.21 (1H, m), 3.32-3.42 (1H, m), 3.86-3.95 (1H, m), 4.02-4.11 (1H, m), 4.16-4.24 (2H, m), 4.64 (1H, d, J = 10.1 Hz), 7.31-7.92 (8H, m), 9.98 (1H, br s); HRESI-MS, calcd for $C_{21}H_{25}N_3O_3S$+H m/z 400.1689, found m/z 400.1690 $(M+H)^+$.

Compound **3_5e**

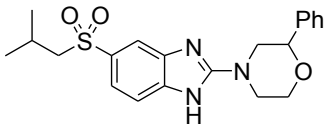

Cream amorphous, 43.4% yield; ^{1}H NMR ($CDCl_3$): δ = 1.01 (6H, d, *J* = 6.6 Hz), 2.12-2.22 (1H, m), 3.00 (2H, d, *J* = 6.6 Hz), 3.16 (1H, dd, *J* = 12.7, 10.6 Hz), 3.33-3.43 (1H, m), 3.87-3.96 (1H, m), 3.96-4.05 (1H, m), 4.10-4.18 (1H, m), 4.21 (1H, dd, *J* = 11.7, 3.0 Hz), 4.64 (1H, dd, *J* = 10.6, 2.5 Hz), 7.32-7.81 (8H, m), 9.50 (1H, br s); HRESI-MS, calcd for $C_{21}H_{25}N_3O_3S$+H m/z 400.1689, found m/z 400.1691 $(M+H)^+$.

Compound **3_5g**

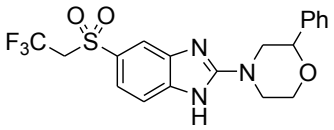

White solid, 31.1% yield; ^{1}H NMR ($CDCl_3$): δ = 3.18 (1H, dd, *J* = 12.4, 10.9 Hz), 3.35-3.47 (1H, m), 3.84-4.25 (6H, m), 4.64 (1H, dd, *J* = 10.6, 2.5 Hz), 7.26-7.98 (8H, m), 9.34 (1H, br s); HRESI-MS, calcd for $C_{19}H_{18}F_3N_3O_3S$+H m/z 426.1094, found m/z 426.1092 $(M+H)^+$.

Compound **3_5h**

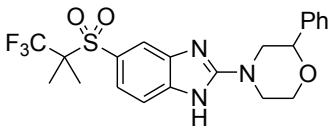

White solid, 25.7% yield; ^{1}H NMR ($CDCl_3$): δ = 1.59 (6H, s), 3.18 (1H, dd, *J* = 12.4, 10.9 Hz), 3.34-3.45 (1H, m), 3.87-3.96 (1H, m), 3.97-4.18 (2H, m), 4.21 (1H, dd, *J* = 11.7, 3.0 Hz), 4.64 (1H, dd, *J* =

10.6, 2.5 Hz), 7.32-7.76 (8H, m), 9.38 (1H, br s); HRESI-MS, calcd for $C_{21}H_{22}F_3N_3O_3S$+H m/z 454.1407, found m/z 454.1406 $(M+H)^+$.

Synthesis of compound **4_1a**

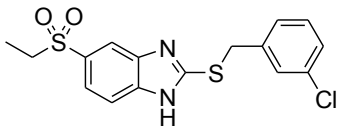

Compound **6_5** (0.200 g, 0.999 mmol) was dissolved in DMF (5.0 mL). After addition of TCDI (0.214 g, 1.20 mmol), the solution was stirred at room temperature over night. The reaction mixture was quenched with water (30 mL) and extracted with EtOAc (2 x 30 mL) and $CHCl_3$ (2 x 30 mL). The combined organic phase was dried with $MgSO_4$. After removal of the drying agent by filtration, the filtrate was concentrated under reduced pressure. The resulting precipitates were collected by filtration. A part of the resulting solid (50.0 mg, 0.206 mmol) was dissolved in CH_3CN (5.0 mL). After addition of 28% NH_3 aq.(0.251 mL, 4.13 mmol), the mixture was stirred at room temperature for 30 minutes. After addition of 1-(bromomethyl)-3-chlorobenzene (26.0 μL, 0.206 mmol), the mixture was stirred at room temperature for 4 hours. The reaction mixture was quenhced with water (30 mL) and extracted with EtOAc (2 x 30 mL) and $CHCl_3$ (2 x 30 mL). The combined organic phase was dried with $MgSO_4$. After removal of the drying agent by filtration, the filtrate was concentrated under reduced pressure. The residue was purified by column chromatography on silica gel ($CHCl_3$/MeOH) to give compound **4_1a** (63.0 mg, 55.3%).

Pink amorphous; ^{1}H NMR (DMSO-d_6): δ = 1.09 (3H, t, J = 7.4 Hz), 3.28 (2H, q, J = 7.4 Hz), 4.62 (2H, s), 7.31-7.37 (2H, m), 7.43-7.47 (1H, m), 7.55-7.70 (3H, m), 7.93 (1H, s), 13.17 (1H, br s); HRESI-MS, calcd for $C_{16}H_{15}ClN_2O_2S_2$+H m/z 367.0336, found m/z 367.0342 $(M+H)^+$.

Typical procedure for synthesis of compounds **4_1b-d**, **4_2a-f**, **4_6b-c** and **4_7a**

60% NaH (170 mg, 4.25 mmol) was added to a solution of compound **6_19** (800 mg, 3.27 mmol) in DMF (10 mL). After addition of SEM-Cl (0.696 mL, 3.92 mmol), the mixture was stirred at room temperature. The reaction mixture was quenched with water and extracted with EtOAc. The organic phase was dried with $MgSO_4$. After removal of the drying agent by filtration, the filtrate was concentrated under reduced pressure. The residue was purified by column chromatography on silica gel (*n*-hexane/EtOAc). A part of the resulting solid (50.0mg, 0.133 mmol) was added to a solution of alcohol (0.160 mmol) and 60% NaH (6.40 mg, 0.160 mmol) in DMF (3.0 mL). The reaction mixture was quenched with water (20 mL) and extracted with EtOAc (2 x 20 mL). The organic phase was washed with 10% citric acid aq. (20 mL) and water (2 x 20 mL) and dried with $MgSO_4$. After removal of the drying agent by filtration, the filtrate was concentrated under reduced pressure. The residue was dissolved in THF (3.0 mL). After addition of TBAF (174 mg, 0.655 mmol), the mixture was refluxed. The reaction mixture was quenched with water (20 mL) and extracted with EtOAc (2 x 20 mL). The organic phase was washed with 10% citric acid aq. (2 x 20 mL) and dried with $MgSO_4$. After removal of the drying agent by filtration, the filtrate was concentrated under reduced pressure. The residue was purified by column chromatography on silica gel ($CHCl_3$/MeOH) to give the target compound.

Compound **4_1b**

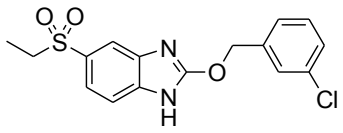

White powder, 25.2% yield; ^{1}H NMR (DMSO-d_6): δ = 1.08 (3H, t, *J* = 7.4 Hz), 3.25 (2H, q, *J* = 7.4 Hz), 5.58 (2H, s), 7.43-7.63 (6H, m), 7.79 (1H, s), 12.61 (1H, br s); HRESI-MS, calcd for $C_{16}H_{15}ClN_2O_3S$+H m/z 351.0565, found m/z 351.0569 $(M+H)^+$.

Compound **4_1c**

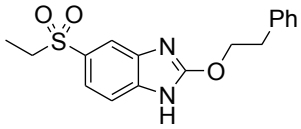

Colorless syrup, 25.3% yield; ^{1}H NMR (DMSO-d$_6$): δ = 1.07 (3H, t, J = 7.4 Hz), 3.13 (2H, t, J = 6.6 Hz), 3.23 (2H, q, J = 7.4 Hz), 4.72 (2H, t, J = 6.6 Hz), 7.21-7.27 (1H, m), 7.30-7.35 (4H, m), 7.45-7.58 (2H, m), 7.75 (1H, s), 12.47 (1H, br s); HRESI-MS, calcd for $C_{17}H_{18}N_2O_3S$+H m/z 331.1111, found m/z 331.1109 $(M+H)^+$.

Compound **4_1d**

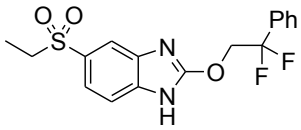

White solid, 73.1% yield; ^{1}H NMR (DMSO-d$_6$): δ = 1.07 (3H, t, J = 7.4 Hz), 3.25 (2H, q, J = 7.4 Hz), 5.15 (2H, t, J = 13.7 Hz), 7.51-7.82 (8H, m), 12.79 (1H, br s); HRESI-MS, calcd for $C_{17}H_{16}F_2N_2O_3S$+H m/z 367.0922, found m/z 367.0924 $(M+H)^+$.

Compound **4_2a**

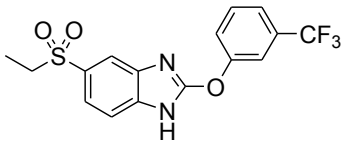

Cream solid, 60.6% yield; ^{1}H NMR (DMSO-d$_6$): δ = 1.08 (3H, t, J = 7.4 Hz), 3.26 (2H, q, J = 7.4 Hz), 7.59-7.93 (7H, m), 13.12 (1H, br s); HRESI-MS, calcd for $C_{16}H_{13}F_3N_2O_3S$+H m/z 371.0672, found m/z 371.0674 $(M+H)^+$.

Compound **4_2b**

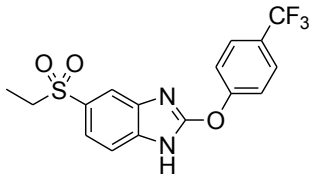

White powder, 27.3% yield; ^{1}H NMR ($CDCl_3$): δ = 1.24-1.28 (3H, m), 3.11-3.22 (2H, m), 7.45-8.15 (7H, m), 9.10-9.30 (1H, br, overlap of NH peaks of two tautomeric forms); HRESI-MS, calcd for $C_{16}H_{13}F_3N_2O_3S$+H m/z 371.0672, found m/z 371.0672 $(M+H)^+$.

Compound **4_2c**

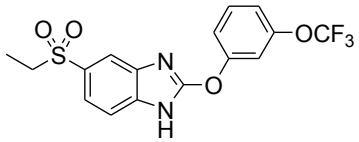

White powder, 14.8% yield; ^{1}H NMR (DMSO-d_6): δ = 1.08 (3H, t, *J* = 7.4 Hz), 3.26 (2H, q, *J* = 7.4 Hz), 7.33-7.38 (1H, m), 7.50-7.54 (1H, m), 7.58-7.67 (4H, m), 7.86 (1H, s), 13.10 (1H, br s); HRESI-MS, calcd for $C_{16}H_{13}F_3N_2O_4S$+H m/z 387.0621, found m/z 387.0619 $(M+H)^+$.

Compound **4_2d**

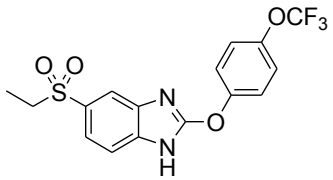

White powder, 10.1% yield; ^{1}H NMR (DMSO-d_6): δ = 1.08 (3H, t, *J* = 7.4 Hz), 3.26 (2H, q, *J* = 7.4 Hz), 7.51 (2H, d, *J* = 8.6 Hz), 7.57-7.65 (4H, m), 7.85 (1H, s), 13.06 (1H, br s); HRESI-MS, calcd for $C_{16}H_{13}F_3N_2O_4S$+H m/z 387.0621, found m/z 387.0616 $(M+H)^+$.

Compound **4_2e**

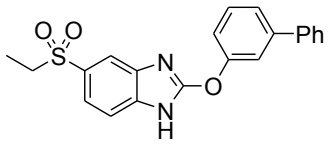

Cream solid, 25.4% yield; ^{1}H NMR (DMSO-d_6): δ = 1.16 (3H, t, *J* = 7.4 Hz), 7.46-7.84 (10H, m), 7.91-8.00 (2H, m), 13.11 (1H, br s), two protons are buried in solvent peak; HRESI-MS, calcd for $C_{21}H_{18}N_2O_3S$+H m/z 379.1111, found m/z 379.1112 $(M+H)^+$.

Compound **4_2f**

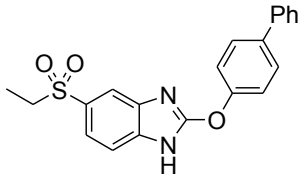

White solid, 82.3% yield; ^{1}H NMR (DMSO-d_6): δ = 1.08 (3H, t, J = 7.2 Hz), 3.26 (2H, q, J = 7.2 Hz), 7.39 (1H, t, J = 7.4 Hz), 7.46-7.56 (4H, m), 7.58-7.66 (2H, m), 7.71 (2H, d, J = 7.3 Hz), 7.75-7.90 (3H, m), 13.03 (1H, br s); HRESI-MS, calcd for $C_{21}H_{18}N_2O_3S$+H m/z 379.1111, found m/z 379.1109 $(M+H)^+$.

Compound **4_6b**

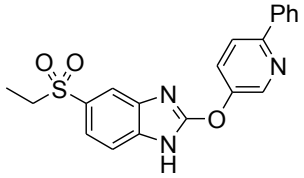

White solid, 65.3% yield; ^{1}H NMR ($CDCl_3$): δ = 1.26 (3H, t, *J* = 7.4 Hz), 3.14 (2H, q, *J* = 7.4 Hz), 7.37-8.09 (10H, m), 8.74 (1H, d, *J* = 2.5 Hz), 10.17-10.32 (1H, br, overlap of NH peaks of two tautomeric forms); HRESI-MS, calcd for $C_{20}H_{17}N_3O_3S$+H m/z 380.1063, found m/z 380.1061 $(M+H)^+$.

Compound **4_6c**

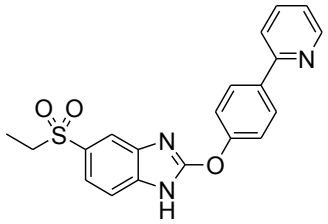

White solid, quant.; ^{1}H NMR (DMSO-d_6): δ = 1.09 (3H, t, J = 7.4 Hz), 3.26 (2H, q, J = 7.4 Hz), 7.35-7.40 (1H, m), 7.53-7.58 (2H, m), 7.59-7.66 (2H, m), 7.86 (1H, s), 7.89-7.94 (1H, m), 8.01 (1H, d, J = 8.1 Hz), 8.18-8.23 (2H, m), 8.68-8.71 (1H, m), 13.06 (1H, br s); HRESI-MS, calcd for $C_{20}H_{17}N_3O_3S$+H m/z 380.1063, found m/z 380.1063 $(M+H)^+$.

Compound **4_7a**

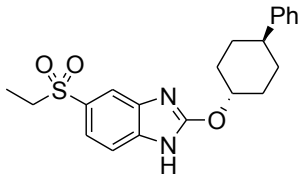

White solid, 64.8% yield; ^{1}H-NMR ($CDCl_3$): δ = 1.25-1.29 (3H, m), 1.62-1.79 (4H, m), 2.01-2.08 (2H, m), 2.40-2.47 (2H, m), 2.55-2.64 (1H, m), 3.10-3.17 (2H, m), 5.14-5.25 (1H, m), 7.19-7.25 (3H, m), 7.30-8.08 (5H, m), 8.45-8.53 (1H, br, overlap of NH peaks of two tautomeric forms); HRESI-MS, calcd for $C_{21}H_{24}N_2O_3S$+H m/z 385.1580, found m/z 385.1580 $(M+H)^+$.

Synthesis of compound **4_3a**

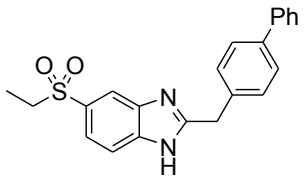

HATU (0.627 mg, 1.65 mmol) and Et_3N (0.311 mL, 2.25 mmol) were added to a solution of 2-(biphenyl-4-yl)acetic acid (318 mg 1.50 mmol) in DMF (3.0 mL) and the mixture was stirred at room temperature for 2 min. After addition of compound **6_5** (300 mg, 1.50 mmol) and DMF (3.0 mL) at 0 °C, the mixture was stirred at room temperature. The reaction mixture was quenched with water (30 mL) and the resulting precipitates were collected by filtration. The solid was dissolved in acetic acid (10 mL) and refluxed for 1 hour. After concentration of the reaction mixture, the residue was neutralized with sat. $NaHCO_3$ aq. and extracted with EtOAc/MeOH. The organic phase was washed with brine and dried with $MgSO_4$. After removal of the drying agent by filtration, the filtrate was concentrated under reduced pressure. The resulting precipitates were collected by filtration and washed with EtOAc to give compound **4_3a** (375 mg, 73.0%).

Cream solid; ^1H NMR (DMSO-d_6): δ = 1.08 (3H, t, J = 7.4 Hz), 3.26 (2H, q, J = 7.4 Hz), 4.30 (2H, s), 7.35 (1H, t, J = 7.4 Hz), 7.41-7.48 (4H, m), 7.60-7.75 (6H, m), 8.00 (1H, s), 12.87 (1H, br s); HRESI-MS, calcd for $C_{22}H_{20}N_2O_2S$+H m/z 377.1318, found m/z 377.1315 $(M+H)^+$.

Synthesis of compound **4_4a**

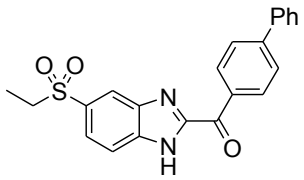

Compound **4_3a** (100 mg, 0.266 mmol) was dissolved in 1,4-dioxane (5.0 mL). After addition of SeO_2 (88.0 mg, 0.797 mmol), the mixture was stirred at 80 °C for 2 hours. The reaction mixture was quenched with sat. $NaHCO_3$ aq. and extracted with EtOAc. The organic phase was washed with sat. $NaHCO_3$ aq. and brine and dried with $MgSO_4$. After removal of the drying agent by filtration, the

filtrate was concentrated under reduced pressure. The residue was purified by column chromatography on silica gel ($CHCl_3$/MeOH) to give compound **4_4a** (87.0 mg, 83.9%).

White powder; ^{1}H NMR (DMSO-d_6): δ = 1.13 (3H, t, J = 7.4 Hz), 7.47 (1H, t, J = 7.4 Hz), 7.55 (2H, dd, J = 7.4, 7.4 Hz), 7.81-7.85 (2H, m), 7.87 (1H, d, J = 8.1 Hz), 7.94-7.99 (3H, m), 8.32 (1H, brs), 8.70 (2H, d, J = 8.6 Hz), 14.05 (1H, br s), two protons are buried in solvent peak; HRESI-MS, calcd for $C_{22}H_{18}N_2O_3S$+H m/z 391.1111, found m/z 391.1107 $(M+H)^+$.

Synthesis of compound **4_5a**

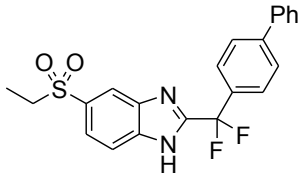

Compound **4_4a** (54.0 mg, 0.138 mmol) was dissolved in THF (3.0 mL). After addition of deoxofluor (153 mg, 0.692 mmol), the mixture was stirred at 60 °C. The reaction mixture was quenched with sat. $NaHCO_3$ aq. and extracted with EtOAc. The organic phase was washed with sat. $NaHCO_3$ aq., 10% critic acid aq., and brine. After removal of the drying agent by filtration, the filtrate was concentrated under reduced pressure. The residue was purified by column chromatography on silica gel ($CHCl_3$/MeOH) to give compound **4_5a** (31.0 mg, 54.3%).

White powder; ^{1}H NMR (DMSO-d_6): δ = 1.10 (3H, t, J = 7.4 Hz), 7.43 (1H, t, J = 7.4 Hz), 7.48-7.54 (2H, m), 7.69-7.93 (8H, m), 8.18 (1H, s), 14.05 (1H, br s), two protons are buried in solvent peak; HRESI-MS, calcd for $C_{22}H_{18}F_2N_2O_2S$+H m/z 413.1130, found m/z 413.1126 $(M+H)^+$.

Caution: MOM-Cl and SEM-Cl are carcinogens and must be handled in a hood with care.

Compound **6_1**

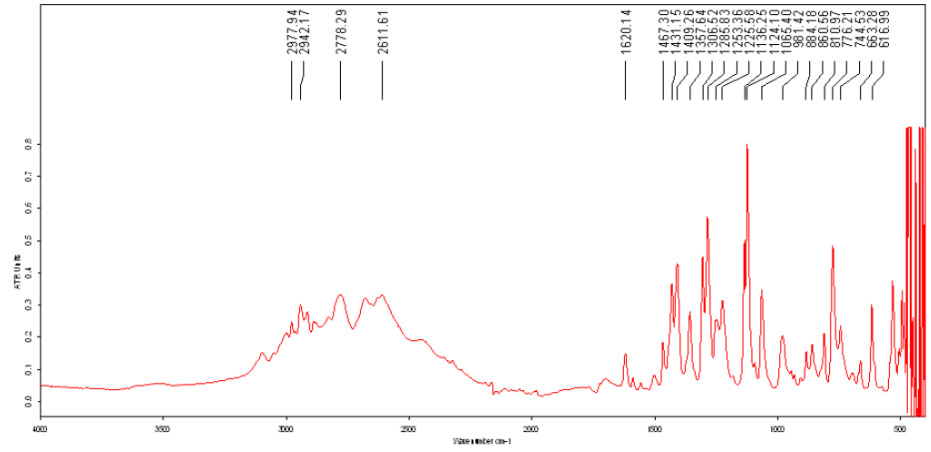

Compound **2_2a**

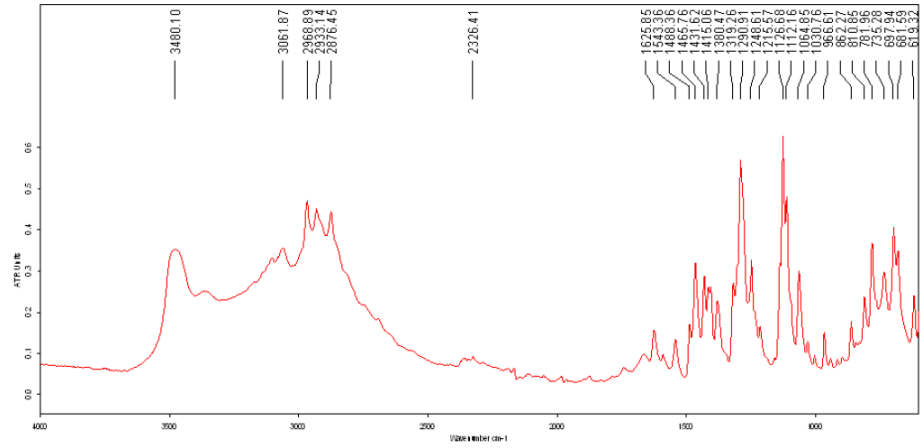

Compound **2_2b**

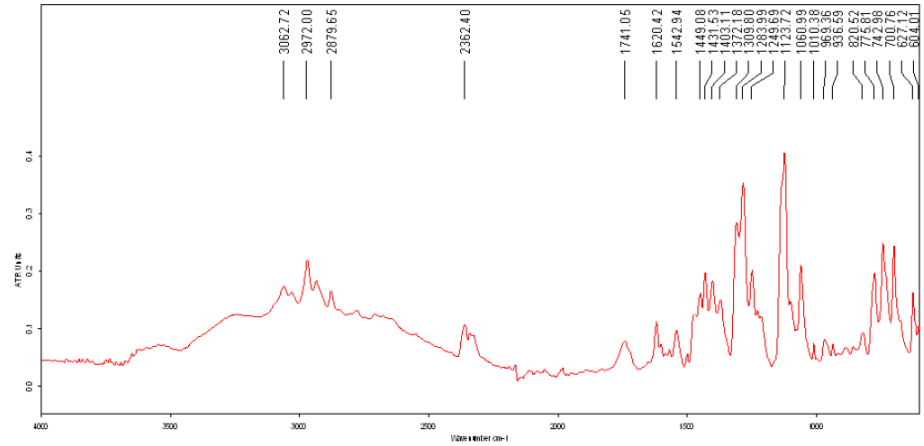

Compound **2_2c**

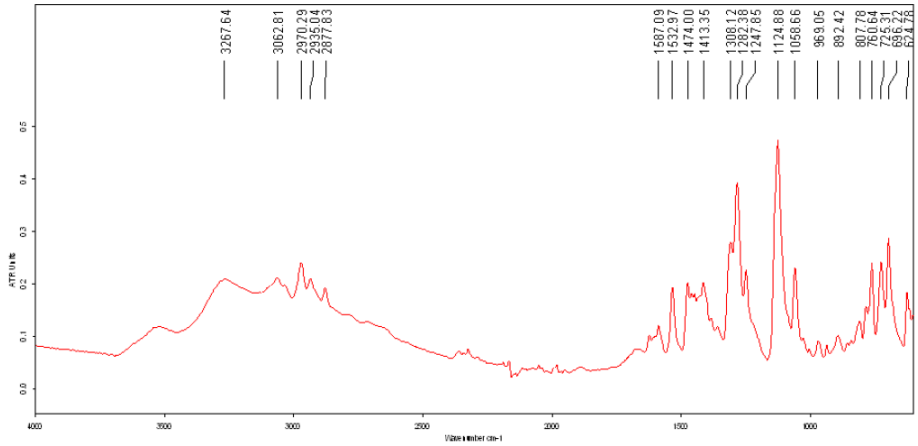

Compound **2_2d**

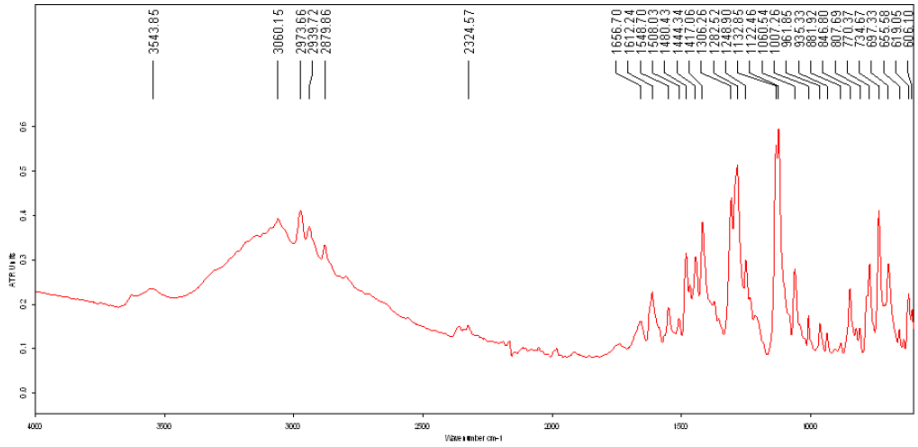

Compound **2_2e**

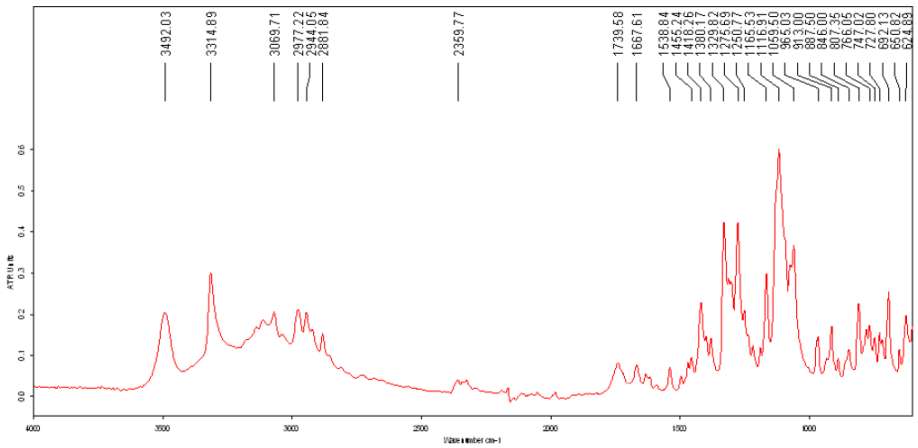

Compound **2_2f**

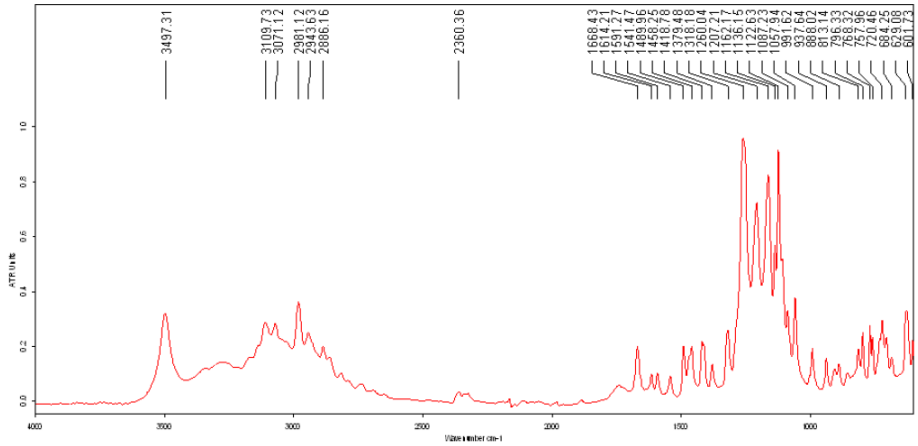

Compound **6_4**

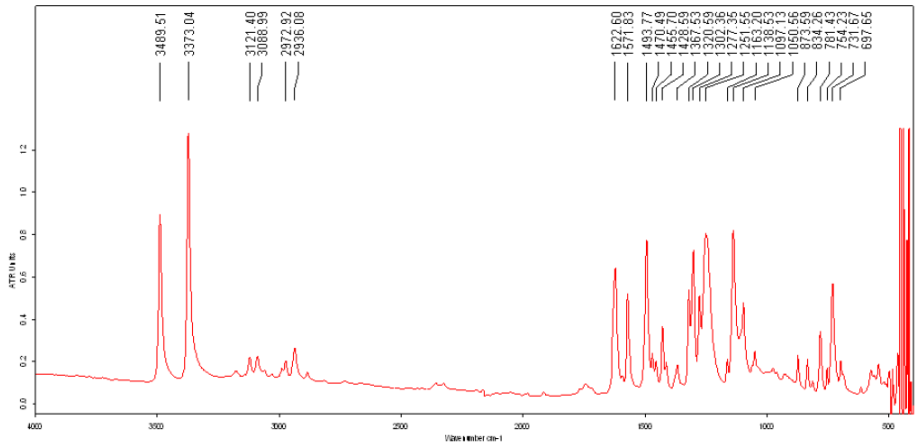

Compound **6_5**

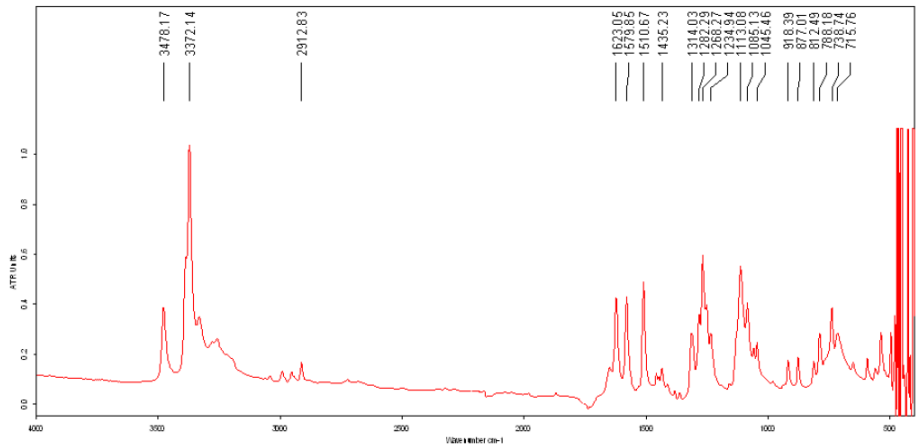

Compound **6_11a**

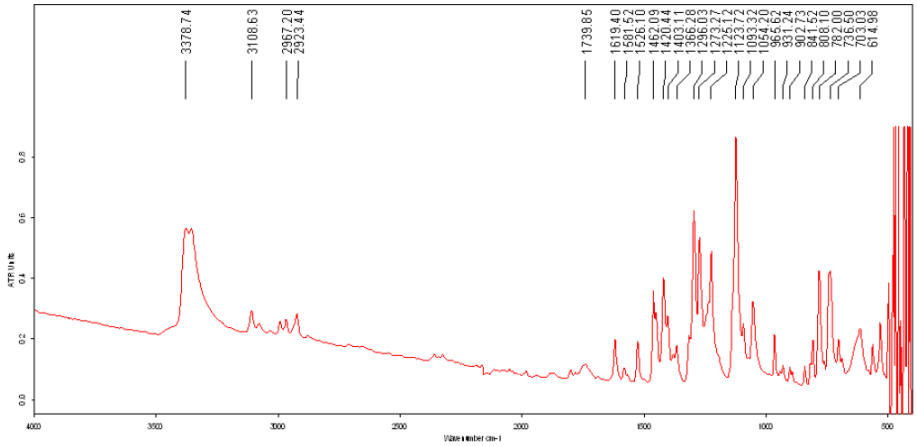

Compound **6_11b**

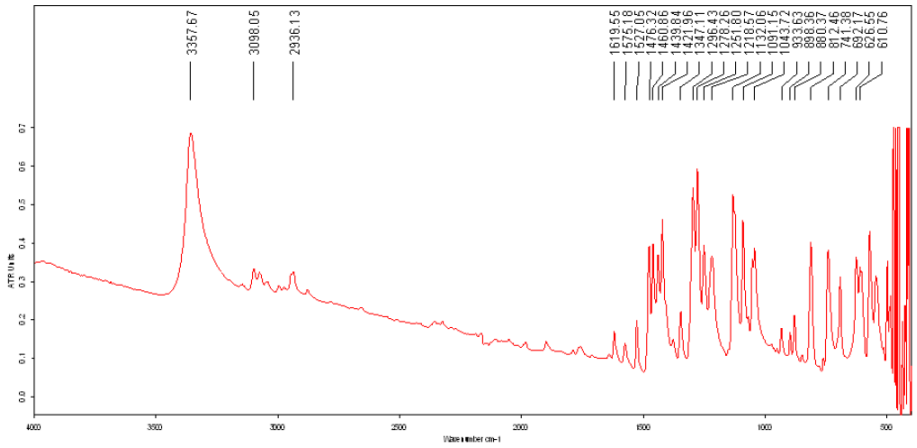

Compound **2_4a**

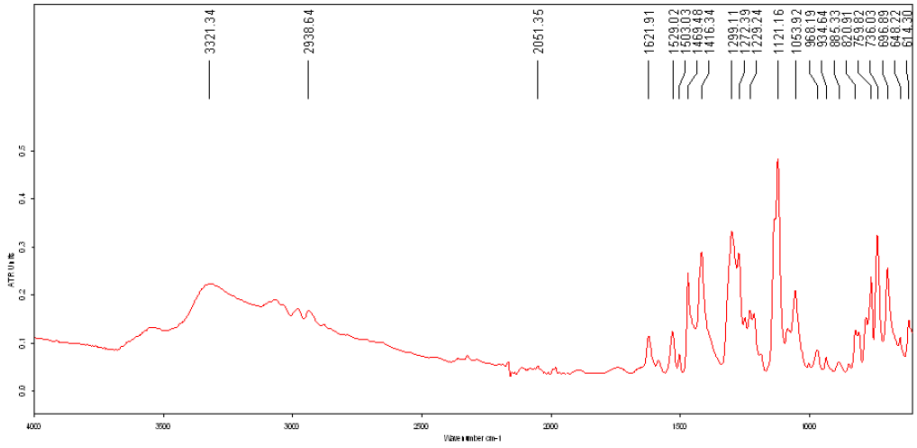

Compound **2_4b**

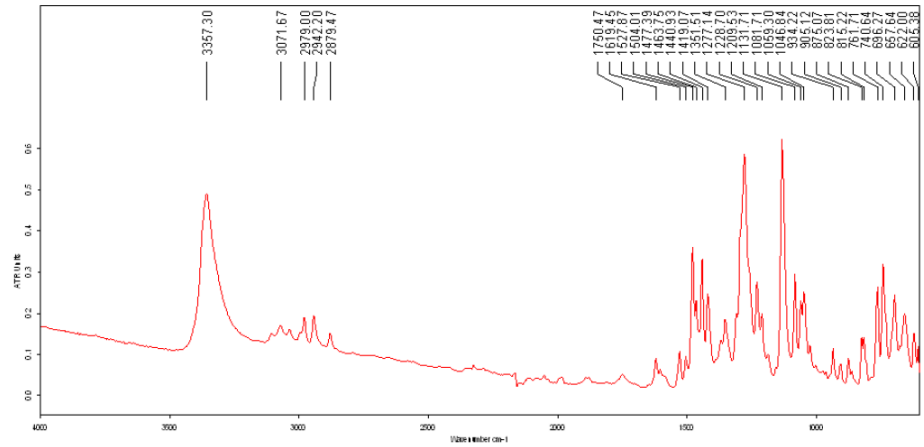

Compound **6_12c**

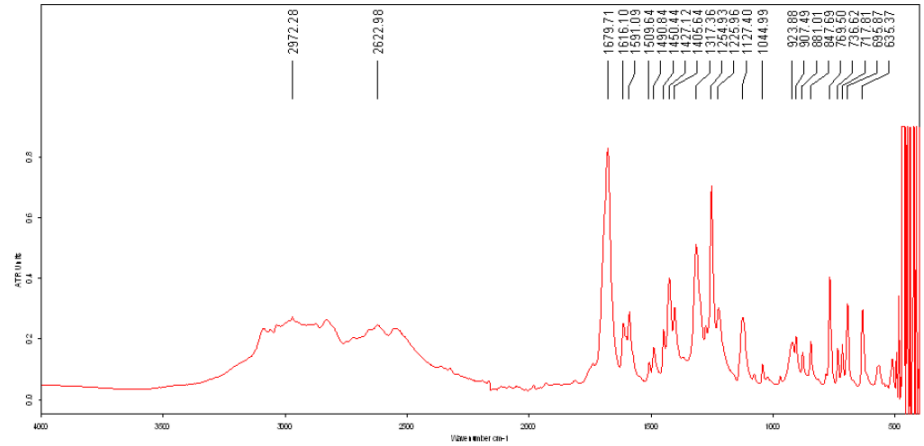

Compound **6_12d**

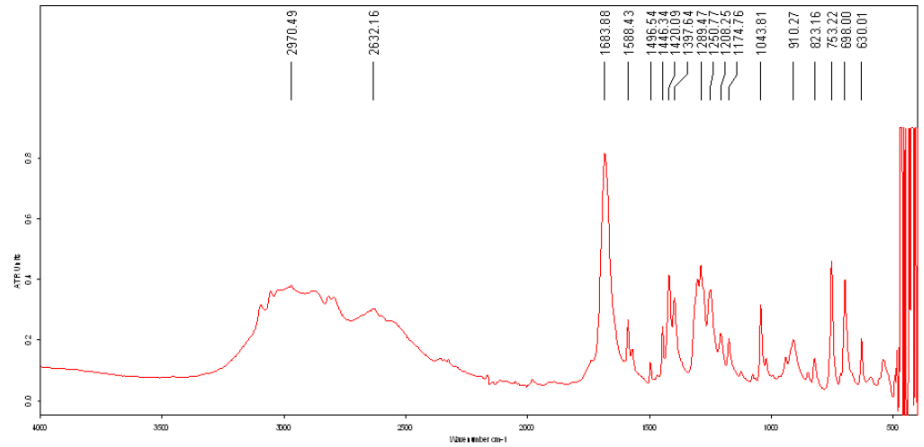

Compound **6_12e**

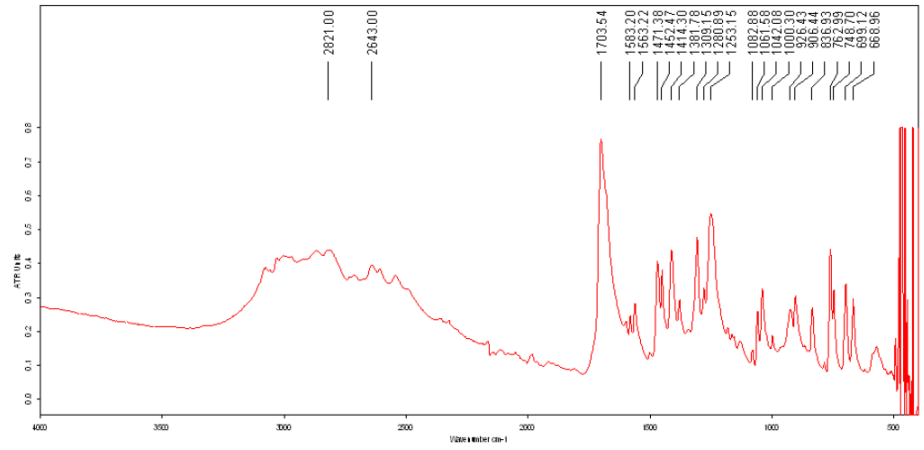

Compound **6_12f**

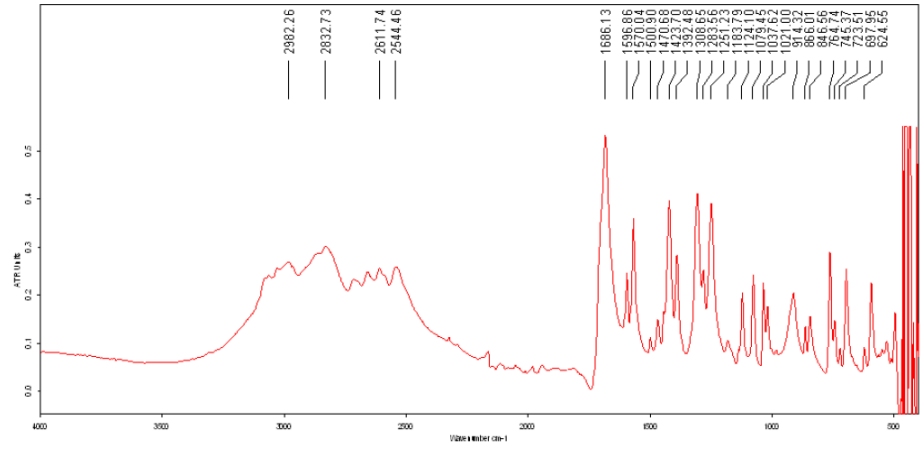

Compound **6_12g**

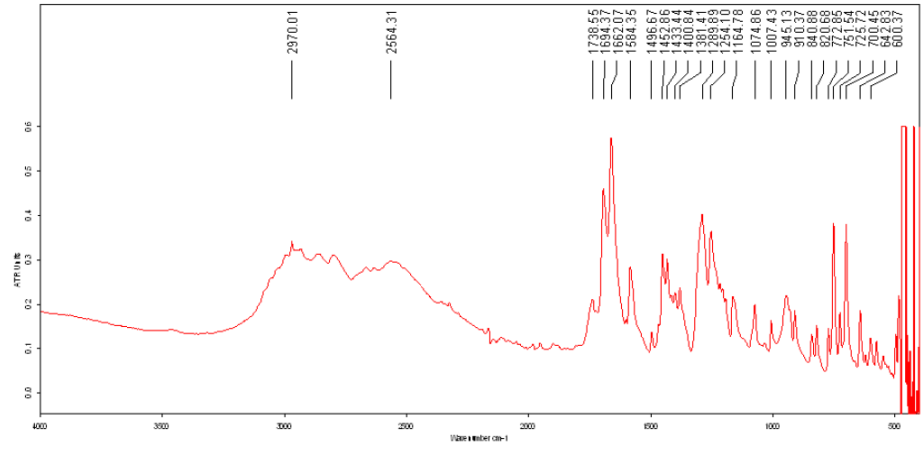

Compound **6_12h**

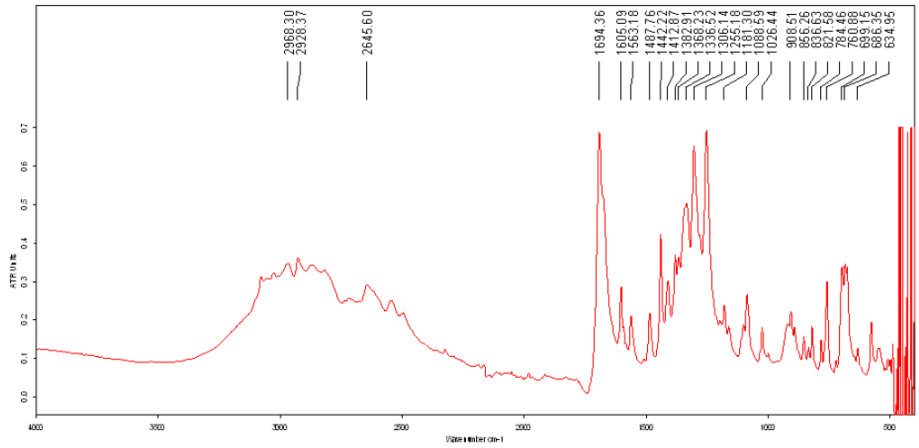

Compound **6_12i**

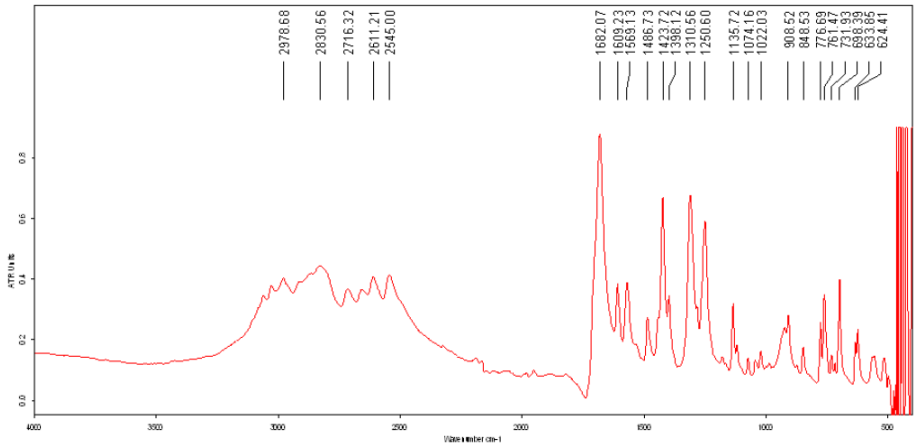

Compound **6_15**

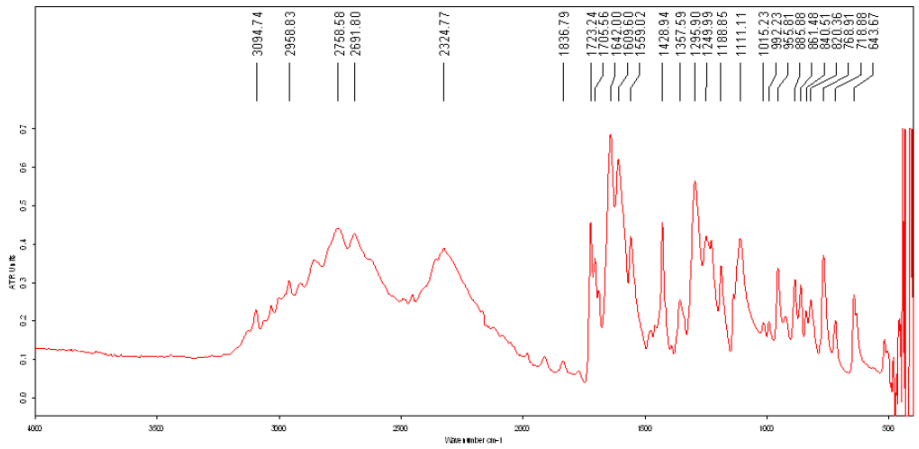

Compound **6_16**

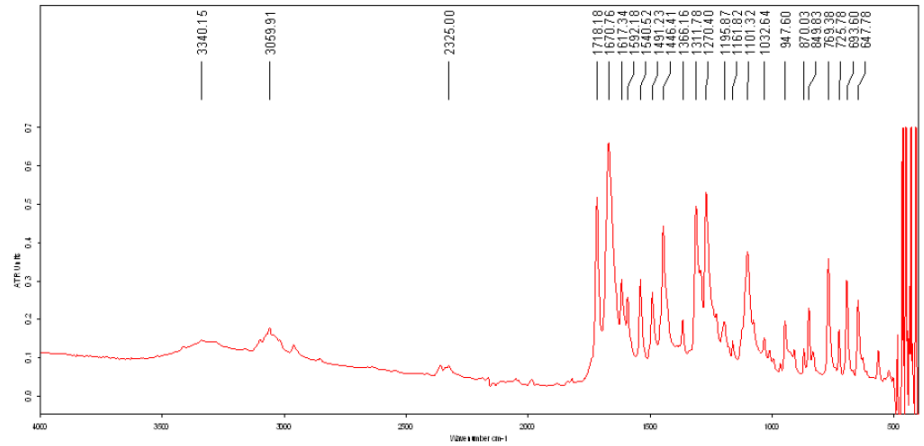

Compound **6_17**

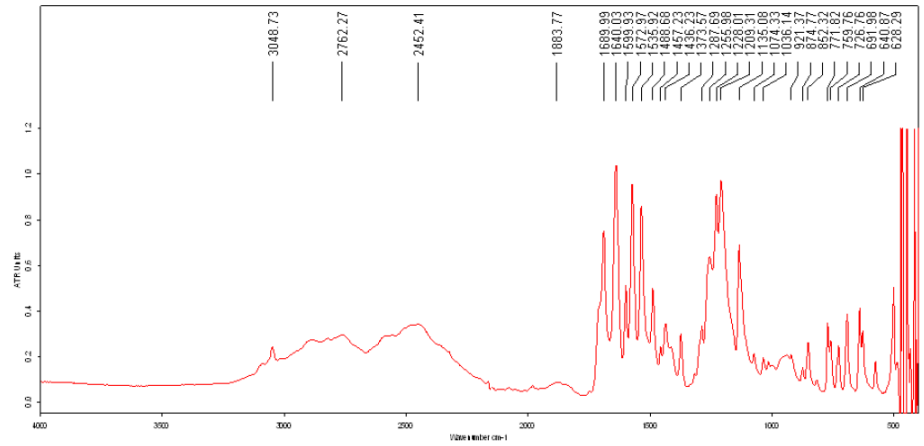

Compound **2_2g**

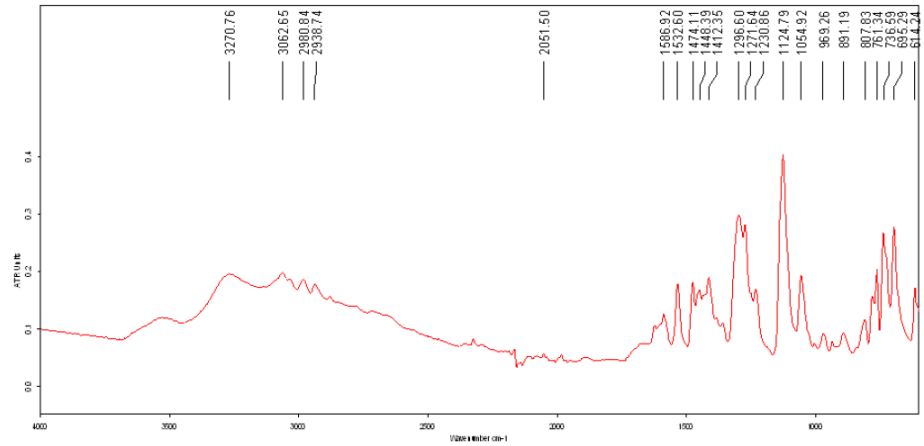

Compound **2_4c**

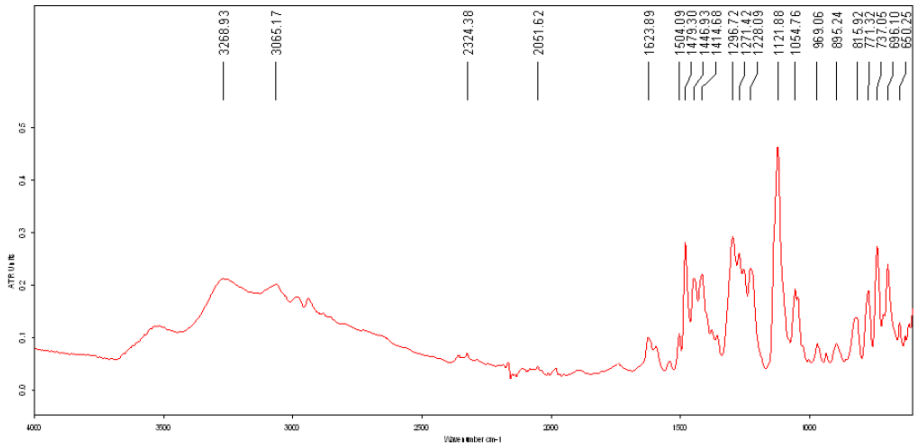

Compound **2_4d**

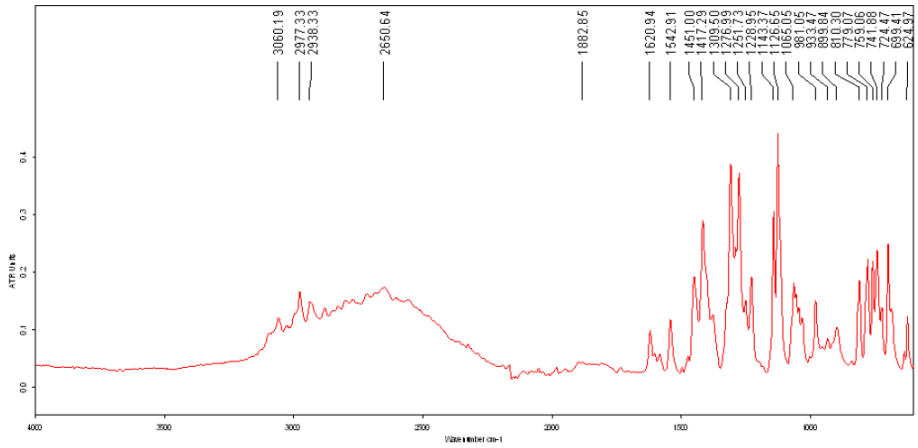

Compound **2_4e**

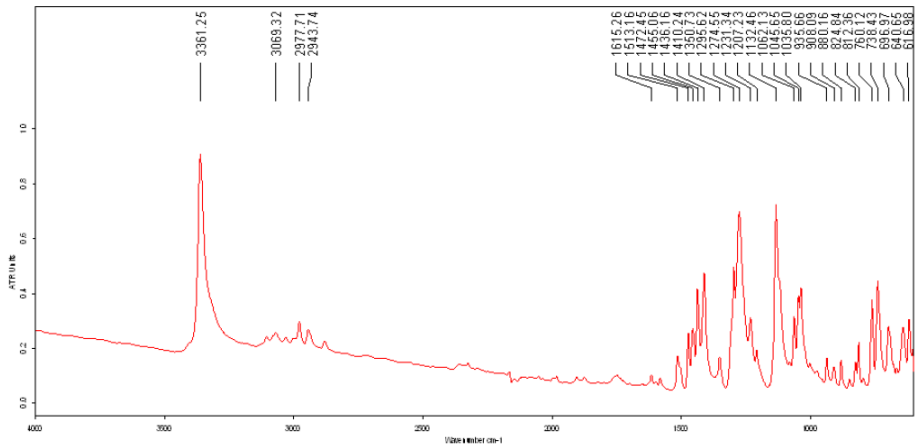

Compound **2_4f**

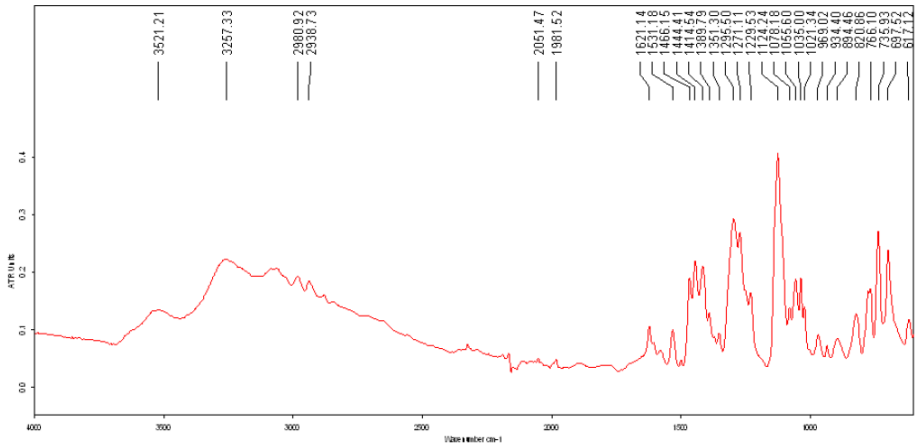

Compound **2_4g**

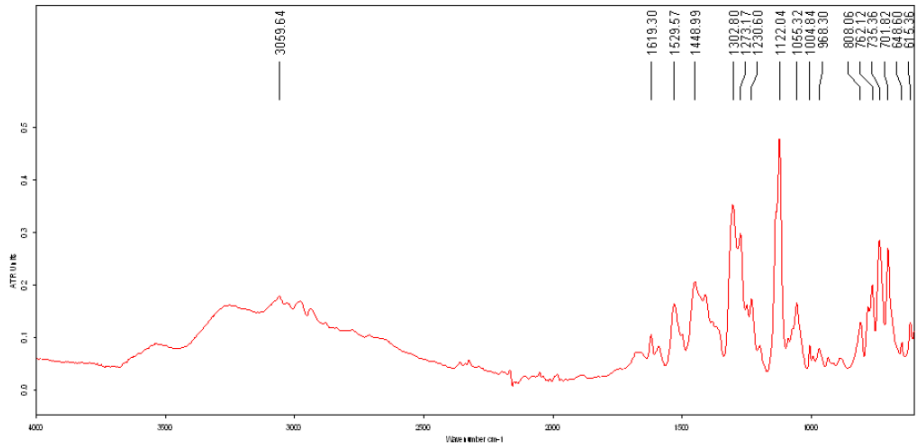

Compound **2_4h**

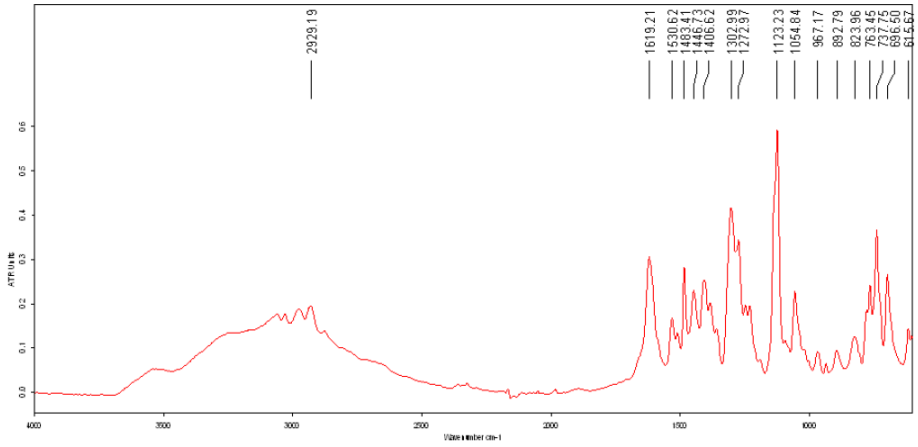

Compound **2_4i**

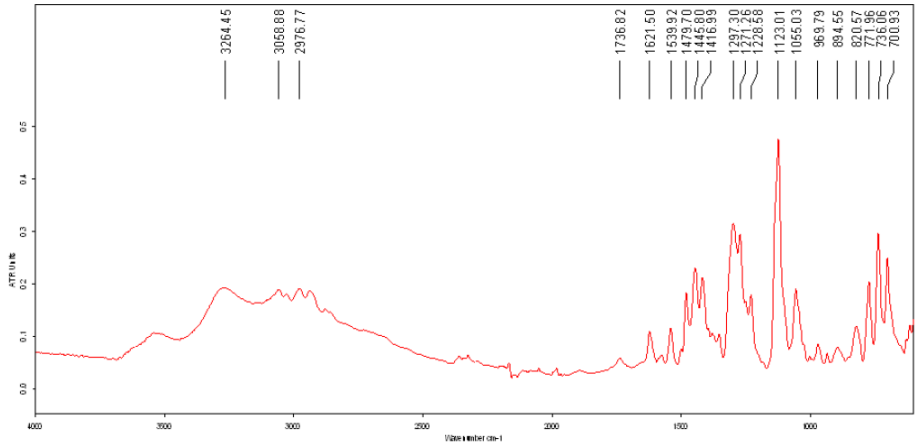

Compound **2_5a**

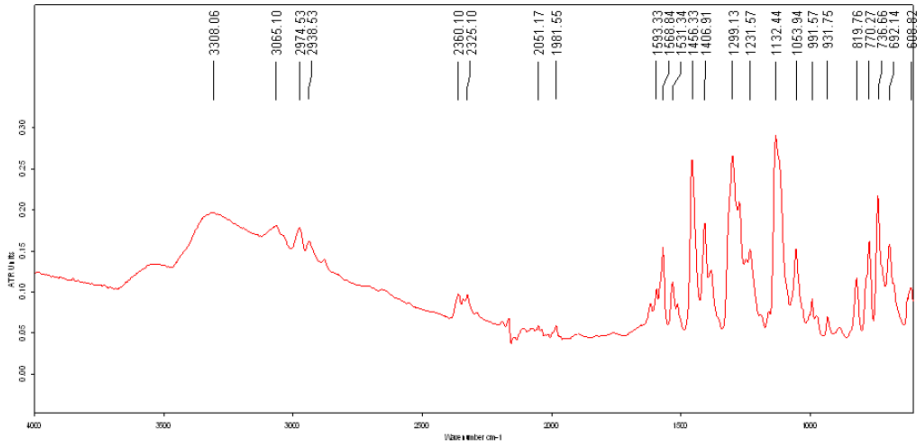

Compound **2_5b**

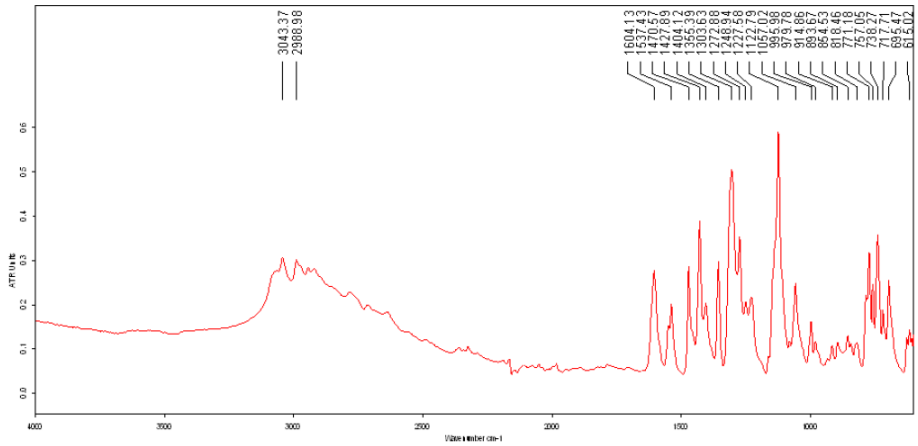

Compound **2_5c**

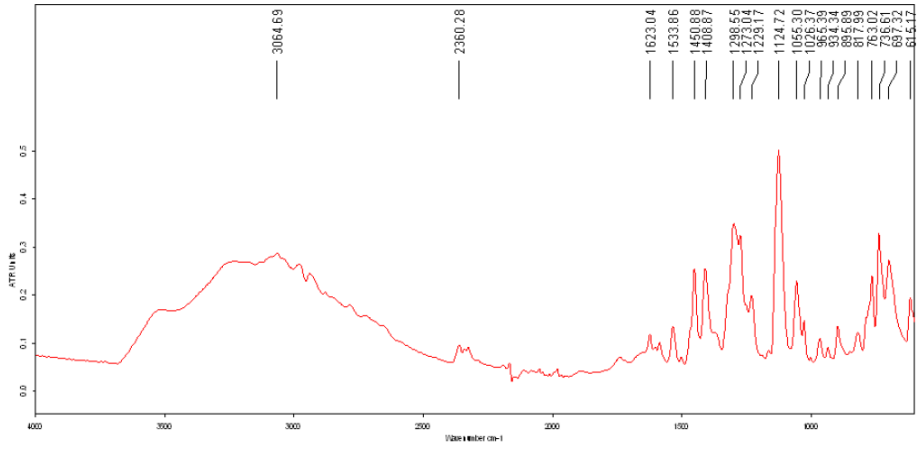

Compound **2_5d**

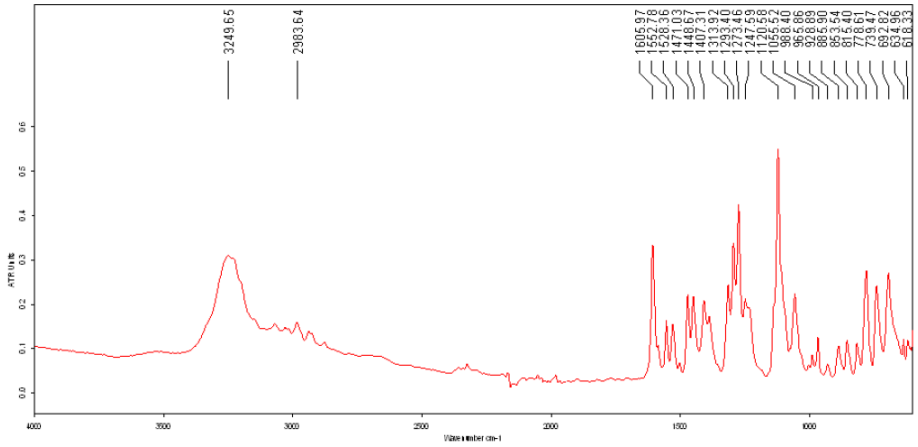

Compound **2_8a**

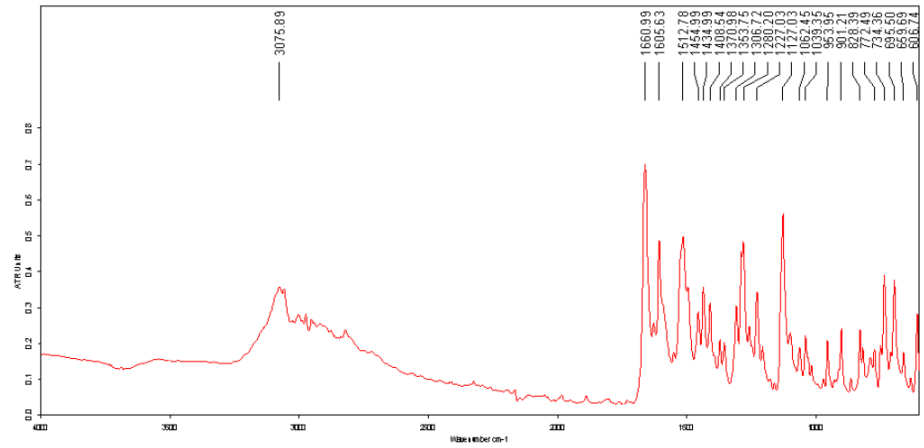

Compound **2_8b**

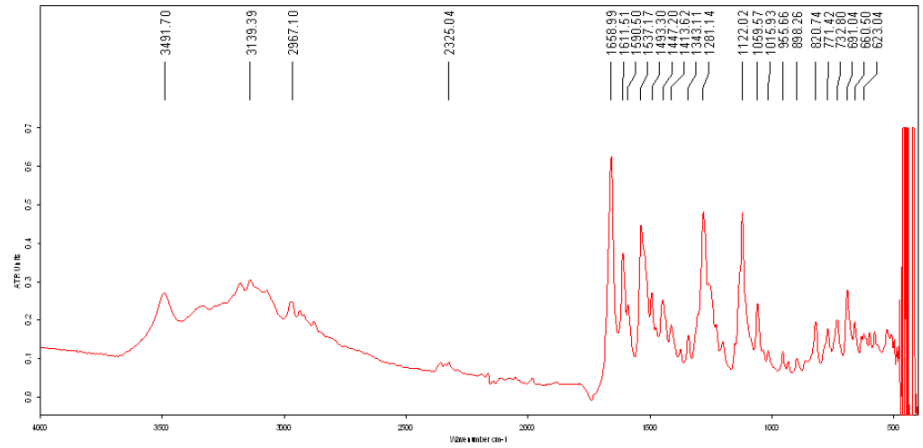

Compound **3_1a**

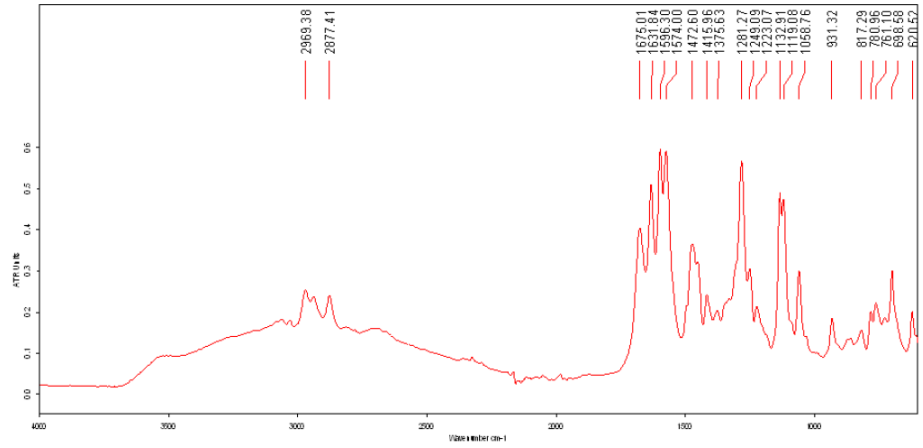

Compound **3_2a**

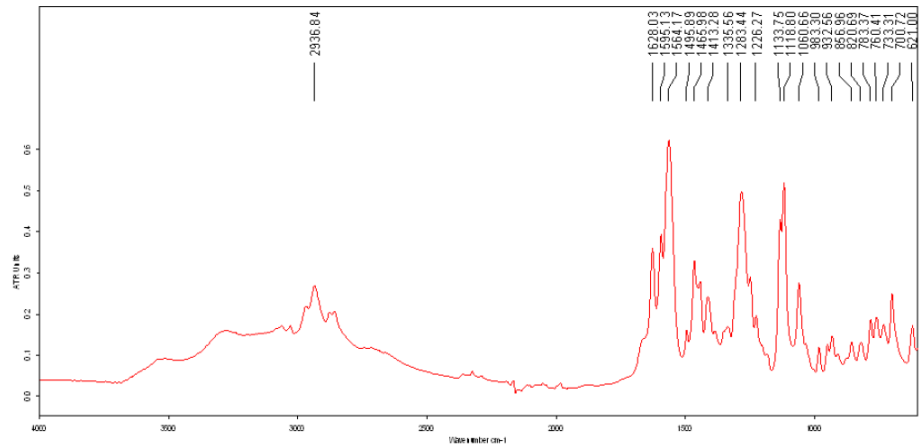

Compound **3_3a**

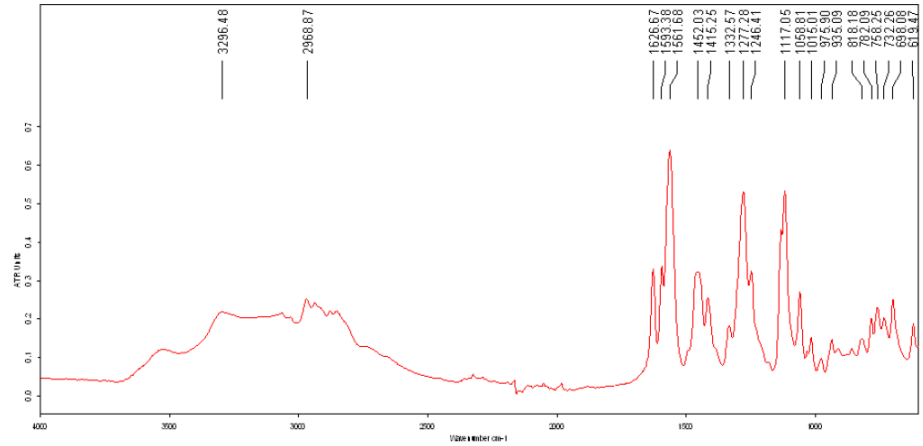

Compound **3_4a**

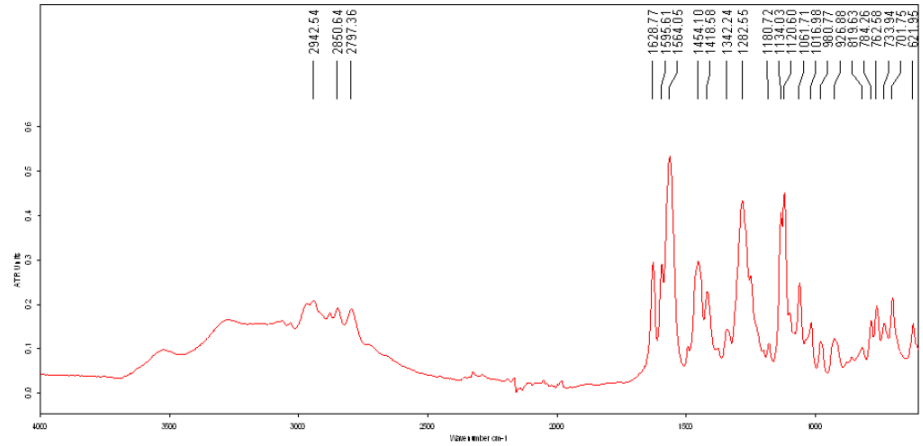

Compound **3_5a**

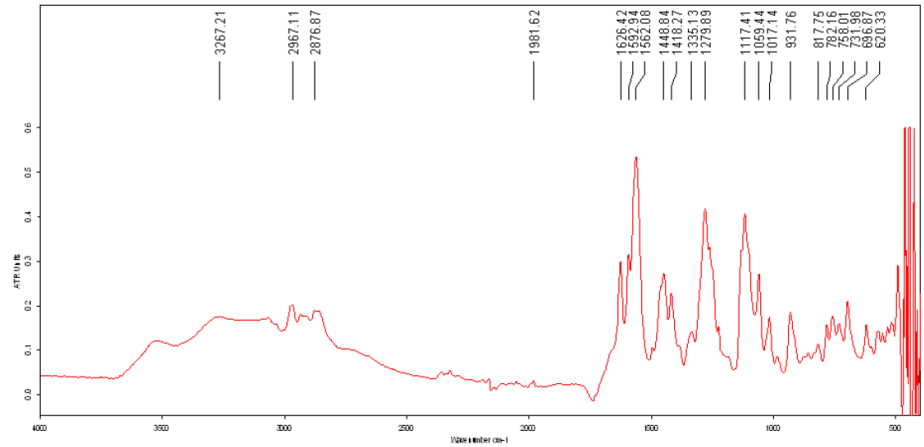

Compound **6_20**

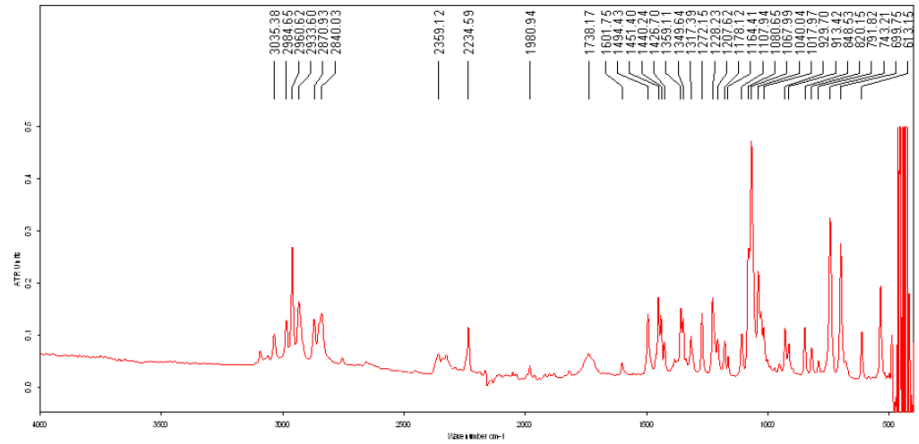

Compound **6_21**

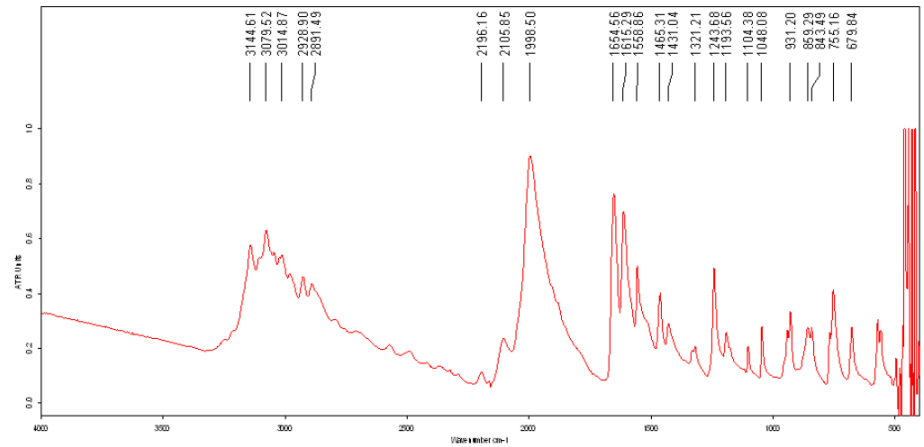

Compound **3_6a**

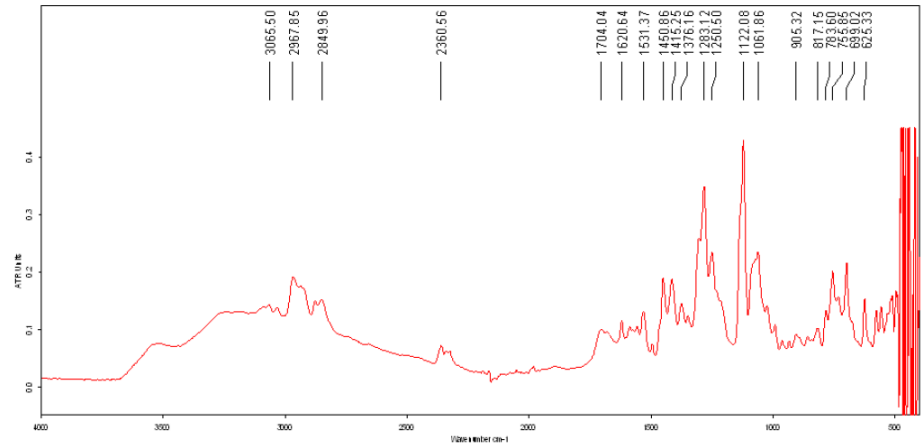

Compound **6_22**

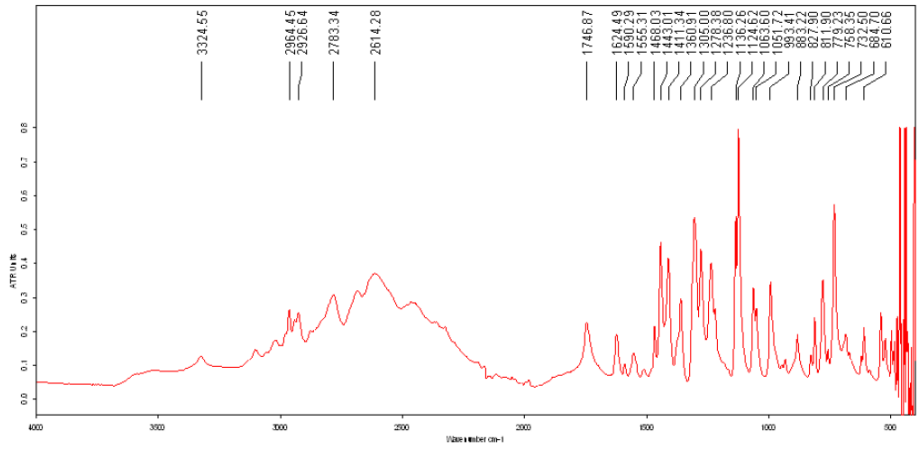

Compound **6_23**

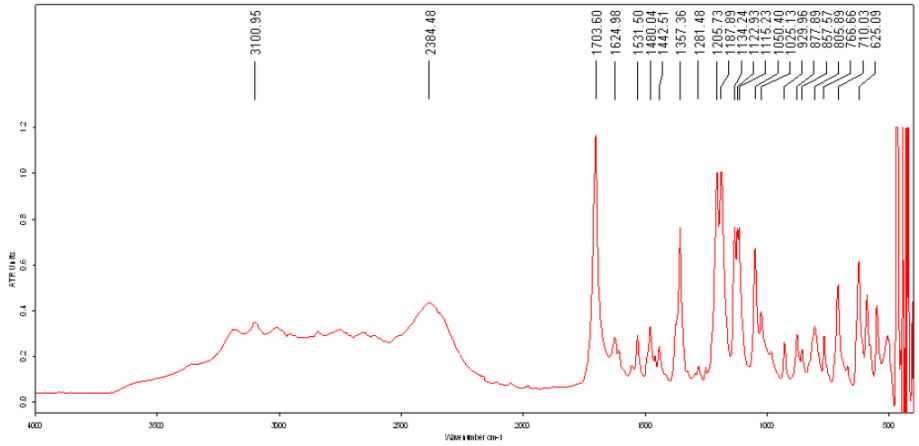

Compound **3_5b**

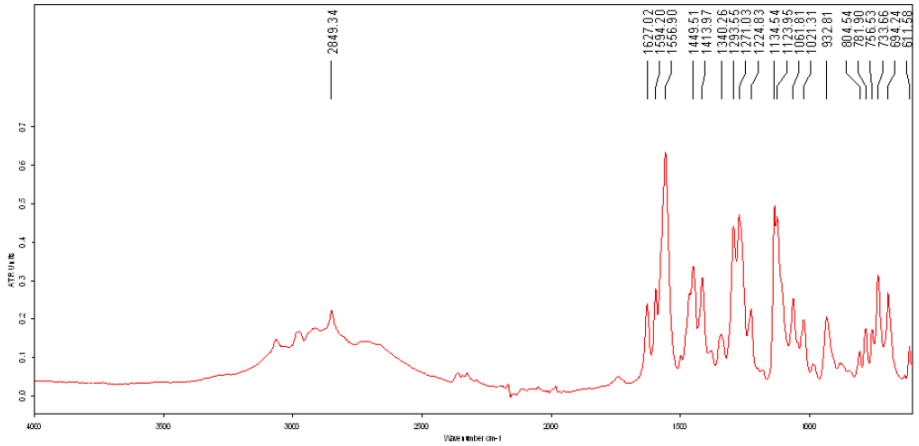

Compound **3_5i**

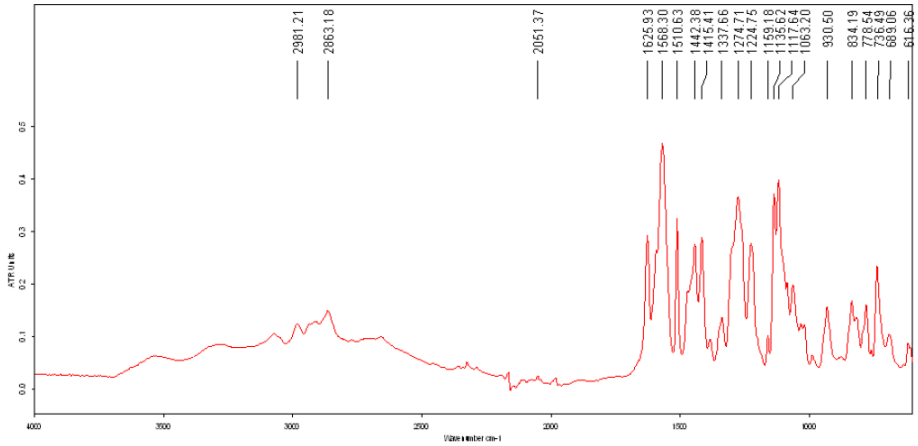

Compound **3_5j**

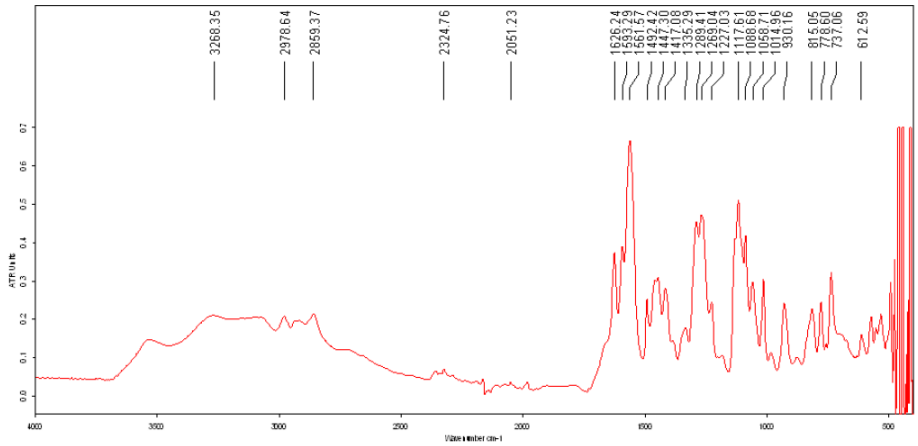

Compound **3_5k**

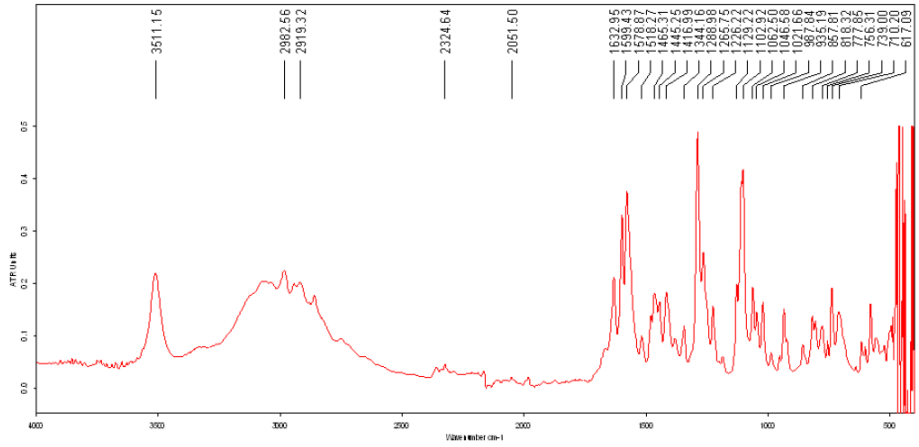

Compound **3_5l**

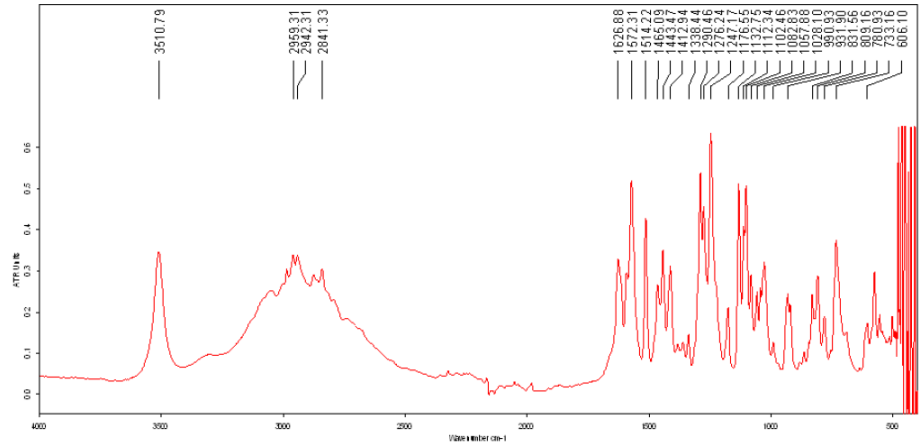

Compound **3_5f**

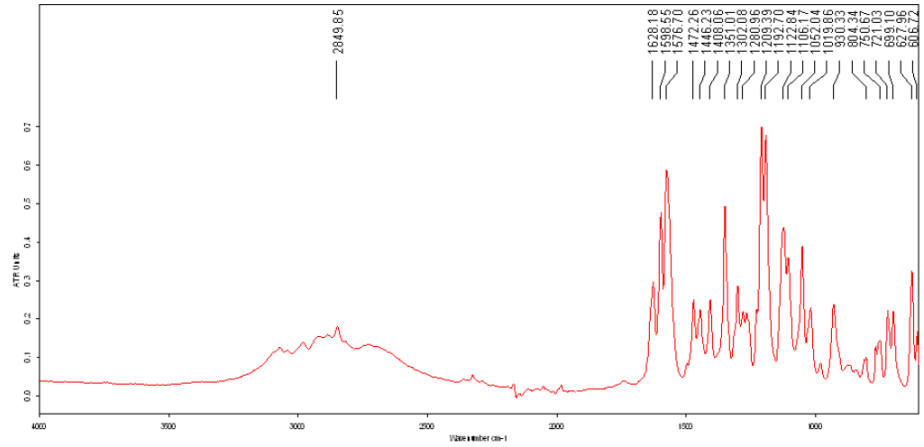

Compound **6_25**

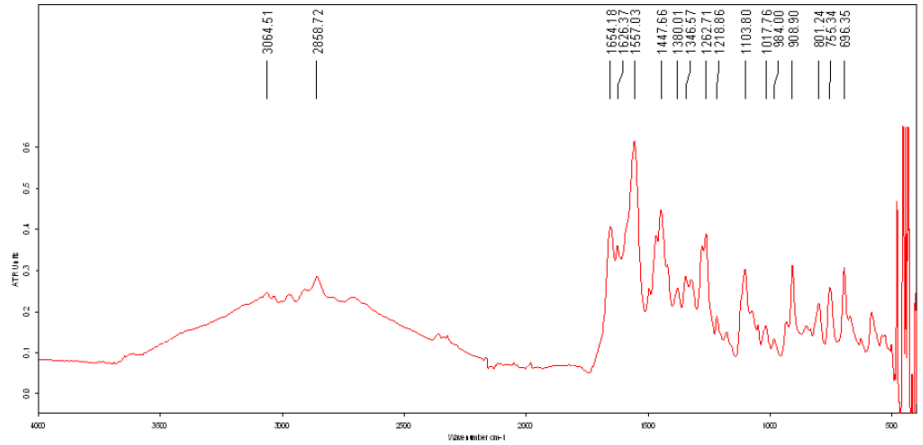

Compound **3_5c**

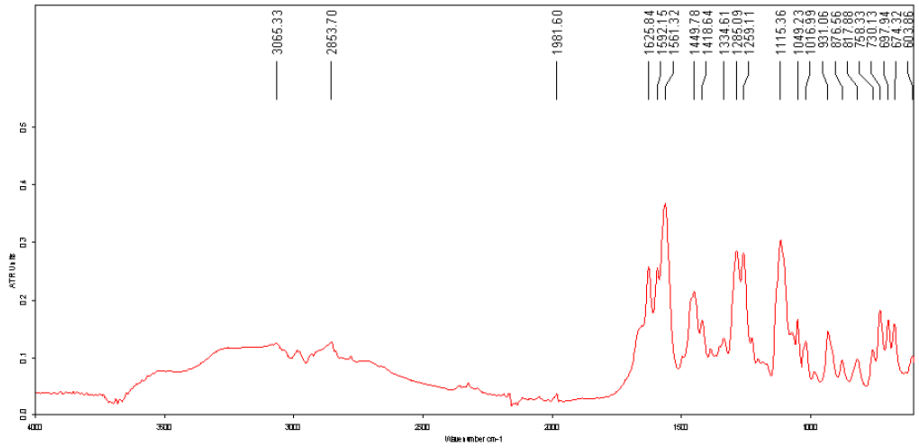

Compound **3_5d**

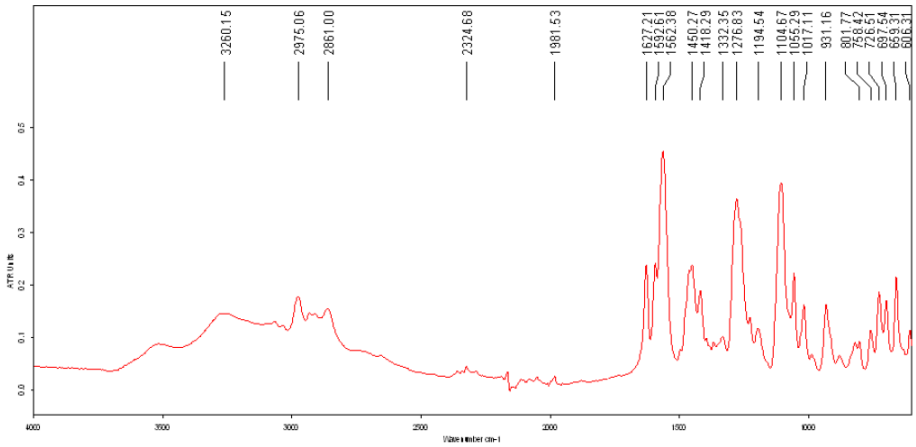

Compound **3_5e**

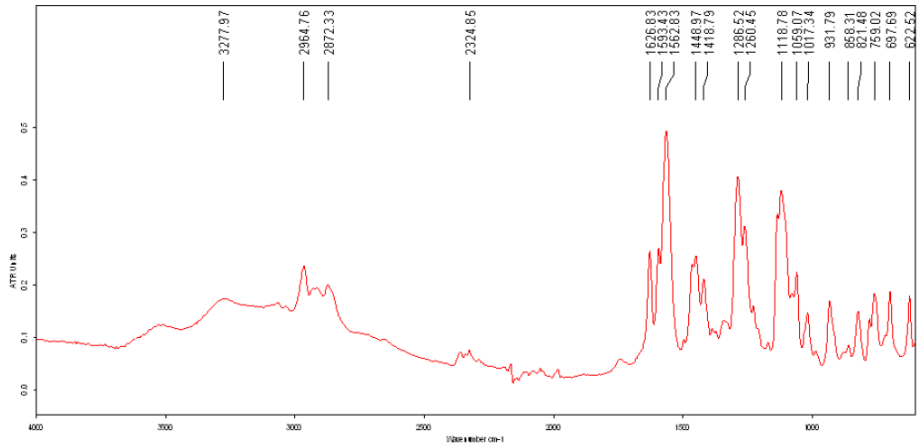

Compound **3_5g**

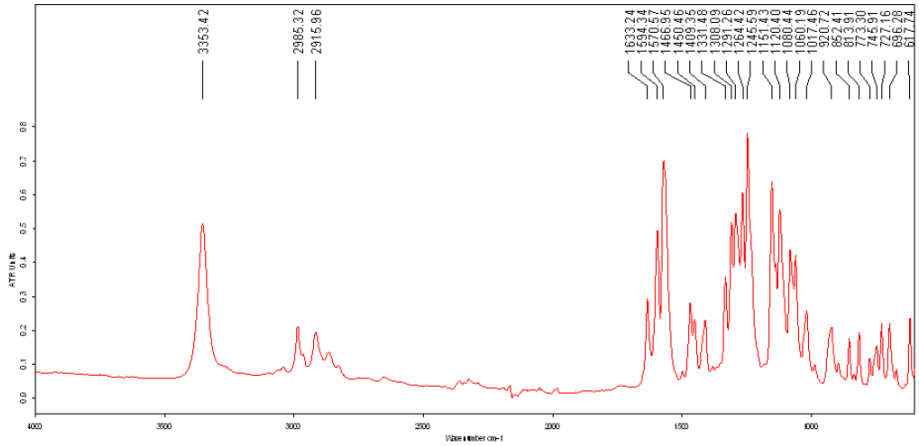

Compound **3_5h**

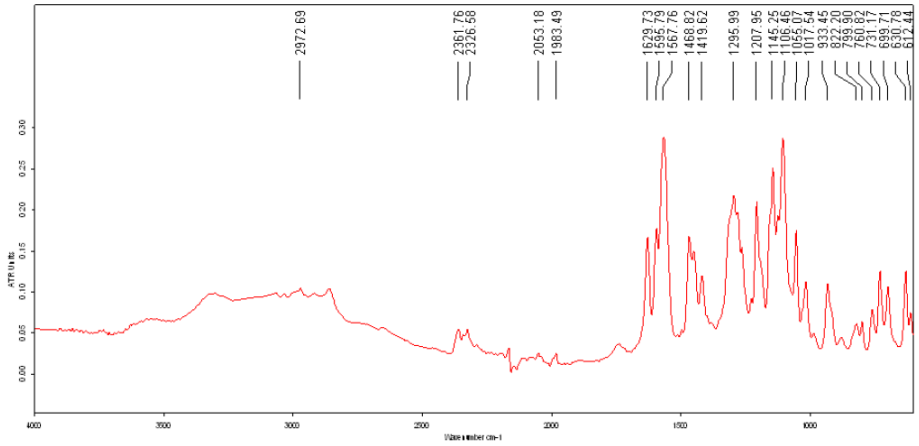

Compound **4_1a**

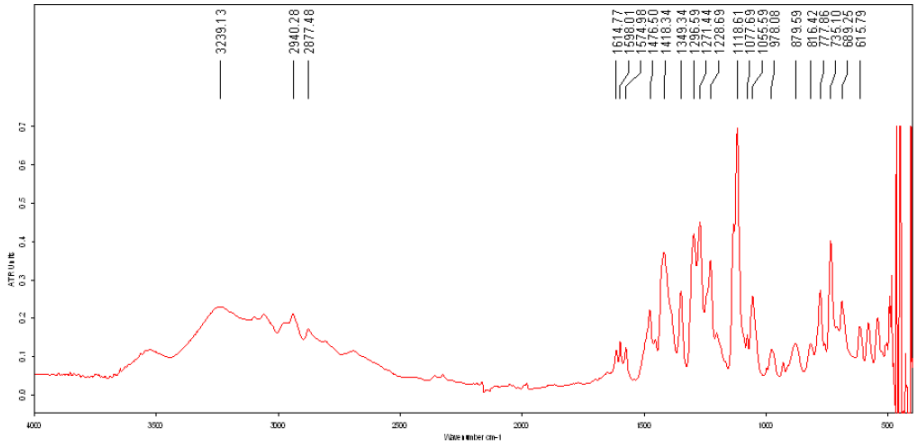

Compound **4_1b**

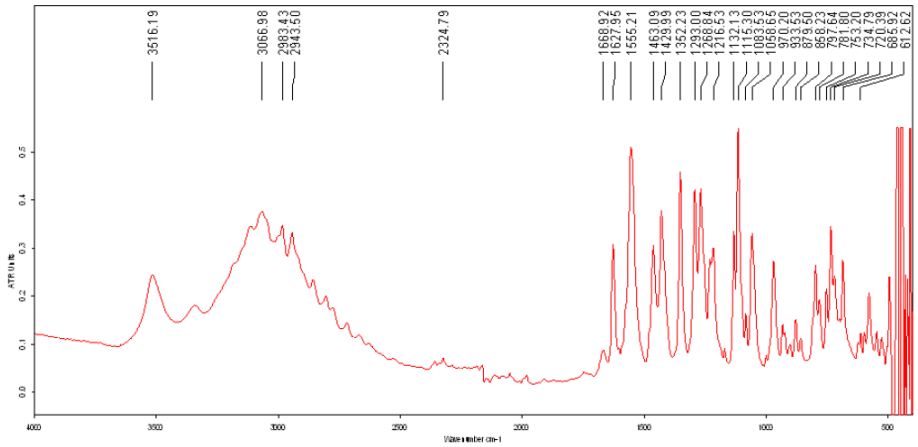

Compound **4_1c**

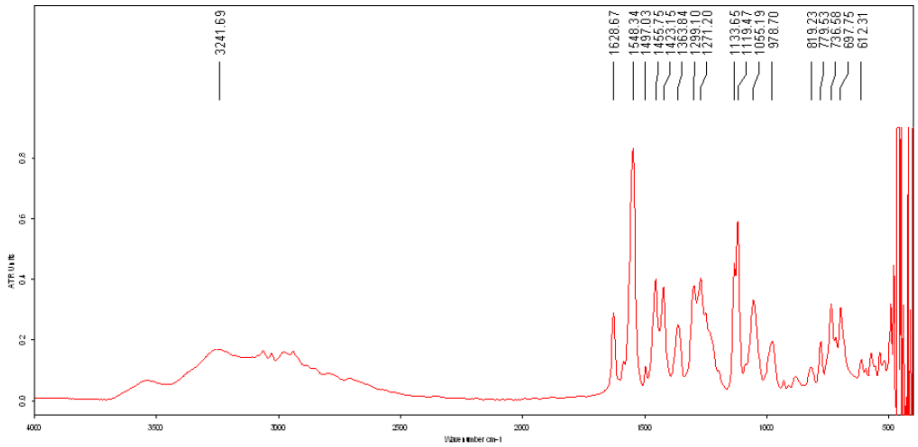

Compound **4_1d**

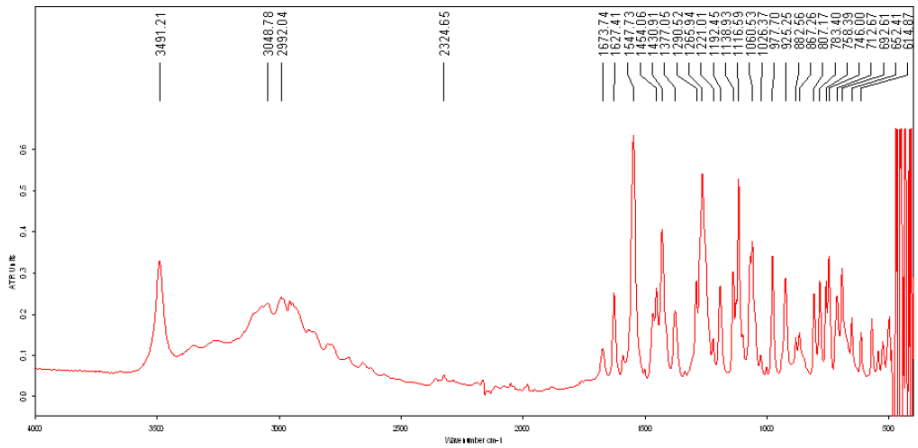

Compound **4_2a**

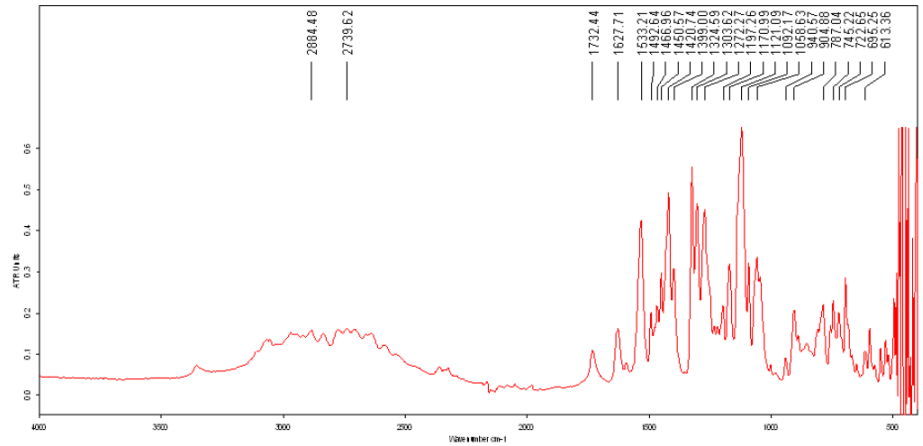

Compound **4_2b**

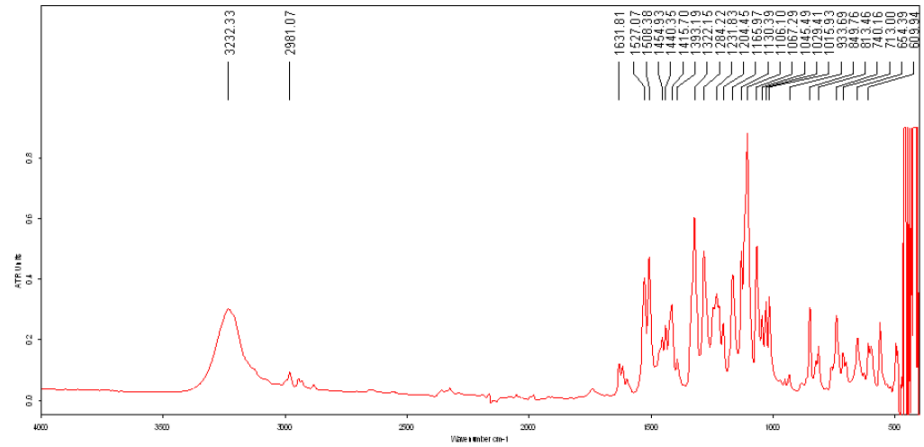

Compound **4_2c**

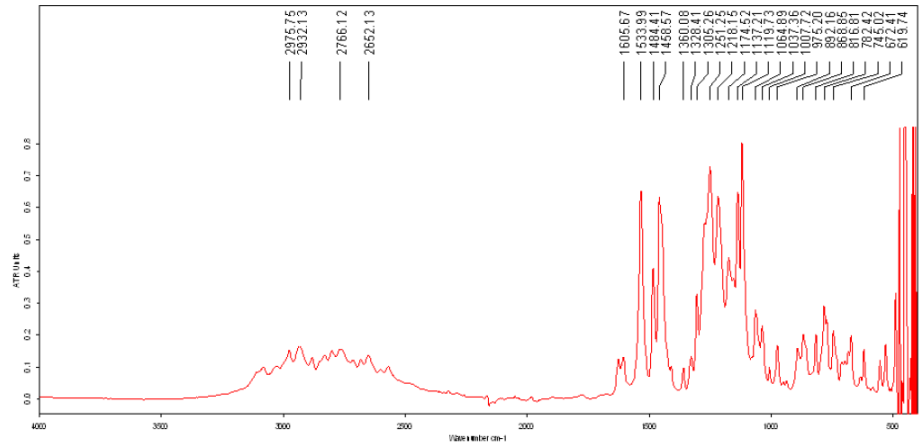

Compound **4_2d**

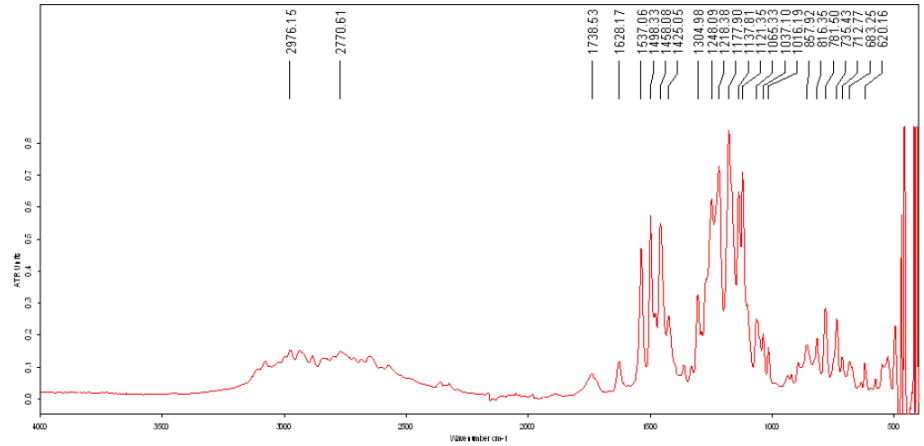

Compound **4_2e**

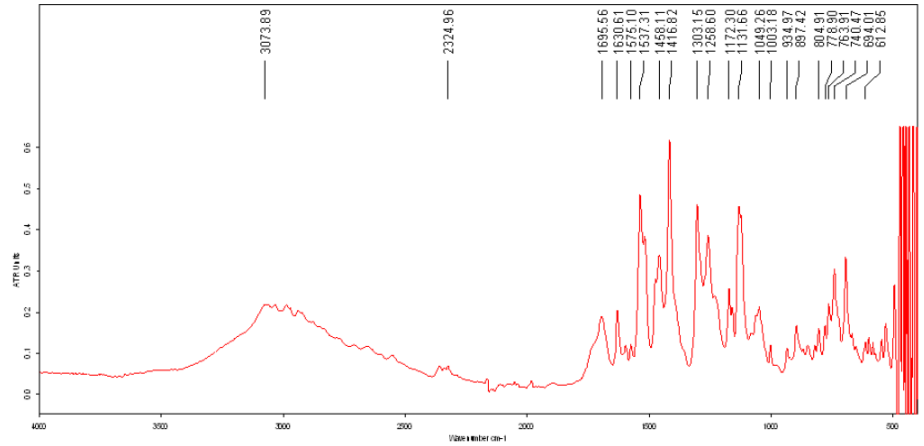

Compound **4_2f**

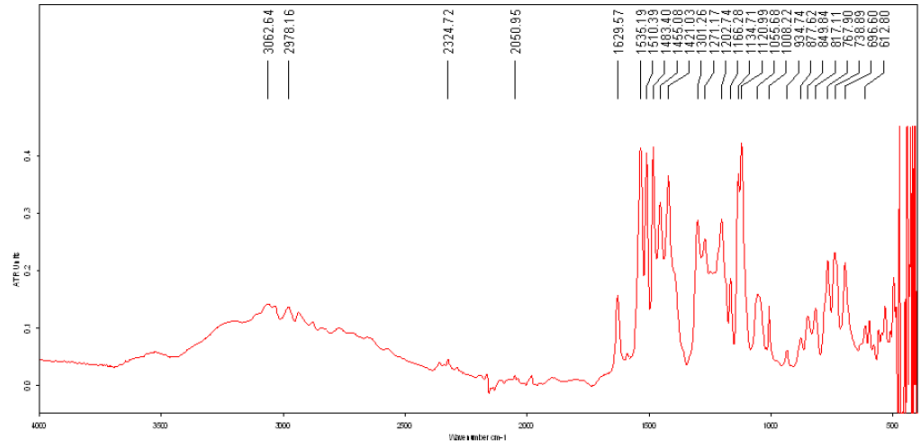

Compound **4_6b**

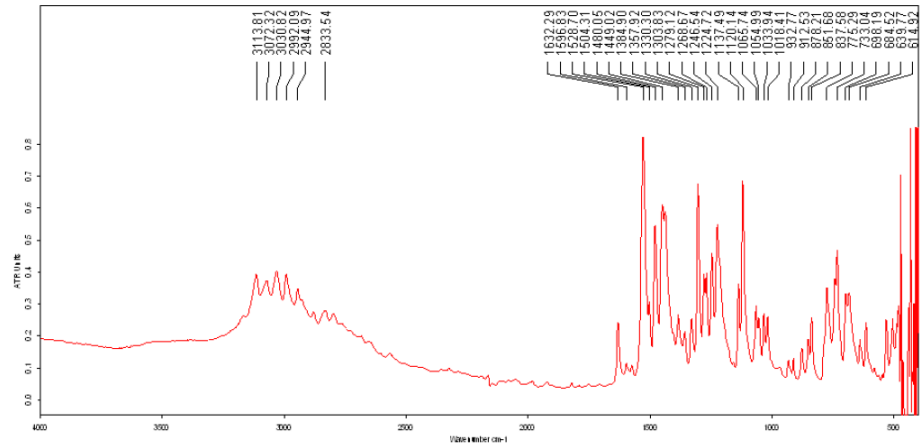

Compound **4_6c**

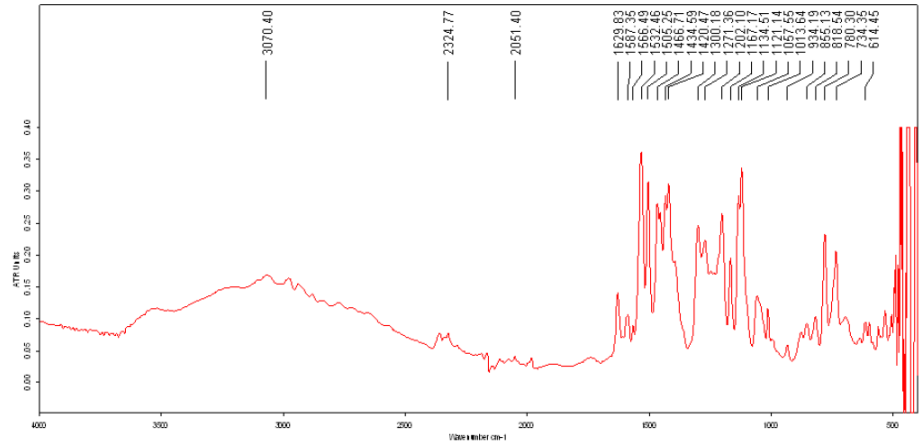

Compound **4_7a**

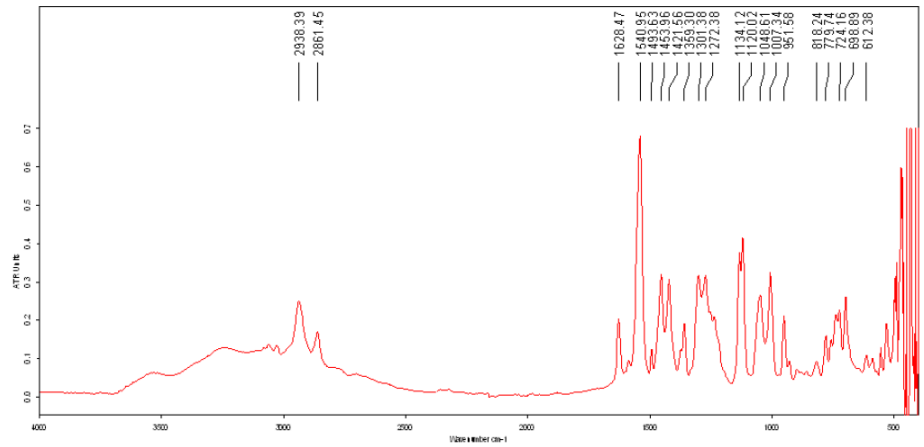

Compound **4_3a**

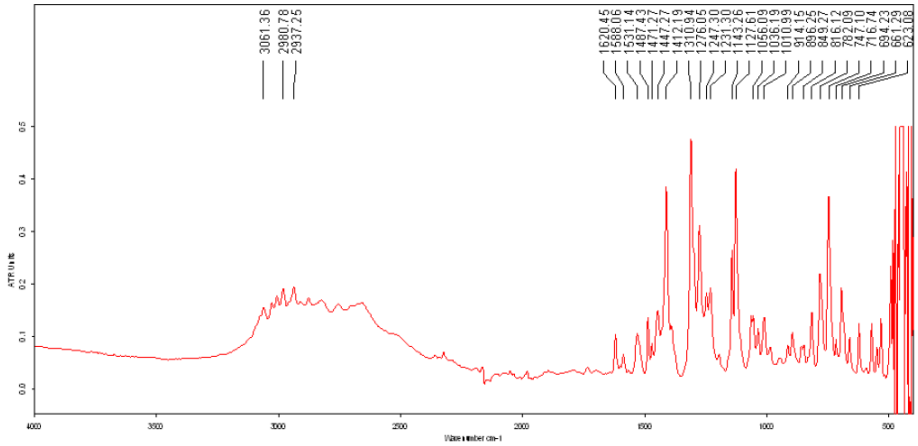

Compound **4_4a**

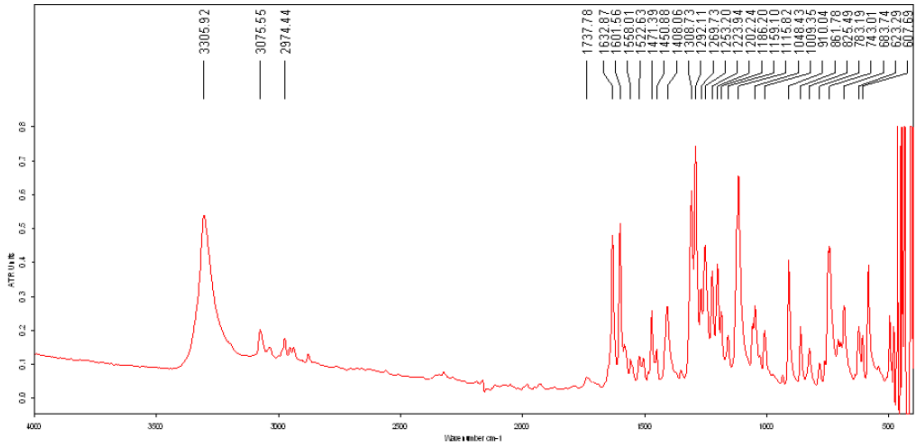

Compound **4_5a**

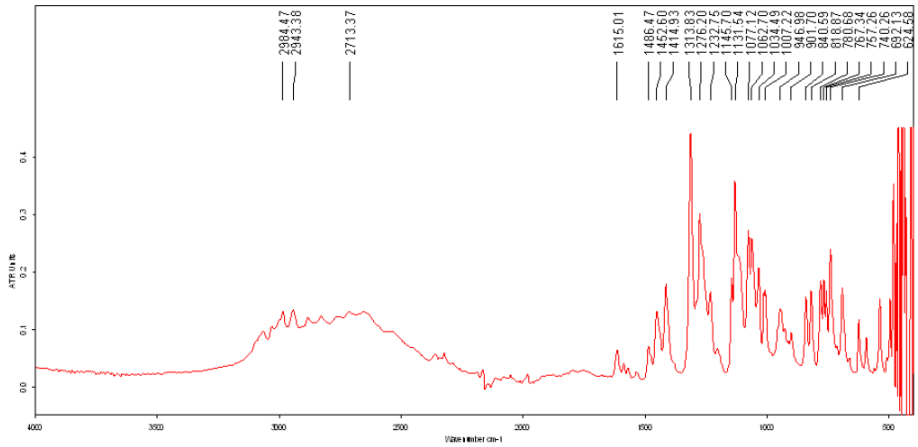

Acknowledgment

The author would like to express his deepest respect and gratitude to Professor Tsutomu Katuski[a] for his constant instruction from undergraduate days. The author got hooked on organic chemistry because of him.

The author owes his debt of gratitude to Professor Tohru Oishi,[a] Professor Ryoichi Kuwano,[a] and Professor Makoto Tokunaga[a] for kindly reviewing of his thesis.

The author expresses cordial gratitude to Dr. Hiroki Sato[b] for providing the opportunity for publication of this research.

This research has been carried out under the supervision of Mr. Takayuki Okuno[b] and Dr. Naoki Omori[b] to whom the author would like to express all his gratitude for their helpful discussions and suggestions.

The author acknowledges Dr. Naoki Kouyama,[b] Dr. Yuji Nishiura,[b] Dr. Kyouhei Hayashi,[b] Ms. Kana Watanabe,[b] Dr. Nobuyuki Tanaka,[b] Dr. Masahiko Fujioka,[b] and Mr. Akira Yukimasa[b] for their collaboration and discussions.

The author is gratitude to Dr. Hideo Yukioka,[b] Dr. Hirohide Nambu,[b] Mr. Hideki Tanioka,[b] Dr. Yasunori Yokota,[b] Ms. Yumiko Saito,[b] Mr. Takeshi Chiba,[b] Dr. Yukari Tanaka,[b] Ms. Kyoko Kadono,[b] and Mr. Tohru Mizutare[b] for the in vitro and in vivo assay of the compounds.

The author wishes to thank Dr. Yasuo Ida,[b] Ms. Naomi Umesako,[b] and Ms. Izumi Fujisaka[b] for support in the analytical characterization of the compounds.

The author would like to express his respect and gratitude to Dr. Ryuichi Kiyama,[b] Dr. Takeshi Shiota,[b] Dr. Kenji Matsuo,[b] and Mr. Yukio Tada[b] for their instruction since his joining the company. The author got hooked in medicinal chemistry because of them.

The author is grateful for Mr. Takeshi Endoh,[b] Dr. Hideki Shimizu,[b] Dr. Masahide Ohdan,[b] Dr. Tatsuya Uchida,[a] and Dr. Kazuhiro Matsumoto[a] for hearty encouragement.

[a]Kyushu University

[b]Shionogi & Co., Ltd.

References and notes

1. Itoh H. *Nihon Rinsho* **2003**, *61*, 1837.
2. Bays, H. E.; Chapman, R. H.; Grandy, S. *International Journal of Clinical Practice* **2007**, *61*, 737.
3. Tsai, A. G.; Williamson, D. F.; Glick, H. A. *Obesity Reviews* **2011**, *12*, 50.
4. Powell, A. G.; Apovian, C. M.; Aronne, L. J. *Clinical Pharmacology & Therapeutics* **2011**, *90*, 40.
5. Tatemoto, K.; Carlquist, M.; Mutt, V. *Nature* **1982**, *296*, 659.
6. Adrian, T. E.; Allen, J. M.; Bloom, S. R.; Ghatei, M. A.; Rossor, M. N.; Roberts, G. W.; Crow, T. J.; Tatemoto, K.; Polak, J. M. *Nature* **1983**, *306*, 584.
7. O'Donohue, T. L.; Chronwall, B. M.; Pruss, R. M.; Mezey, E.; Kiss, J. Z.; Eiden, L. E.; Massari, V. J.; Tessel, R. E.; Pickel, V. M.; DiMaggio, D. A.; Hotchkiss, A. J.; Crowley, W. R.; Zukowska-Grojec, Z. *Peptides* **1985**, *6*, 755.
8. Wahlestedt, C.; Reis, D. *Annu. Rev. Pharmacol. Toxicol.* **1993**, *32*, 309.
9. Grundemar, L.; Hakanson, R. *Gen. Pharmacol.* **1993**, *24*, 785.
10. Lungberg, J.; Franco-Cerecada, A.; Lacroix, J. S.; Pernow, J. *Ann. N. Y. Acad. Sci.* **1990**, *611*, 166.
11. McDermott, B. J.; Millat, B. C.; Peper, H. M. *Cardiovasc. Res.* **1993**, *27*, 893.
12. Blomqvist, A. G.; Herzog, H. *Trends Neurosci.* **1997**, *20*, 294.
13. Kamiji, M. M.; Inui, A. *Endocr. Rev.* **2007**, *28*, 664.
14. Ladyman, S. R.; Woodside, B. *Physiol. Behav.* **2009**, *97*, 91.
15. Félétou, M; Galizzi, J. -P.; Levens, N. R. *CNS Neurol. Disord. Drug Targets* **2006**, *5*, 263.
16. Marsh, D. J.; Hollopeter, G.; Kafer, K. E.; Palmiter, R. D. *Nat. Med.* **1998**, *4*, 718.
17. (a) Nonaka, K.; Erondu, N.; Kanatani, A. *Bio Clinica* **2006**, *21*, 1199. (b) Erondu, N.; Gantz, I.; Musser, B.; Suryawanshi, S.; Mallick, M.; Addy, C.; Cote, J.; Bray, G.; Fujioka, K.; Bays, H.; Hollander, P.; Sanabria-Bohórquez, S. M.; Eng, W.; Långström, B.; Hargreaves, R. J.; Burns, H.

D.; Kanatani, A.; Fukami, T.; MacNeil, D. J.; Gottesdiener, K. M.; Amatruda, J. M.; Kaufman, K. D.; Heymsfield, S. B. *Cell Metabolism* **2006**, *4*, 275. (c) Erondu, N.; Addy, C.; Lu, K.; Mallick, M.; Musser, B.; Gantz, I.; Proietto, J.; Astrup, A.; Toubro, S.; Rissannen, A. M.; Tonstad, S.; Haynes, W. G.; Gottesdiener, K. M.; Kaufman, K. D.; Amatruda, J. M.; Heysmfield, S. B. *Obesity* **2007**, *15*, 2027.

18. (a) Puopolo, A.; Heshka, S.; Karmally, W.; Alvarado, R.; Kakudo, S.; Ochiai, T.; Archambault, W. T.; Kobayashi, Y.; Albata, B. *Obesity Soc. Ann. Sci. Meeting.* **2009**, 214-P. (b) Smith, D.; Heshka, S.; Karmally, W.; Doepner, D.; Narukawa, Y.; Ochiai, T.; Archambault, W. T.; Kobayashi, Y.; Albata, B. *Obesity Soc. Ann. Sci. Meeting.* **2009**, 221-P. (c) Okuno, T.; Takenaka, H.; Aoyama, Y.; Kanda, Y.; Yoshida, Y.; Okada, T.; Hashizume, H.; Sakagami, M.; Nakatani, T.; Hattori, K.; Ichihashi, T.; Yoshikawa, T.; Yukioka, H.; Hanasaki, K.; Kawanishi, Y. *Abstr. Pap. Am. Chem. Soc.* **2010**, *240*, 284.
19. Omori, N.; Kouyama, N.; Yukimasa, A.; Watanabe, K.; Yokota, Y.; Tanioka, H.; Nambu, H.; Yukioka, H.; Sato, N.; Tanaka, Y.; Sekiguchi, K.; Okuno, T. *Bioorg. Med. Chem. Lett.* **2012**, 22, 2020.
20. Metabolic stability in human or rat liver microsome was measured as the percentage of drug remaining after 30 min incubation.
21. Ritchie, T. J.; Macdonald, S. J. F.; *Drug Discovery Today* **2009**, *14*, 1011.
22. (a) Gleeson, M. P. *J. Med. Chem.* **2008**, *51*, 817. (b) Lovering, F.; Bikker, J.; Humblet, C. *J. Med. Chem.* **2009**, *52*, 6752. (c) Ishikawa, M.; Hashimoto, Y. *J. Med. Chem.* **2011**, *54*, 1539.
23. CLogP values were estimated with ChemDraw Ultra, version 9.0.
24. To further characterize the pyridone analogue **2_8b**, in vivo cassette studies (0.5 mg/kg iv, 1.0 mg/kg po) were conducted. Unfortunately, this analogue exhibited low plasma levels with high

clearance (CL_{tot} = 46.7 ml/min/kg, C_{max} = N.D.) in spite of their acceptable solubility and high metabolic stability in rat liver microsomes. The poor correlation between the metabolic stability in liver microsomes and the in vivo clearance suggests that extrahepatic clearance routes may operate.

25. King, J. F.; Gill, M. S. *J. Org. Chem.* **1996**, *61*, 7250.
26. The rats (n = 2) were dosed at 0.5 mg/kg iv and 1.0 mg/kg po.
27. [cPP^{1-7}, NPY^{19-23}, Ala^{31}, Aib^{32}, Gln^{34}]-human pancreatic polypeptide.
28. Peters, J.-U.; Lubbers, T.; Alanine, A.; Kolczewski, S.; Blasco, F.; Steward, L. *Bioorg. Med. Chem. Lett.* **2008**, *18*, 262.
29. Meanwell, N. A. *J. Med. Chem.* **2011**, *54*, 2529.
30. Crowell, T. A.; Halliday, B. D.; McDonald, J. H. III; Indelicato, J. M.; Pasini, C. E.; Wu, E. C. Y. *J. Med. Chem.* **1989,** *32,* 2436.
31. Ulman, A.; Urankar, E. *J. Org. Chem*. **1989**, *54*, 4691.
32. Colacot, T. J.; Shea, H. A. *Org. Lett.* **2004**, *6*, 3731.
33. Patent WO 200856898, **2008**.
34. Itoh, T.; Mase, T. *Org. Lett.* **2004**, *6*, 4587.
35. Takada, S.; Fujishita, T.; Sasatani, T.; Matsushita, A.; Eigyo, M. Patent US 4940714, **1990**.

List of publications

1. **Highly enantioselective (OC)Ru(salen)-catalyzed sulfimidation using *N*-alkoxycarbonyl azide as nitrene precursor**

   Tetrahedron Letters, **2003**, *44*, 3301-3303.

   Yuusuke Tamura, Tatsuya Uchida, and Tsutomu Katsuki

2. **Mechanism of asymmetric sulfimidation with *N*-alkoxycarbonyl azide in the presence of (OC)Ru(salen) complex**

   Tetrahedron Letters, **2003**, *44*, 7965-7968.

   Tatsuya Uchida, Yuusuke Tamura, Masaaki Ohba, and Tsutomu Katsuki

3. **Oxidative desymmetrization of *meso*-cyclic ethers (2): Recognition of the core structure of substrates of the Mn(salen) catalyst**

   Heterocycles, **2007**, *71*, 2587-2593.

   Hidehiro Suematsu, Yuusuke Tamura, Hiroaki Shitama, and Tsutomu Katsuki.

4. **Design, synthesis and identification of novel benzimidazole derivatives as highly potent NPY Y5 receptor antagonists with attractive in vitro ADME profiles**

   Bioorganic & Medicinal Chemistry Letters, **2012**, *22*, 5498-5502

   Yuusuke Tamura, Naoki Omori, Naoki Kouyama, Yuji Nishiura, Kyouhei Hayashi, Kana Watanabe, Yukari Tanaka, Takeshi Chiba, Hideo Yukioka, and Takayuki Okuno

5. **Identification of a novel and orally available benzimidazole derivative as an NPY Y5 receptor antagonist with in vivo efficacy**

   Bioorganic & Medicinal Chemistry Letters, **2012**, *22*, 6554-6558

   Yuusuke Tamura, Naoki Omori, Naoki Kouyama, Yuji Nishiura, Kyouhei Hayashi, Kana Watanabe, Yukari Tanaka, Takeshi Chiba, Hideo Yukioka, and Takayuki Okuno

6. **Identification of a novel benzimidazole derivative as a highly potent NPY Y5 receptor antagonist with an anti-obesity profile**

   Bioorganic & Medicinal Chemistry Letters, **2013**, *22*, 90-95

   Yuusuke Tamura, Kyouhei Hayashi, Naoki Omori, Yuji Nishiura, Kana Watanabe, Nobuyuki Tanaka, Masahiko Fujioka, Naoki Kouyama, Akira Yukimasa, Yukari Tanaka, Takeshi Chiba, Hideki Tanioka, Hirohide Nambu, Hideo Yukioka, Hiroki Sato, and Takayuki Okuno